Cardiosphere-derived stem cell culture, characterisation and labelling for *in vivo* testing in the infarcted heart

Jun Jie Tan

Oriel College

Department of Physiology, Anatomy and Genetics

University of Oxford

Hilary Term 2011

Supervisor: Professor Kieran Clarke

Acknowledgements

First of all, I am deeply grateful to my supervisor, Professor Kieran Clarke, for giving me the opportunity of working in her laboratory as a DPhil student. She has given me endless help and advice for all the problems I had encountered during my studies.

I would also like to say a big thank you to my co-supervisors, Dr. Carolyn Carr and Dr. Daniel Stuckey, for their exceptional understanding and patience. Moreover, their guidance, scientific directions, and ability to solve scientific problems, have altogether made this thesis possible. I also owe my deepest gratitude to Dr. Georgina Ellison. Without her help and guidance, setting up immuno-labelling experiments in the laboratory would have been a lot more difficult. I would also like to thank Dr. Philip Lee and Dr. Lowri Cochlin for their technical support, ideas, and efforts on the magnetic resonance cell-labelling project.

I am also indebted to Dr. Lisa Heather, Dr. Marie Schroeder, Dr. Damian Tyler, Dr. Gil Bub, Dr. Lien-Cheng Hsiao, Kah Keng Wong, Alice Kwok, Mattea Finelli, Siaw Wei Ng, Mike Dodd, Fiona Woods, Emma Carter, Yvonne Green, and all of whom have given me endless motivation and support during times when work did not progress as smoothly as I would have liked. I would also like to thank all Cardiac Metabolism Research group members; it would have been next to impossible to complete my project without your help. Thanks also to my beloved wife and parents for their love and support.

Last but not least, I would like to thank Universiti Sains Malaysia and the Malaysian Ministry of Higher Education, for sponsoring my DPhil studies at the University of Oxford.

Abstract

Cardiac stem cells (CSCs), isolated from heart tissue explants and expanded via the formation of cardiospheres (Csp), are a promising candidate for cell therapy to prevent heart failure following myocardial infarction. To allow early administration to patients, isolation and expansion of CSCs must be performed in the shortest time possible. Hence, this project aimed to optimize culture conditions and characterize the cardiac explant-derived cells (EDCs), Csp and Csp-derived cells (CDCs) produced. Rat neonatal EDCs contained 4-7% c-kit$^+$ cells, measured using flow cytometry. Optimal Csp growth conditions were determined, such that plating 3 x 10^4 EDCs per well of a 24-well plate coated with 16.7 µg/ml poly-D-lysine, in CGM containing 7% serum, improved Csp production and generated 1.5 x 10^7 CDCs in 16 days, a sufficient number for cell therapy. The CDCs expressed the stemness markers; c-kit, Oct3/4, SOX2, and Klf-4, and the cardiac differentiation markers; GATA4 and Nkx2.5. The therapeutic effect of CDCs may be limited by the low, 3 ± 0.1%, c-kit$^+$ cell numbers. To increase c-kit$^+$ cells in CDCs, an alternate culture method for Csp and different extracellular matrices (ECM) for cell expansion were tested. The hanging drop culture method produced Csp with higher levels of c-kit$^+$ cells (9 ± 2%) than poly-D-lysine-coated and low-bind culture dishes. Of five ECM tested, collagen IV was found to enhance EDC migration and CDC proliferation, and produced 11 ± 0.4% c-kit$^+$ cells, with Csp cultured in hanging drops. Intramyocardial injection of CDCs improved left ventricular ejection fractions of infarcted rat hearts by 9% and prevented the peri-infarct wall from thinning, measured *in vivo* using MRI over 16 weeks. To improve cell tracking using MRI, two MR positive contrast agents, gadolinium-DTPA and gadonanotubes were tested. Gd-DTPA had low sensitivity after labelling (1.4 x 10^5 cells/mm^2); whereas gadonanotubes did not provide positive contrast at 11.7 T. Thus, neither contrast agent could be used for cell tracking using high magnetic field. In conclusion, CDCs were an effective source of stem cells that could be used for heart repair, although cells could not be tracked using positive MR contrast.

Table of Contents

Abbreviations

αSA	A-sarcomeric actin
ABCG2	ATP-binding cassette transporter2
ACE	Angiotensin converting enzyme
BMMNCs	Bone marrow mononuclear cells
BM-MSCs	Bone marrow derived mesenchymal stem cells
CADUCEUS	CArdiosphere-Derived aUtologous Stem Cells to reverse ventricUlar dySfunction
CDCs	Cardiosphere-derived cells
CEM	Cardiac explant medium
CGM	Cardiosphere-growth medium
CSCs	Cardiac resident stem cells
CXCR-4	C-X-C chemokine receptor type 4
DAPI	4',6-diamidino-2-phenylindole
DDR2	Discoidin domain receptor-2
DMSO	Dimethy sulfoxide
EDCs	Explant-derived cells
EMT	Epithelial-mesenchymal transition
EPCs	Endothelial progenitor cells
EPDCs	Epicardial derived cells
ESCs	Embryonic stem cells
Gd^{3+}@US	Gadonanotubes
Gd-DTPA	Gadolinium diethylenetriamine penta-acetic acid
GFP	Green fluorescent protein
GLUT	Glucose transporter
HSC	Haematopoietic stem cells
IGF-1	Insulin-like growth factor-1
LVEF	Left ventricular ejection fraction
MAGIC	Myoblast Autologous Grafting in Ischemic Cardiomyopathy
MEF2C	Myocyte-specific enhancer factor 2C
MPIO	Micron-sized particles of iron oxide
MRI	Magnetic resonance imaging
Oct4	Octamer-binding transcription factor 4
PBCs	Phase-bright cells
PGC1-α	PPARγ coactivator 1-α
PPAR	Peroxisome proliferator-activated receptors
Sca-1	Stem cell antigen-1
SCF	Stem cell factor
SCIPIO	Cardiac Stem Cell Infusion in Patient with Ischemia cardiomyopathy
SMA	Smooth muscle actin
SP cells	Side population cells
SSEA-1	Stage-specific embryonic antigen-1
Tβ4	Thymosin-β4
VSEL	Very small-embryonic like cells
vWF	von-Willebrand factor

Chapter 1

Introduction

1.1 MYOCARDIAL INFARCTION

Myocardial infarction remains a major cause of morbidity and mortality worldwide. In 2004, 17 million people around the world died of cardiovascular disease, of which 45% had previously suffered from coronary heart disease, which is the major cause of myocardial infarction (1). Despite use of the most advanced therapies, myocardial infarction can progress to heart failure. The London Heart Failure Study showed that 62 % of patients in the UK survived one year after diagnosis of heart failure and more than 60% had died after 5 years (2) (Figure 1.1).

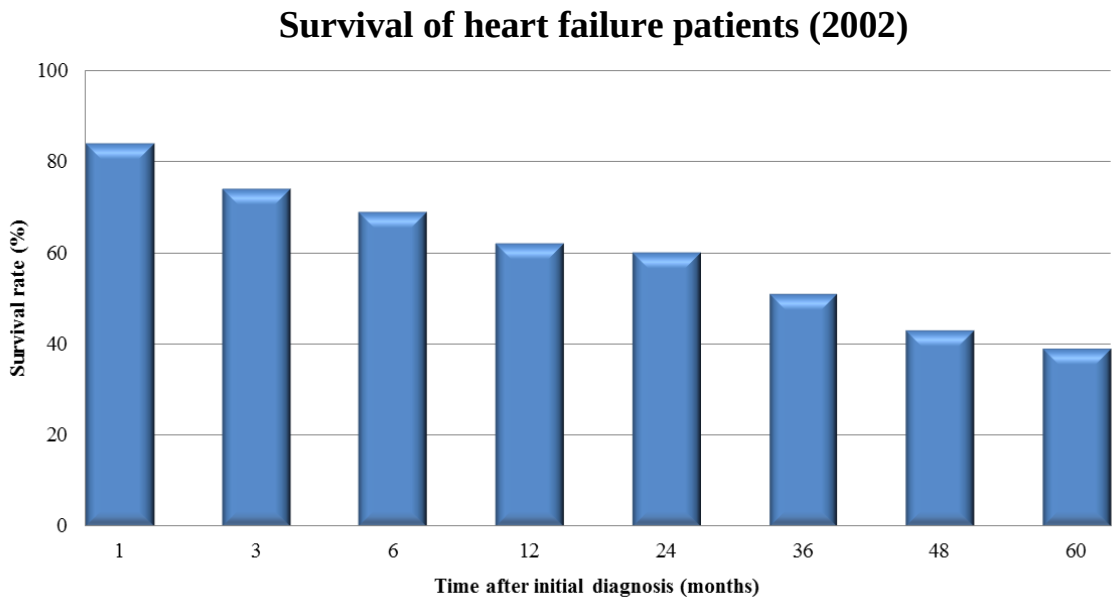

Figure 1.1: Only ~40% of the heart failure patients survive 5 years after initial diagnosis. (London Heart Failure Study, 2005)

Myocardial infarction occurs when the blood supply to the myocardium is reduced, commonly due to blockage of a coronary artery, resulting in significant myocardial cell death through apoptosis or necrosis (3). Acute loss of cardiomyocytes triggers the activation of several complex biochemical signalling cascades that modulate reparative mechanisms, including the formation of non-contractile scar tissue. The resultant scar leads to hypokinesis (diminished contractility) in the infarcted region, and hyperkinesis (increased contractility) of the remaining viable cardiomyocytes in the remote region, in order to maintain delivery of a

normal amount of blood to the whole body. The uncompensated haemodynamic stress leads to cardiac remodelling, which can be phenotypically recognized by cardiac hypertrophy and ventricular dilatation. Sustained wall stress recruits the remote region into the scar, further deteriorating the contractility, and subsequently culminating in heart failure (4).

1.2 CURRENT THERAPIES FOR MYOCARDIAL INFARCTION

1.2.1 Coronary reperfusion

When a patient with myocardial infarction is admitted to hospital, restoration of circulation to the affected myocardium is attempted as soon as possible. Treatments include thrombolytic agents, primary balloon angioplasty or stenting or, in the more extreme cases, artery by-pass surgery (5-7). These approaches aim to re-establish vessel patency and prevent further induction of irreversible injury to the myocardium. Although these therapies have significantly reduced the early mortality rate, they are not the absolute cure, as the cardiac tissue has already been damaged.

1.2.2 Pharmacological treatment

A pharmacological approach is also used to alleviate the patient's symptoms and attenuate remodelling. Two common drugs given to heart failure patients are beta-blockers, and angiotensin-converting enzyme (ACE) inhibitors. Beta blockers reduce heart rate and workload by antagonising increased adrenergic activity induced by weakening heart contractility; while ACE inhibitors act on peripheral vasodilation and attenuates ventricular remodelling. Although drugs are available and have been shown in the clinic to reverse heart remodelling and progression to heart failure (8), they do not replace the akinetic scar with functional cardiomyocytes.

1.2.3 Cell therapy

Cell-based therapy is the only treatment capable of replacing the akinetic scar of the infarcted myocardium, as it aims to replace the fibrotic scar tissue with viable cardiomyocytes. This was demonstrated by Huwer et al. (2003), who injected neonatal rat cardiomyocytes into the infarcted rat heart, and showed improvement in ejection fraction and increased wall thickness (9). However, ethical and immunological problems may preclude the use of human neonatal cardiomyocytes clinically. Instead, cardiomyocytes may be cultured or generated from adult cardiomyogenic stem cells.

1.3 STEM CELLS

Stem cells are cells that are capable of self-renewal, proliferate indefinitely, and are multipotent, thus are able to differentiate into daughter cells, which are different from the mother cells. Stem cells are primitive, unspecialised cells that can be isolated and cultured *in vitro* and can be directed to differentiate along a desired lineage using defined chemicals or growth factors. There are three general categories of stem cells, namely embryonic stem cells, iPS cells and adult/somatic stem cells.

1.3.1 Embryonic stem cells

Embryonic stem cells (ESCs) originate from the inner mass of the blastocyst (10). These cells are pluripotent and are able to differentiate into all cells of the three germ-layers. They are capable of indefinite *in vitro* expansion while maintaining a normal karyotype. However, there are limitations to the use of ESC for therapy. The pluripotent characteristics of ESCs result in a high chance of teratoma formation after administration (11, 12). In addition, the allogenicity of ESCs provokes an immune reaction, as the body recognise ES cells as foreign due to high expression level of HLA class I antigen (13). An immunosuppressive regimen may address this problem, but may also compromise the subject's immune system against

common infectious diseases and affect quality of life. Moreover, ESC research often encounters ethical and legal issues because the isolation of ESCs requires sacrifice of a live embryo.

1.3.2 Induced pluripotent stem cells

Induced pluripotent stem (iPS) cells are generated from adult skin fibroblast cells by *ex vivo* nuclear reprogramming to become embryonic-like stem cells, through ectopic expression of a combination of stemness-related pluripotent genes Oct4, Sox 2, Klf-4 and c-Myc (14). Unlike ESCs, the protocol does not involve killing an embryo and the source of the cells can readily be taken from the patient, thereby avoiding ethical controversy and providing patient-specific cells. iPS cells can undergo indefinite expansion and are able to differentiate into beating cardiomyocytes (15), providing an alternate cell source to treat myocardial infarction. However, the risk of tumorigenesis remains, as iPS cells are pluripotent, like ESCs, and currently there are no Good Manufracturing Practices (GMP) compliant strategies available. Furthermore, the generation of iPS cells involves genetic reprogramming of adult cells, which may retain an epigenetic memory of their origin (16).

1.3.3 Adult stem cells

Adult stem cells are undifferentiated, multipotent cells that reside within a tissue or organ amongst the differentiated cells. These cells can self-renew, and differentiate to specialized cells in order to maintain homeostasis within their host tissue. Generally, there are limited in number and difficult to access. In some cases, adult stem cells are able to undergo transdifferentiation, and become developmentally unrelated cells (17). Several types of adult stem cells have been studied for their regenerative potential for the treatment of the damaged myocardium, including bone marrow mononuclear cells (18, 19), hematopoietic stem cells

(20, 21) , endothelial progenitor cells (22, 23), mesenchymal stem cells (24, 25) , skeletal myoblasts (26, 27), and endogenous cardiac stem cells (28).

1.3.3.1 Bone marrow-derived stem cells

Bone marrow cells represent a complex assortment of differentiated cells (adipocytes, osteoblast, osteoclast, and vascular cells) and a diverse multipotent stem and progenitor cell population. The interest in using bone marrow cells for cardiac cell therapy was initiated by the identification of an extracardial source of cardiac progenitor cells, following detection of recipient-derived cardiomyocytes in sex-mismatched donor hearts (29-31). Most clinical studies showed a small, yet clinically significant (32), improvement in cardiac function following bone marrow mononuclear cell (BMMNC) injection (*Supplementary Table 1*). The mechanism for the improvement was unclear, but scepticism exists regarding the transdifferentiation of the injected donor BMMNCs into cardiomyocytes (33). However, there is evidence that BMMNCs contributed to angiogenesis (34) and neovascularisation (35), by secreting paracrine factors (18).

A landmark report from Orlic *et al.* showed that a subset of bone marrow derived Lin^- $ckit^+$ hematopoietic stem cells (HSCs) trans-differentiated into cardiomyocytes, reconstituted the infarct, and improved cardiac function in a mouse infarct model (20). However, Murry and Balsam utilized genetic methods to track cell fate following administration (36) and did not observe transdifferentiation of HSCs into cardiomyocytes or improvement in cardiac function. Nygren and coworkers suggested that HSCs generated cardiomyocytes through cell-fusion as opposed to transdifferentiation (37). However, a few *in vitro* studies have shown that transforming growth factor-beta (38) or cell c-kit/SCF signalling (39) can induce

cardiomyogenesis of HSCs. Yet, no consensus exists regarding HSC cardiomyogenic differentiation and heart regenerative potential in *vivo*.

1.3.3.2 Endothelial progenitor cells

Endothelial progenitor cells (EPCs) are a subset of bone marrow-derived HSCs that express KDR (a marker for the angioblast lineage), CD133 and CD34 (hematopoietic progenitor cells), and have a high capacity to differentiate into endothelial cells (40, 41). It has been shown that intravenously injected EPCs home to the infarcted heart, slow the progression of the ventricular remodelling and improve heart function (42, 43). The observed improvement in cardiac function following EPC transplantation was attributed mainly to their angiogenic and neovasculogenic potential (44). However, evidence has shown that EPCs are capable of cardiomyocyte differentiation *in vitro* (45) and *in vivo* (46), not due to cell fusion (47).

1.3.3.3 Bone marrow-derived mesenchymal stem cells (BM-MSC)

BM-MSCs represent a very small fraction of cells (less than 0.01%) of the total bone marrow stem cell population (48). Recently, a clear definition has been given for MSCs by the International Society on Cellular Therapy (49), as positive for CD105, CD73 and CD90, but negative for CD45, CD34, CD14, or CD11b, CD79, CD19, and HLA-DR. They are adherent to plastic under standard culture conditions and able to different into osteoblasts, adipocytes, and chondroblasts. BM-MSCs have been shown to augment cardiac function in the infarcted animal heart (50-53), but conflicting results have been reported (54). There is no robust evidence to suggest that the improvement in cardiac function *in vivo* results from direct regeneration through differentiation of MSCs into cardiomyocytes, and the underlying mechanism by which the injection of MSCs improved cardiac function is poorly defined.

1.3.3.4 Skeletal myoblasts

Skeletal myoblasts (SMs), or satellite cells, are responsible for skeletal muscle maintenance and regeneration (55). Myoblasts can be isolated from muscle biopsies and amplified *in vitro* (56). Several clinical trials of myoblast treatment have shown improved left ventricular ejection fraction (LVEF) in myocardial infarct patients (57, 58). However, incidents of early phase ventricular arrhythmia were reported (57, 59) and, in the MAGIC trial (60), the SMs failed to improve echocardiographically-determined heart function and were associated with life-threatening ventricular tachycardia. It is unlikely that SMs can transdifferentiate into cardiomyocytes, due to their lineage constraint (61) , nor can they integrate with host tissue via gap junctions (62). However, modification of the preimplantation methods has reduced the occurrence of arrhythmias after SM transplantation and Phase II clinical studies are now underway (63).

1.3.3.5 Very small-embryonic like cells

Very small-embryonic like cells (VSELs) were first described as a subset of the non-hematopoietic cell population within the bone marrow mononuclear cells (0.01-0.02%), which expressed $CXCR4^{+}$ $Sca\text{-}1^{+}$ $CD45^{-}$ (64), but were later found to reside in many adult organs (65). They are recognized by their uniquely small size (2-4 μm), and express several embryonic stem cell transcription factors, such as Oct-4, Nanog, SSEA-1 and Rex-1. VSELs possess ESC-like pluripotent plasticity, and are able to differentiate into neuronal, pancreatic and cardiomyogenic lineages (64). VSEL transplantation improved left ventricular function after myocardial infarction in animal models (66, 67), but the oncogenic risk and the rarity of the cells need to be resolved before translation to the clinic.

1.3.4 ENDOGENOUS CARDIAC STEM CELLS

The heart had been defined as a terminally differentiated, post-mitotic organ. However, the paradigm was challenged when measurement of the rate of apoptosis and necrosis of cardiomyocytes in the failing heart (68) suggested that a heart would disappear in 2 months if no cycling stem cells replenished the lost myocytes (69). A sophisticated genetic fate-mapping study reported by Hsieh (2007) demonstrated the existence of stem cells which replenished lost cardiomyocytes following myocardial infarction or pressure overload (70). Subsequent studies have proved the presence of endogenous cardiac stem cells (71), and confirmed their important role in the heart (72). Several types of endogenous cardiac stem cells (CSCs) have been identified, which will be discussed below based on different markers and characteristics.

1.3.4.1 Cardiac side population

Side population (SP) cells, were first described in mouse hematopoiectic stem cells, are characterized by the ability to efflux DNA-binding dye Hoechst 33342. The unique dye efflux ability is mediated by the ATP-binding cassette transporter (ABCG2) which is then used as an identity marker. Several studies have shown that SP cells are not only present in bone marrow, skeletal muscle, brain and liver, but are also found within the heart, and are capable of forming cardiomyocytes (73-75), endothelial cells, and smooth muscle cells (73). Other studies involving ABCG2 knockout models demonstrated that ABCG2 expression is important to endothelial cell survival, migration and tubule formation following myocardial infarction (76). *In vitro* cell models showed that overexpression of the ABCG2 transporter increased proliferation of cardiac SP cells, but at the same time impaired cardiomyogenic differentiation (73). The cardiogenic potential is greater in the cell subset co-expressing Sca-1, but negative for CD31, an endothelial marker (77). However, no study has evaluated the regenerative potential *in vivo* following SP cell transplantation.

1.3.4.2 c-kit$^+$ cells

A distinct population of CSCs, which express c-kit (CD117) but are haematopoietic lineage (CD45) and lineage (Lin) negative, was first identified in the rodent heart (28). These c-kit$^+$ cells are self-renewing, clonogenic, multipotent, and can differentiate into cardiomyocytes, smooth muscle cells and endothelial cells. Some Lin$^-$c-kit$^+$ cells are also positive for early myocyte differentiation transcription factors (Nkx2.5, GATA-4 and MEF2C), indicating that the population contains cells which are committed to the cardiac lineage (28). Many studies have demonstrated that c-kit$^+$ cells are activated and differentiate into cardiomyocytes following an ischemic insult (78, 79), and that activation is mediated by insulin-like growth factor 1 (IGF) and hepatocyte growth factor, either in a paracrine or autocrine fashion (80). Isolation from the heart yields very low numbers of lin$^-$ ckit$^+$ cells (1 cell in every 10^4 myocytes), (28) but the cells can be expanded *in vitro* for up to 60 passages without introducing culture senescence (81). In addition, evidence also showed that c-kit$^+$ cells have pro-survival effects on isolated rat left ventricular cardiomyocytes (81), which can be enhanced by high GATA-4 expression through the IGF signalling pathway (82). Furthermore, c-kit$^+$ cells have also been shown to improve left ventricular ejection fraction (28) and activate endogenous stem cells following cell transplantation (83). This encouraging pre-clinical evidence has led to a clinical trial (Cardiac Stem Cell Infusion in Patients With Ischemic CardiOmyopathy (SCIPIO)).

1.3.4.3 Stem cell antigen -1$^+$ cells

A population of cells has been isolated from the murine heart based on the expression of stem cell antigen-1 (Sca-1), a member of the Ly-6 family (84). These cells are self-renewing, clonogenic and can be phenotypically distinguished from hematopietic lineages (negative for CD45, CD34, vWF, Flk-1, Flt-1, vascular endothelial cadherin). Only 0.3% of cells isolated

from the mouse heart were Sca-1$^+$, and among the Sca-1$^+$ cells, 40% are positive for CD45, and 10% of them co-expressed CD34 and c-kit (85).

Many studies have demonstrated that cardiac Sca-1$^+$ cells are capable of self-renewal, are clonogenic, and multipotent (86), and are capable of cardiomyogenic differentiation, both *in vitro* upon treatment with 5-azacytidine (84) or oxytocin (85), and *in vivo* after administration to the infarcted murine myocardium (84, 86). Smits and coworkers described a successful isolation of human heart-derived Sca-1-like cells with a high efficiency of *ex vivo* cardiomyocyte differentiation upon stimulation with ascorbic acid, 5'azacytidine and transforming growth factor-β (87). The therapeutic effect has also been demonstrated *in vivo* by transplantation of cardiac-derived Sca-1$^+$ cells following insulin-like growth factor-1and preconditioning by oxygen-glucose deprivation, thereby improving heart function (88), and attenuating left ventricular remodeling (89). Sca-1 transcript knockdown resulted in diminishing cell proliferation, survival and engraftment *in vivo* after cell transplantation (90).

1.3.4.4 Islet-1 cells

Laugwitz described a distinct subpopulation of cells expressing Islet-1 (Isl1), a LIM-homeodomain transcription factor which is expressed in cardiac progenitors and cardioblasts (91). Islet-1$^+$ cells are present in heart at low levels and do not express c-kit or Sca-1, but are capable of differentiation into fully functional cardiomyocytes, and express cardiac transcription factor Nkx2.5 and Gata4. However, these cells are present at a very low numbers, 500-600 per heart, which limits their use in cell therapy (92).

1.3.4.5 Epicardial-derived stem cells (EPDCs)

During heart development, a subset of epicardial cells delaminate from the epicardium and acquire a mesenchymal phenotype with superior migratory capability to enter the

subepicardium through a process called epithelial-mesenchymal transition (93). These migratory epicardial-derived cells (EPDCs) have the potential to give rise to various cell types including fibroblasts, coronary smooth muscle cells, endothelial cells (94) and cardiomyocytes (95).

Recently, Smart and coworkers found that EPDCs can be isolated from cultured epicardial explants using the potent stimulant thymosin-β4 (Tβ4), which releases the quiescent EPDCs from a state of dormancy and enhances extensive activation of EPDC migration, and differentiation into fibroblasts, smooth muscle and endothelial cells (96). By modulating Tβ4, human adult EPDCs can easily be isolated for cell therapy. Nonetheless, most evidence supports the notion that EPDCs are a source of progenitors of coronary vasculature during embryonic development, whereas the cardiogenic differentiation potency of EPDCs has yet to be fully unveiled.

In 2008, Zhou reported that EPDCs expressing Wilms' tumor 1 suppressor protein (WT1), predominantly differentiated into smooth muscle cells and, to a lesser extent, endothelial cells. Interestingly, they also found that 4% of the total cardiomyocytes in fetal heart were derived from Wt-1+ cells. Similarly, Cai and collegues reported that T-box transcription factor-18 (Tbx18)-expressing EPDCs contribute to the cardiomyocyte lineage during heart development (97). However, they failed to detect cardiomyogenic differentiation in postnatal and adult Tbx-18+ EPDCs under *in vitro* conditions. Moreover, intramyocardial injection of human EPDCs in immunodeficient mice caused significant improvement in infarcted mouse hearts after 6 weeks, but only a few engrafted cells were detected and none of them had differentiated into endothelial cells or cardiomyocytes (98). Hence, future research is required to support the cardiomyogenic potential of adult EPDCs for translation into therapy for myocardial infarction in humans.

1.3.4.6 Cardiospheres

In 2004, Messina and coworkers developed a method for isolating and culturing cardiac stem cells from mouse and human tissue explants (99). Explant-derived cells (EDCs) were selectively enriched for c-kit through the formation of cardiospheres, multicellular clusters that aggregated upon stimulation with several growth factors. They showed that the cardiosphere-forming cells were clonogenic, and expressed several stem cell markers including c-kit, Sca-1 and CD34. Mouse cardiospheres cultured in growth medium spontaneously differentiated into cardiomyocytes and contracted, confirming that these cells possess cardiomyogenic potency. Human cardiospheres were only seen to beat after co-culture with rat cardiomyocytes. Furthermore, immunostaining of cardiospheres revealed a heterogenous cell population containing cardiac stem cells, differentiated progenitor cells and cardiomyocytes.

A modified protocol has used cardiospheres as the cell source for extensive *ex vivo* expansion (100). These cardiosphere-derived cells (CDCs) expressed the stem cell marker c-kit, mesenchymal markers CD90 and CD105, and to a lesser extent, hematopoietic markers CD34 and CD31. CDCs from porcine and human heart were found to differentiate into electrically functional cardiomyocytes *in vitro* and improved function in the infarcted heart following CDC administration. The advantage of the wide feasibility and safety margin in the isolation and use of CDCs for heart regeneration therapy has led to a clinical trial in the United States (CADUCEUS: http://clinicaltrials.gov/ct2/show/NCT00893360).

1.4 SCALABILITY FOR CARDIAC CELL THERAPY

Although the precise mechanism is uncertain, most studies of endogenous cardiac stem cells (eCSCs) have shown attenuation of dysfunction after myocardial infarction. Cardiac stem cells can be isolated using magnetic or fluorescent cell sorting using specific cell-surface

markers, including c-kit, Sca-1 and Isl-1. Because these isolation methods yield relatively few cells (~2% per total heart cells) (Table 1.1), substantial *in vitro* expansion is required to generate sufficient cell numbers for therapy. This may preclude early administration of the therapeutic cells to myocardial infarcted patients, who are at risk of progressive heart remodelling. Alternatively, the generation of cells from tissue by explantation produces a reasonably high number of cells in a cell population. These cells are cardiogenic and, upon induction in a specific growth medium, c-kit^{+} cells can be enriched by the formation of cardiospheres. The main focus of this thesis centered on culturing cardiosphere-derived cells, given their advantages over the use of an homogenous stem cell population in terms of number of cells obtaining from the starting materials (heart tissue biopsies) by *in vitro* expansion (101), the time for expansion (100) and the therapeutic effect in treating infarcted myocardium (102). However, the growth of cardiospheres is slow in that ~45 days are needed to generate 1.7 ± 0.4 million CDCs, which precludes rapid treatment for acute MI patients. Hence, a method is required that can shorten the length of time needed to obtain sufficient cells for therapy, while preserving cellular stemness and differentiation capability.

Table1.1: Cell density of endogenous cardiac stem cells

Reference	Marker	Species	Cell density per heart
(28)	c-kit	Adult rat	0.01%
(79)	c-kit	Adult human	20,000 cells/cm3 (border region) 40,000 cells/cm3 (remote region)
(103)	c-kit	Adult dog	0.006%
(104)	Sca-1	Adult mouse	2.1%
(105)	Sca-1	Adult mouse	0.3%
(104)	ABCG2	Adult mouse	0.03%
(106)	ABCG2	Neonatal rat	2%
(106)	ABCG2	Adult rat	1.2%
(107)	ABCG2	Adult mouse	1%
(108)	Islet-1	1 day neonatal rat	Negligible

Sca-1; stem cell antigen-1

C-kit and Sca-1 are among the common markers used to identify endogenous cardiac stem cells and these markers were found within the cardiosphere-derived cell population (100, 101, 109). As there is no Sca-1 antibody available for immunolabelling, c-kit was used as the only stem cell marker analysed for the culture optimization experiments described in this thesis.

1.5 *IN VIVO* CELL TRACKING

The therapeutic effects of stem cells are directly related to the cell retention, migration, engraftment, long-term viability and subsequent cell fate after administration. In order to determine the best cell type for therapy, cell tracking studies are needed. Many different imaging modalities have been designed and established for *in vivo* tracking of stem cells.

The most straight-forward method for examining cell migration, engraftment and fate after injection is to perform histological microscopy. Implanted cells are pre-labeled with green fluorescent protein, or a reporter transgene, such as LacZ (36, 110). These cells can be tracked by dissecting the target tissue, and processed with immuno-fluorescent labelling, which can then be visualized using a fluorescence microscope. This technique permits identification of cell engraftment, as well as differentiation after engraftment in the target tissue. However, this method requires sacrifice of the subject followed by whole organ removal for tissue processing, which disallows long-term evaluation of injected cells, or requires a large number of animals for statistical significance.

Radioactive tracers such as ^{111}In-oxyquinoline (^{111}In) and ^{99m}Tc-hexamethylpropylene amine oxime (^{99m}Tc), are clinically approved radionuclides. Imaging of radioactive isotopes can be achieved by positron emission tomography (PET) or single photon emission computed tomography (SPECT). Direct cell labelling with radionuclides allows measurement of biodistribution of intravenously infused cells plus tracking in the myocardium. However, this

method can only be used for short-term tracking, due to short isotope half-life (e.g. ^{111}In 1/2t= 2.8d), and may compromise cellular function as a result of radiation exposure (111).

1.5.1 Magnetic resonance imaging (MRI)

In vivo MRI has become the gold standard for imaging heart function. MRI is a non-invasive procedure and it provides three dimensional imaging with high spatial resolution and soft tissue detail. The principle of MRI lies in the polarization of a spinning proton in a sample in an applied magnetic field, forming a net magnetization of the sample. The application of a short pulse of radio frequency energy, perpendicular to the main magnetic field, allows energy transfer from an RF pulse to the spinning protons at the same frequency, creating a resonance. The intensity of the MR signal is affected by two types of proton spin relaxation: T1 and T2 relaxation. T1 (also called longitudinal or spin-lattice relaxation) describes the exponential decay of signal intensity after the RF pulse as proton spins relax back to equilibrium. While T2 (transverse, or spin-spin proton relaxation) describes the process of signal dephasing (loss of proton coherence) in the transverse plane, which is perpendicular to the main magnetization. Generating a gradient of magnetization across the sample and altering proton precession frequency in a predetermined manner allows acquisition of MR signals encoded with spatial resolution. These signals can be transformed to reveal the spatial characteristic of the sample using two-dimensional Fourier transformation (112).

1.5.2 MR contrast agent for cell labelling

Cell labelling for MRI enables accurate localization of transplanted cells in the imaged tissue and allows serial monitoring of cell engraftment and viability over long-term follow up. To achieve this, cells must be labelled with an MR contrast agent, which is incorporated into stem cells and generates sufficient signal for detection. The contrast agent may act by affecting the longitudinal (T1) or the transverse (T2) relaxation time of the neighbouring

water or lipids, and thereby influence the endogenous magnetic homogeneity. This allows the area containing the contrast agent to be clearly discriminated from the tissue background. There are two types of contrast agent commonly used for cell labelling and MR imaging: negative contrast (T2/T2* based) agent and positive contrast (T1-based) agent.

1.5.2.1 MR negative contrast agent

A negative contrast agent produces signal voids or hypointensities in MR images by shortening spin-lattice (T2/T2*) proton relaxation. Superparamagnetic iron oxide particles are the most widely used negative contrast agent for *in vivo* stem cell tracking and most of the superparamagnetic formulations are biocompatible, with many studies showing that iron particles do not alter cellular viability and function (113). Micron-sized particles of iron oxide (MPIO) can be used to label mesenchymal stem cells that can be tracked *in vivo* for up to 16 weeks (54, 114). Cells can be tracked in the mouse or pig (115-117) heart using MRI, with smaller superparamagnetic iron oxide nanoparticles (SPIO). In addition to *in vivo* imaging and cellular tracking, the magnetic properties of iron particles can facilitate re-isolation of transplanted cells (114), or improve engraftment by magnetic targeting with an external magnet, following cell injection (118).

1.5.2.2 MR positive contrast agent

Gadolinium (III) (Gd^{3+}) chelates differ from iron particles as they shorten T1 longitudinal relaxation, thereby increasing the MR signal and appearing bright in T1-weighted MR images. Gadolinium-diethylene-triamine penta-acetic acid (Gd-DTPA) is the first FDA approved contrast agent for clinical MRI applications, for angioplasty or to visualise regions of hypo-perfusion and to identify the necrotic region in the infarcted myocardium. Evaluation of phantoms using Gd-DTPA, or other Gd^{3+} chelates including gadonantubes, for stem cell labelling, has been mainly performed using clinical MR scanners (1.5 Tesla) (119, 120). Only

a few studies described cell labelling using other Gd^{3+} based contrast media, such as gadolinium hexanedione nanoparticles (121) or gadofluorine (122), have used at higher magnetic field strength (3 T and 9.4 T, respectively).

Pre-clinical cell tracking using small animals is typically performed at high magnetic field strength (e.g. 7 T, 9.4 T and 11.7 T). Dominant relaxation mechanisms are often different at different field strengths and a simple extrapolation of the behaviour of contrast media is not possible. Therefore, the validity of using contrast media, which have been shown to give MR signal at low field, needs to be tested at high field.

The main objectives of this thesis were:

1. To establish protocol modifications to isolate, expand and characterize cardiosphere-derived cells *in vitro* for testing in the infarcted rat heart.
2. To evaluate the effect of cardiac-relevant extracellular matrices on explant cell migration, cardiosphere growth and CDC proliferation, adhesion and clonogenicity, and examine the changes in the number of c-kit expressing cardiac stem cells in CDCs.
3. To test the validity of using MR positive contrast agent, gadolinium-DTPA, and gadonanotubes for stem cell tracking at 11.7 Tesla.

Chapter 2

General Methods

GENERAL METHODS

2.1 ANIMALS

All protocols involving live animals were reviewed and approved by an Institutional Animal Care and Use Committee (IACUC), the Home office and conformed to government regulations for the care and use of laboratory animals (Home office licence: 30/2278). Sprague Dawley (SD) rats were obtained from a commercial breeder (Harlan, UK) and kept under controlled conditions of temperature, light and humidity, with *ad libitum* access to rat chow and water. Neonatal SD rats (1-2 days) were used in all cell culture optimization experiments described in *Chapter 3* except for the *in vivo* study and post-study histology examinations, in which the cell source was from 1-2 day-old neonatal SD-Tg(GFP)2BalRrrc rats (Rat Resource and Research center, US) ; whereas in *Chapter 4* and *Chapter 5*, 5-week-old SD rats (Harlan, UK) were used.

2.2 HEART TISSUE EXPLANTATION

Sprague Dawley rats (neonatal; 1-2 days, young; 5 weeks) were sacrificed under schedule one and the hearts were rapidly excised using sterile scissors and placed in a petri dish filled with sterile Dulbecco phosphate buffered saline (DPBS; Invitrogen, UK). The heart was cut into several pieces and rinsed with DPBS to remove excess blood, as blood inhibits cell growth. The heart tissue was digested using 0.05% trypsin (Invitrogen, UK) and minced further into small pieces (1 - 1.5 mm^3) for 3 minutes. Then, 2 ml of cardiac explant medium (CEM, see Appendix 1) was added to the tissue to neutralize trypsin activity. Approximately 30-35 explants were plated on a fibronectin-coated dish containing 1.5 ml pre-warmed CEM. The distance between explants was kept to 0.5 - 1 cm. Explants adhered to the petri dish overnight and cells started migrating out from the explants after 1 to 2 days. The CEM was topped up to

2 ml the day after plating and refreshed every 2 days. Explant-derived cells reached 80-90% confluency after 7 days.

2.3 CULTURE OF CARDIOSPHERES FROM EXPLANT-DERIVED CELLS

Cardiosphere growth medium (CGM) was prepared using growth factor/cytokine stock solutions (Appendix 1). Each confluent dish of explants was washed twice with 2 ml DPBS and once with 1 ml Versene (Invitrogen, UK). The supernatant was saved in a 15 ml centrifuge tube to prevent loss of loosely adherent phase-bright cells. Explant-derived cells (EDCs) were dissociated using 0.05% trypsin and centrifuged at 1300 rpm for 3 minutes to form a cell pellet, which was then resuspended in 2 ml of fresh CGM. Cells were counted, using the haemocytometer under the inverted light microscope (Nikon, UK), and diluted to a density of 1 x 10^5 cells/ml. About 3 x 10^4 cells per 300 µl were dispensed into each well of a 24-well plate coated with poly-D-lysine (Sigma, UK).

2.4 CARDIOSPHERE ISOLATION AND CARDIOSPHERE-DERIVED CELL CULTURE AND EXPANSION

Cardiospheres, formed after 4 days in culture, were harvested and gently dissociated using a 1 ml Gilson pipette, and then centrifuged. The cell pellet was resuspended in 7 ml of CEM and transferred to a fibronectin-coated 25 cm^2 cell culture flask (Corning, UK). Cardiosphere-derived cells were maintained at 37^oC with 5% CO_2. The medium was replaced with fresh medium every 3 days. CDCs were trypsinized and split into two when the cells reach 80-90% confluency.

2.5 CULTURING CARDIOSPHERES IN HANGING DROPS

Isolated EDCs were centrifuged for 5 minutes at 1300 rpm, after which cells were resuspended in CGM at a final concentration of 2 x 10^4 cells/ml. EDCs were plated at 500 cells/25 µl in droplets on non-treated 60 mm x 15 mm petri dishes. A few droplets of PBS (10 µl) were placed on the inner side of the cover to increase the humidity inside the dish. The plates were flipped to invert drops and maintained at 37^{o}C in a 5% CO_2 incubator for 3 days.

2.6 CELL VIABILITY AND PROLIFERATION ASSAYS

2.6.1 MTT viability assay

The yellow tetrazolium salt, 3-(4, 5-dimethylthiazolyl-2)-2, 5-diphenyltetrazolium bromide, MTT (Sigma, UK), assay is commonly used to determine cell proliferation and viability (123); cleavage of the tetrazolium ring requires mitochondrial dehydrogenase activity and produces purple MTT formazan crystals, which are insoluble in water but can be dissolved in dimethylsulfoxide (DMSO; Sigma, UK). The number of viable cells correlates directly with the amount of MTT formazan formed, which can be measured by reading the absorbance at 544 nm.

MTT powder was dissolved in phenol red-free IMDM (5 mg/ml) and sterile-filtered using a 0.2 µm syringe-driven filter (Millipore, UK). CDCs were cultured in a sterile 24-well plate (0.5 ml per well) at a starting density of 5,000 cells/well. At the indicated time, 50 µl of 5 mg/ml MTT was added directly to each well and the cells were incubated at 37^{o}C in 5% CO_2. After 4 hours, the medium was removed and the formed tetrazolium salt was dissolved in 500 µl DMSO. The absorbance of the purple MTT formazan was measured at 544 nm using a fluorescence microplate reader (Fluostar OPTIMA, BMG Labtech, UK). Cell viability was expressed as the ratio of labelled cells to unlabelled cells.

2.6.2 AlamarBlue ® Cell proliferation assay

AlamarBlue® (Serotec, UK) is reduced within cells to yield a pink solution. The primary advantage of using AlamarBlue® is that it does not interfere with the reactions of the electron transport chain, and thus allows cells to remain viable after the experiment is performed. Passage 2 CDCs were seeded onto a 96-well plate at a density of 5,000 cells/ml in CEM and allowed to adhere overnight. The cells were washed three times with sterile PBS and incubated with 10% AlamarBlue® in phenol-red free Iscove's modified Dulbecco's medium (IMDM; Invitrogen, UK) at 37^{o}C for 4 h, after which the fluorescence of the reduced AlamarBlue® was read at an emission wavelength of 590 nm (Fluostar Optima, BMG Labtech, UK). A standard curve was created from serial dilution of CDCs starting at 5000 cells per well of 96 well plate) (Figure 2.1), and the relative fluorescence intensities obtained after 4 hours AlamarBlue® incubation.

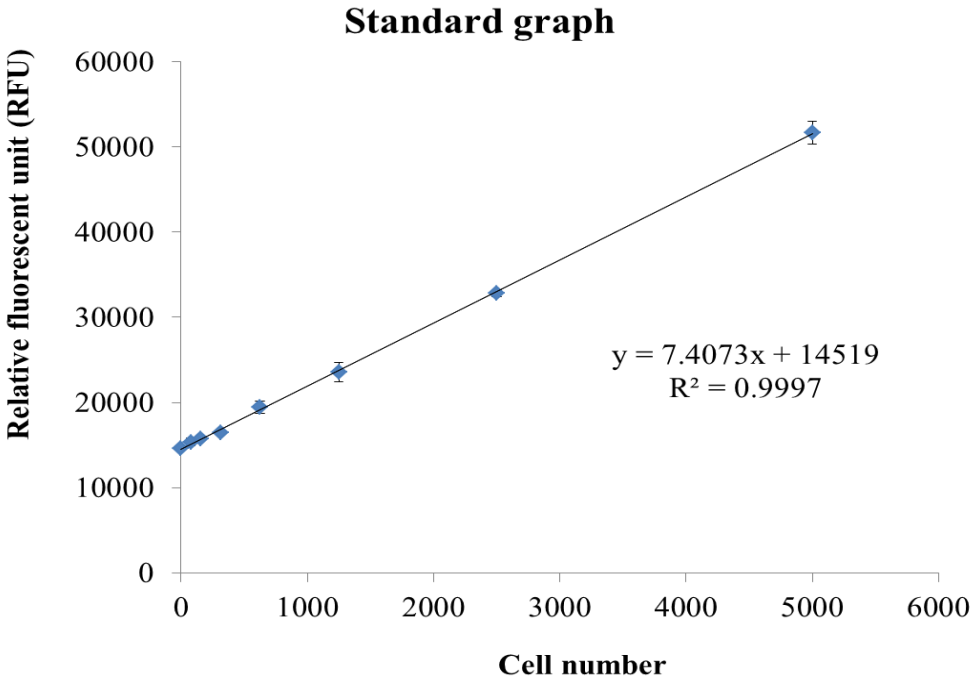

Figure 2.1: Standard graph for AlamarBlue ® Cell proliferation assay. Relative fluorescent intensity of 0, 78, 156, 313, 625, 1260, 2500 and 5000 cells were measured after 4 hours incubation with AlamarBlue ® at 37^{o}C. Values are presented as mean of 3 sample replicates. Relative cell number of test sample was calculated based on the equation obtained from the standard.

2.6.3 LIVE/DEAD assay

The LIVE/DEAD cell cytotoxicity kit (Molecular Probes, UK) uses calcein-AM, and ethidium homodimer-1, to measure live and dead cells, respectively. Calcein-AM (1 μM) and ethidium homodimer-1 (1 μM) were freshly prepared and made up in serum-free, phenol red-free IMDM for each experiment. At the indicated time, CDCs were washed three times in PBS and then stained with freshly prepared Calcein-AM and ethidium homodimer for 30 minutes at room temperature. Cell viability was directly assessed by counting all cells within each well using a fluorescence microscope (CETI).

2.7 CELL ADHESION ASSAY

Passage 2 CDCs were seeded at a density of 50,000 cells/ml in 96 well plates. Cells were washed three times with PBS to remove non-adherent cells after 5 hours. Media was replaced with serum-free IMDM containing AlamarBlue® (10% v/v) to measure the number of adhered cells. Plates were incubated at 37^{o}C for 4 hours prior to reading fluorescence, as described in Section 2.6.2. Cell adhesion was expressed as the ratio of fluorescent intensity of test samples (coated with extracellular matrix) to control samples (uncoated plates).

2.8 WESTERN BLOTTING

Whole cell lysates were used for the measurement of α-ketoglutarate dehydrogenase, glucose transporter-1, glucose transporter-4, and PPAR-γ coactivator 1-α protein levels using western blotting. A general description of the blotting technique is outlined below, with variations for the individual proteins described in Table 2.4.

2.8.1 Preparation of lysates

Approximately 50 mg of powdered frozen heart tissue was added to an equal volume (w/v) of lysis buffer (see Appendix 2) and homogenized using a Polytron homogenizer. For preparing cell lysate, cells from a single confluent flask were mechanically lysed in 500 µl lysis buffer supplemented with protease inhibitor cocktails (Roche, UK) using a 21 gauge needle. Lysates were boiled for 5 min and clarified by centrifugation at 13,000 rpm for 10 min. The pellets were discarded and protein concentrations of the supernatants were determined using a Bradford protein assay kit. β-mercaptoethanol (5% v/v; Sigma, UK) was added to the remaining supernatant, followed by boiling for 5 min and storage at -80 ^{o}C.

2.8.2 Polyacrylamine gel electrophoresis and protein transfer

Equal concentrations (20 µg for tissue lysates, 50 µg for cell lysates) of protein were diluted in Laemmli loading buffer (Appendix 2) and loaded onto 12.5% polyacrylamide gels. Gels were run at 120 V for approximately 2 h. A piece of Immobilon-P membrane (Millipore, UK) and two pieces of extra thick chromatography paper (BioRad, UK) were cut to the same size as the gel. These were soaked with the gel for 30 min in SDS transfer buffer (Appendix 2), layered onto the semi-dry transfer apparatus (Biorad, UK) and transferred at 0.07 A per gel for 1 h. The membranes were stained with Ponceau S stain (Sigma, UK) to determine successful protein transfer and even protein loading. Blots were washed in TBS-Tween (Appendix 2) and blocked in 5% (w/v) dried milk powder in TBS-Tween for at least 1 hour.

2.8.3 Immunoblotting, detection and band quantification

Membranes were washed for 1 h in TBS-Tween, with the solution changed every 15 min. The specific primary antibody was diluted in 5% (w/v) dried milk powder in TBS-Tween, and incubated with the membranes (see Table 2.4). The membranes were then washed for 2 h in TBS-Tween, with the solution changed every 15 min. The appropriate horseradish

peroxidase-conjugated secondary antibody was diluted in 5% (w/v) dried milk in TBS-Tween, and added to the incubated membrane (see Table 2.4). Membranes were washed for a further hour in TBS-Tween, with the solution changed every 15 min. The membrane was covered in enhanced chemiluminescence (ECL) detection solution (Amersham, UK) and sandwiched between acetate sheets. Membranes were exposed to X-ray film and developed using a Compact X4 automatic X-ray film processor (X-ograph Imaging systems, UK). Protein bands were quantified using Un-Scan-It, Version 6.1 (Silk Scientific, USA).

2.9 TISSUE SECTIONING

Heart tissue was embedded in Optimal Cutting Temperature (O.C.T.) compound (Miles Scientific, UK) and kept frozen at -20^{o}C until blocks were sectioned on a cryostat (10 µm) (Leica Microsystem, UK), and carefully placed on a cold slide. The slide was fixed with chilled 2% paraformaldehyde (Sigma, UK) for 10 minutes at room temperature. After fixation, the tissue was permeablized (using PBS with 0.1% Triton and 0.1% Tween) and blocked with 10% donkey serum (Biosera, UK) for 30 minutes. The immuno-staining procedure was similar to that for staining of cells, as described in Section 2.10.3.

2.10 IMMUNOCYTOCHEMISTRY

Cell phenotypes were characterized using the expression of surface markers and intracellular proteins. A general description of this technique is outlined below, with the relevant antibodies and dilution factors listed in Table 2.1.

2.10.1 Culture of CDCs on chamber slides

About 3-5 x 10^4 rat CDCs per 500 µl CEM were grown on a 4-well chamber slide (Nunc® Lab-Tek® Chamber Slide™ system, UK) pre-coated with 10 µg/ml fibronectin (Sigma, UK).

The chamber slide was then placed in the incubator for 4-6 hours to allow cell adhesion prior to fixation.

2.10.2 Cell fixation, permeabilization and blocking

CEM was removed from the chamber slides, which were washed three times with sterile DPBS. The cells were fixed by filling each well with cold 4% paraformaldehyde (PFA; Sigma, UK), left on ice for 20 minutes, and then washed three times with washing solution containing PBS with 0.1% Tween for 5 minutes, each on a rotating/shaker platform at 30 rpm. The fixed cells were permeabilized with PBS containing 0.1% Tween and 0.1% Triton-X100 for 10 minutes at room temperature. Cells were not permeabilized when staining for surface markers, such as CD117. After washing the cells three times for 5 minutes with PBS containing 0.1%Tween on a rotating/shaker platform at 30 rpm, each well was incubated with blocking solution (10% normal donkey serum (Biosera, UK) in 0.1% PBS-tween) for an hour at room temperature.

2.10.3 Primary antibody incubation, secondary antibody labelling, DAPI staining and mounting

Primary antibody was diluted in PBS according to the dilution factors shown in Table 2.1. The blocking solution was aspirated and the well was covered with the diluted primary antibody solution (~300 µl/well). The chamber slides were incubated at 4^{o}C overnight in an humidified chamber. The cells were washed gently with PBS, three times for 5 minutes, on a rotating/shaker platform at 30 rpm. An appropriate secondary antibody solution (Table 2.1) was added to each well and plates were incubated at 37^{o}C for an hour. Nuclei were stained by covering each well with 1 µg/ml DAPI solution (Sigma, UK) for 14 minutes at room temperature in an humidified chamber protected from sunlight. Slides were mounted by putting a drop of Vectashield mounting medium (Vector laboratories, UK) on each well/rectangle and covering the sample with a 22 x 50 mm cover glass.

2.10.4 Confocal Microscopy

All immuno-labelled samples were imaged using Zeiss LSM META 510 confocal laser scanning microscope. The laser power was kept to a minimum and the image contrast was optimized by adjusting the gain. The pinhole was set to ~1 to minimize background signal. Scanning was performed in 8-bit multi-track scan mode and a 1024 x 1024 pixel image was generated. Type of lasers and filters used are listed in Table 2.5. All Images were processed using Zeiss LSM image browser software.

2.11 FLOW CYTOMETRY

CDCs in T75 flasks were digested with 3 ml trypsin for 3 minutes at 37^{o}C after washing twice with PBS. The cells were collected in centrifuge tubes and resuspended in incubation medium (DPBS with 0.5% BSA (Sigma, UK), 2 uM EDTA (Sigma, UK) and 1% penicillin/streptomycin (Invitrogen, UK)), and then spun at 2,000 rpm for 5 minutes. The cell pellets were resuspended in the incubation medium, and diluted to 5 x 10^5 cells in 1.5 ml eppendorf tubes. The suspended cells were stained with primary antibody, at the dilutions shown in Table 2.2, and rotated at 4^{o}C for an hour in the dark. After the primary antibody incubation, the cells were washed once with incubation medium and counterstained with Alexa Fluor-488 secondary antibody at 4^{o}C for an hour in the dark. The labelled CDCs were washed once again to remove excessive secondary antibody and resuspended in 500 µl buffer and analysed using FACS Calibur (BD). The results were analysed using CellQuestPro software.

2.12 CARDIOMYOGENIC DIFFERENTIATION

CDCs (10,000) were seeded in 6-well plates coated with 0.1% gelatin and incubated with CEM overnight. The medium was changed to cardiomyocyte differentiation medium (see

Appendix 1). The medium was changed every two days. The experiment was terminated at day 5.

2.13 CLONOGENIC ASSAY

CDCs were prepared in a suspension of about 50 cells per 10 ml of CEM. The cells were mixed and seeded (100 µl) onto a 96-well plate using a multichannel transfer pipette. The plated cells were incubated at 37^{o}C for 30 minutes. Wells containing a single cell were identified under a light microscope. Wells with more than one cell or no cells were disregarded. Clones were allowed to grow for 20 days and the clones derived from a single cell were counted. Six of the identified clones were randomly picked and trypsinized separately to expand in a 6-well plate to confirm the cell clonogenicity. Clonal efficiency was counted using the following formula:

$$\textbf{Clonal efficiency}\ (\%) = \frac{\textbf{total wells with clone}}{\textbf{total wells with single cell}}\ \ \textbf{x 100}$$

2.14 CELL LABELING FOR MR EXPERIMENTS

2.14.1 MPIO and CellTracker™ CM-DiI labeling

Passage two CDCs at 80-90% confluency in 75 cm^2 flasks were labelled with micron-sized particles of iron oxide (MPIO: 2 µl/cm^2, encapsulated magnetic microspheres; Bangs, Fishers, IN) in CEM overnight. MPIO-CDCs were washed twice with PBS and stained with CellTracker™ CM-DiI (Molecular Probes, UK) in PBS for 30 minutes before trypsinization. Approximately 2 x 10^6 cells were prepared in 50 µl IMDM for *in vivo* cell therapy.

2.14.2 Gadolinium-DTPA labeling (Gd-DTPA)

Cells were cultured in six well plates (35 mm in diameter) at a density of 5 x 10^5 cells per well in 2 ml serum-free IMDM. Gd-DTPA was transfected into cells by using calcium-phosphate precipitation. Gd-DTPA (50 µl 0.5 M) was precipitated with 60 µl $CaCl_2$ (0.25 M), 10 µl H_2O and 120 µl phosphate solution (2xBBS: 50 mM BES (pH 6.96), 280 mM NaCl, 1.5 mM Na_2HPO_4). CDCs were incubated with the transfection-Gd-DTPA complexes for 4 hours at 37^{o}C under 5% CO_2.

2.14.3 Gadonanotube labeling

Gadonanotubes were provided by Lon J. Wilson, Rice University, US. CDCs were cultured with gadonanotubes in CEM for 24 hours under standard cell culture conditions (37^{o}C and 5% CO_2). Then the cells were washed with phosphate buffered saline (1×PBS) and gently stripped using ice-cold acid strip buffer solution (50 mM glycine-HCl, 100 mM NaCl, and 2 mg/mL polyvinylpyrrolidone at pH 3.0) for 10 min at 4 °C. The stripping buffer was removed; the cells were washed with 1×PBS and trypsinized for 3 minutes. The labeled cells were then passed through a 100 µm nylon filter to remove large cell-gadonanotube aggregates and the filtrate was collected in 50 ml centrifuge tubes.

2.15 MR PHANTOM STUDY (IN COLLABORATION WITH DR PHILIP LEE)

Labelled CDCs were washed three times with PBS to remove excessive extracellular contrast agent. The cells were centrifuged in a 1.5 ml tube and diluted to the indicated cell number in a 200 µl PCR tube, topped with 2 % agar solution in DMEM/F12. MRI was performed in a vertical bore 500 MHz, 11.7 Tesla MR system with a Bruker console and a birdcage coil (60 cm). MR images of phantoms GD-DTPA and gadonanotube-labeled samples were acquired in a vertical plane using T1-weighted gradient recalled echo sequence (T1W-GRE) with a matrix

of 256 x 256 pixels, 1.5 mm thickness and a field of view (FOV) of 25.6 x 60 mm, with a repetition time (TR) of 4500 ms, and a echo time (TE) of 1.7 ms.

2.16 RAT MYOCARDIAL INFARCTION AND CDC ADMINISTRATION (PERFORMED BY DR CAROLYN CARR AND DR DANIEL STUCKEY)

The left anterior descending (LAD) coronary artery of female SD rats (200-250 g, n = 14) was occluded using the method of Michael *et al* (124). In brief, following anaesthesia and thoracotamy, the pericardium was removed and a 5-0 prolene suture was placed under the LAD, about 2 mm from the origin. The suture was tied around a small piece of PE tubing, occluding the LAD, and the chest closed. After 50 minutes, the chest was re-opened and the tubing removed to allow reperfusion. Ten minutes after ischaemia/reperfusion, CDCs (2×10^6 in 50 µl CEM; n = 7) or control medium (50 µl CEM; n = 7) were injected in the peri-infarct region. Two days after MI, a bolus of CDCs (4×10^6 in 500 µl CEM) or control medium (500 µl CEM) was administered *via* the tail vein. In sham operated animals (n = 3), the thoracotamy was performed, but no stitch was placed in the heart, and the chest was closed.

2.17 CARDIAC CINE MRI (PERFORMED BY DR CAROLYN CARR AND DR DANIEL STUCKEY)

Cardiac cine MRI was performed as described (125). Briefly, rats were anaesthetised with 2.5% isoflurane in O_2, positioned supine in a purpose built cradle and lowered in a 60 mm birdcage coil in a vertical bore 500 MHz, 11.7 T MR system with a Bruker console running Paravision 2.1.1. A stack of 7-8 contiguous 1.5 mm true short axis ECG-gated cine images (field of view 51.2 mm^2, matrix size 256 x 256 zero filled to 512 x 512 giving a voxel size of 100 x 100 x 1500 µm, echo time/repetition time (TE/TR) 1.43/4.6 ms, 17.5° pulse, 25-35 frames per cardiac cycle) were acquired to cover the entire left ventricle. The end diastolic and end systolic volumes were measured for each slice using Image J (126) and summed over

the whole heart. Stroke volume was calculated as end diastolic volume minus end systolic volume. The ejection fraction was calculated as the stroke volume divided by the end diastolic volume. The relative infarct size was calculated from the average of the endocardial and epicardial circumferential lengths of the thinned, akinetic region of all slices, measured at diastole, and expressed as a percentage of the total myocardial surface (127). Wall thickness of the peri-infarct (myocardium adjacent to infarct where contraction was observed) and posterior regions of the myocardium were measured in a mid-papillary slice.

2.18 STATISTICAL ANALYSIS

Data were presented as mean ± standard deviation (SD). All statistical analysis was performed using the SPSS software package. Statistical differences between two groups were analysed using a student t-test, whereas multiple comparisons were analysed using a one-way analysis of variance (ANOVA). Tukey post hoc test was used to analyse statistical difference between groups. Significance was set at $P < 0.05$.

Table 2.1: List of antibodies used for immunocytochemistry

Antibody	Manufacturer	Applications (dilution)	Secondary antibody (dilution)
c-kit	Santa Cruz	1:50	AF488 Donkey anti rabbit (1:1000)
Nkx2.5	R&D	1:50	AF488 Donkey anti goat (1:1000)
Troponin I	Santa Cruz	1:100	AF488 Donkey anti rabbit (1:1000)
Troponin T	Abcam	1:200	AF488 Donkey anti mouse (1:1000)
Myosin heavy chain	Abcam	1.:200	AF488 Donkey anti mouse (1:1000)
Klf-4	Santa Cruz	1:50	AF488 Donkey anti rabbit (1:1000)
Sox 2	Santa Cruz	1:50	AF488 Donkey anti goat (1:1000)
Oct 3/4	Santa Cruz	1:50	AF488 Donkey anti rabbit (1:1000)
Smooth muscle actin	Sigma	1:200	AF488 Donkey anti mouse (1:1000)
α-sarcomeric actin	Sigma	1:500	AF488 Donkey anti mouse (1:1000)
Von-Willebrand Factor	Chemicon	1:50	AF488 Donkey anti mouse (1:1000)

Table 2.2: List of antibodies used for flow cytometry

Antibody	Manufacturer	Applications (dilution)	Secondary antibody (dilution)
c-kit	Santa Cruz	1:20	AF488 Donkey anti rabbit (1:1000)
CD45-FITC	BD Bioscience	1:50	-
CD90	BD Bioscience	1:100	AF488 Donkey anti mouse (1:1000)
DDR2	Santa Cruz	1:20	AF488 Donkey anti goat (1:1000)

Table 2.3: List of antibodies used for immunohistochemistry

Antibody	Manufacturer	Applications (dilution)	Secondary antibody (dilution)
GFP	Abcam	1:50	AF488 Donkey anti rabbit (1:1000)
Troponin I	Santa Cruz	1:100	AF488 Donkey anti rabbit (1:1000)
CD68	Abcam	1:200	AF633 Donkey anti mouse (1:1000)

Table 2.4: List of antibodies used for western blotting

Antibody	Manufacturer	Applications (dilution)	Secondary antibody (dilution)
Glucose transporter-1	Santa Cruz	1:500	HRP Goat anti rabbit (1:1000)
Glucose transporter-4	University of Bath, Bath, UK*	1:4000	HRP Goat anti rabbit (1:1000)
α-ketoglutarate dehydrogenase	Santa Cruz	1:500	HRP Goat anti rabbit (1:1000)
PPAR-γ coactivator-1α	Santa Cruz	1:500	HRP Goat anti rabbit (1:1000)

**antibody was received as a gift from Professor Geoff Holman (University of Bath, Bath, UK)*

Table 2.5: Lasers and filters used for confocal microscopy

Fluoresence dye/probes	Peak excitation wavelength (nm)	Peak emission wavelength (nm)	Laser	Filter
DAPI	364	454	Diod (405)	BP 420-480
Propidium Iodide	545	615	HeNe1 (543)	BP 420-480
Alexa Fluor 488	495	519	Argon (488)	BP 420-480
Alexa Fluor 594	590	613	HeNe1 (543)	BP 420-480
Alexa Fluor 633	633	647	HeNe2 (633)	BP 420-480

Chapter 3

Cardiac stem cell characterization from explant tissue

3.1 ABSTRACT

Cardiac-derived stem cells (CSCs) have the potential to repair damaged heart tissue. However, they may be of more benefit if administered as soon as possible after infarction. To date, more than one month has been required to culture sufficient CSCs for therapy. Hence, this chapter describes the isolation, characterization and culture optimizations of CSCs. Optimal cardiosphere growth conditions were determined, and plating 3×10^4 EDCs per well of a 24-well plate coated with 16.7 µg/ml poly-D-lysine, in CGM containing 7% serum, improved cardiosphere production and generated 1.5×10^7 CDCs in 16 days, sufficient for cell therapy. Rat neonatal cardiosphere-derived cells (CDCs), cultured using this protocol, contained stem cells expressing pluripotent markers Oct 3/4, SOX2, and Klf-4, and cardiac differentiation markers GATA4 and Nkx2.5. These cells co-existed with differentiated cells exhibiting α-sarcomeric actin, smooth muscle actin, and von Willebrand factor. Flow cytometry revealed that only 3% CDCs expressed c-kit, and 71% expressed CD90, resembling a more mesenchymal phenotype. CDC proliferation was enhanced by culturing in 11.7 mM and 22.8 mM glucose. Western blot analysis showed that the uptake of glucose in CDCs was regulated by glucose transporter-1. CDCs were labelled with CellTracker™ CM-DiI and iron oxide (MPIO) to track CDCs using *in vivo* MRI. Proliferation and sphere formation of labelled CDCs remained the same as that of unlabelled CDCs over 4 days. Cells engrafted and were retained in the infarcted myocardium for 16 weeks. CDC treatment improved left ventricular ejection fractions by 9% and prevented the peri-infarct wall from thinning. In conclusion, modifications were made in the culture protocol to allow isolation and expansion of sufficient CDCs from neonatal rat hearts for therapy in 16 days. MPIO labelling did not alter CDC proliferation or cardiosphere-forming capacity, making them suitable for *in vivo* cell tracking using MRI.

3.2 INTRODUCTION

Various markers have been used to identify putative cardiac stem cells, including c-kit, Sca-1and Isl-1. Methods of isolation have been reported using magnetic (128), or fluorescent cell sorting (129), or both (28, 84), or by single cell clonogenic amplification (130). However, as the number of stem cells present in the heart is small, isolation based on specific cell surface markers yields relatively few cells and requires substantial *in vitro* expansion to generate sufficient cell numbers for therapy. This is important, as the efficacy of cell therapy appears to be directly related to the number of cells grafted and inversely correlates with time of cell delivery after reperfusion therapy post infarction (131, 132).

Messina et al. (2004) developed a tissue explant culture technique and expanded cells via the formation of cardiospheres using defined growth factors. The resulting cells expressed the stem cell marker, c-kit (CD117), the mesenchymal marker, Thy-1 (CD90), and one of the components of transforming growth factor receptor-β complex important in angiogenesis, endoglin (CD105). Later, Smith et al. (2007) adapted the technique, expanding cardiospheres to cardiosphere-derived cells (CDCs) as a monolayer and generated 2 $x10^6$ human CDCs over 45 days, with the cells expressing CD117 (c-kit), CD90, CD105, CD34 and CD31.

Several studies have shown that nutrient levels in the medium and the cell metabolic characteristics can alter stem cell proliferation and function (133). High glucose (20-30 mM) and fatty acids promote embryonic stem cell (ESC) proliferation (134, 135). However, others have reported that high glucose attenuated VEGF expression in rat bone marrow stem cells (136), and reduced the invasiveness of circulating endothelial cells (137). This suggested that nutrient concentration and availability could influence cell metabolic phenotype and behaviour. In addition, a change in mitochondrial mass and activity may be related to cell

‘stemness’ state and differentiation (138), also demonstrated in ESCs (139) and induced pluripotent stem cells (140).

As energy metabolism is implicated in stem cell function and fate, it is valuable to understand stem cell energetics involved in cell expansion and differentiation. The role of substrate metabolism in CSC proliferation and differentiation has yet to be investigated and may provide useful insights for optimizing cell growth and function *in vitro*. Furthermore, studying CSC metabolism may prove especially useful when isolating CSC from heart failure patients, who have altered cardiac metabolism (141).

Here, glucose metabolism in cardiosphere-derived cells (CDCs) was evaluated and the effects of various glucose concentrations on CDC proliferation and metabolic phenotype were examined. Modifications were made to Smith’s technique (100) to culture heart explants from neonatal rat hearts and generate therapeutically relevant numbers of cells, without compromising the original cellular phenotype, properties and function. To do this, cardiosphere growth was optimized and the cultured CDCs were characterized, tested *in vitro*, and the functional benefits were further confirmed *in vivo* using a rat model of myocardial infarction.

3.3 METHODS

The study design described in this chapter is illustrated in a simplified flow diagram (Figure 3.1). Specific experimental methodologies are described below.

3.3.1 Isolation, expansion and characterization of cardiosphere-derived cells

Explant-derived cells were isolated from 1-2 day old neonatal Sprague Dawley (SD) rat hearts. For the *in vivo* study, EDCs were obtained from 1 day old neonatal SD-Tg(GFP)BalRrrc rat hearts expressing green fluorescent protein. Cardiosphere-derived cells (CDCs) were generated from EDCs according to Smith's protocol (100), with modifications. All experiments in this chapter were performed using Passage 2 CDCs, unless stated otherwise. Phenotypic characterization of CDCs was assessed using immunocytochemistry and/or quantitative flow cytometry, to identify stem cell markers (c-kit, Oct3/4, Sox2, and Klf-4), lineage markers (α-sarcomeric actin, α-smooth muscle actin, von Willebrand factor and discoidin domain receptor-2), and cardiac differentiation transcripton factors (Nkx2.5 and GATA4). To assess cardiomyogenicity of CDCs *in vitro*, cells were induced to differentiate using DMSO.

3.3.2 CDC labelling

CDCs were incubated overnight with micron-sized particles of iron oxide (MPIO; 2 µl/cm^2, encapsulated magnetic microspheres, Bangs Laboratories Inc., Fishers, IN., USA), on the day prior to transplantation. MPIO-labelled CDCs were washed twice with PBS and stained with CellTracker™ CM-DiI (Molecular Probes, UK) in PBS for 30 minutes before trypsinization. Approximately 2 x 10^6 cells were suspended in 50 µl CEM for direct injection to the myocardium and 4 x 10^6 cells were suspended in 500 µl CEM for systemic infusion. Viability and proliferation of CDCs were assessed using MTT and Alamar®Blue, respectively.

3.3.3 Western blotting

The metabolic characteristics of CDCs were determined by western blotting for GLUT-1 and GLUT-4 (See *Chapter Two*). Bands were quantified using UN-SCAN-IT gel software (Silk Scientific, USA).

3.3.4 CDC proliferation

DMEM with no glucose or pyruvate (Invitrogen, UK) was supplemented with 20% FBS and 1% penicillin, streptomycin and glutamate solution (Invitrogen). D-Glucose (Sigma, UK) was added to obtain a final concentration of 5 mM, 10 mM and 20 mM. The glucose concentrations of the formulated media were determined using an ABX Pentra 400 Chemistry Analyzer (analyzed by Emma Carter). Passage 2 CDCs were incubated with the test medium and the cell numbers were calculated at days 0, 4, 8 and 14 using a haemacytometer. All experiments were run in three replicates and results were analysed using a one-way ANOVA.

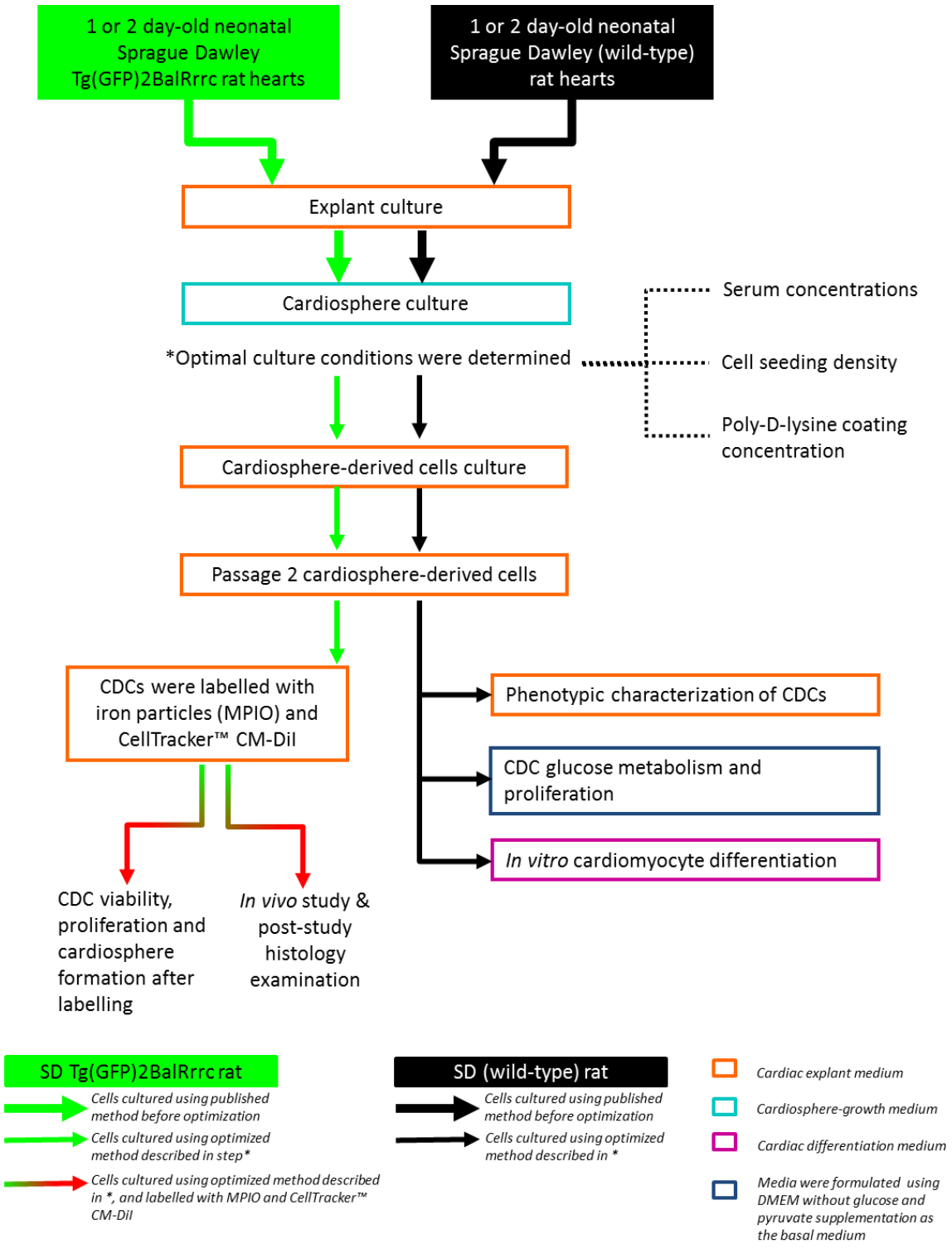

Figure 3.1: Flow diagram showing an overview of study design

3.4 RESULTS

3.4.1 CSC isolation and expansion

Heart explants were cultured from 1 or 2 day-old neonatal SD Tg(GFP)2BalRrrc rats, of which enhanced green fluoresecent protein (eGFP) gene was expressed under the control of the ubiquitin-C promoter, to generate GFP expressing cells for the *in vivo* study and post-study histological examinations. A number of round, loosely adherent, phase-bright cells (PBCs) grew on top of fibroblastic cells 7 days after explantation (Figure 3.2). Approximately 5-7 x 10^5 cells were obtained from each dish of 1 mm^3 explant. Explant-derived cells (EDCs) could be harvested every 7 days for up to 3 times (Figure 3.2C), but the cell yield was lower at the third harvest ($P < 0.05$).

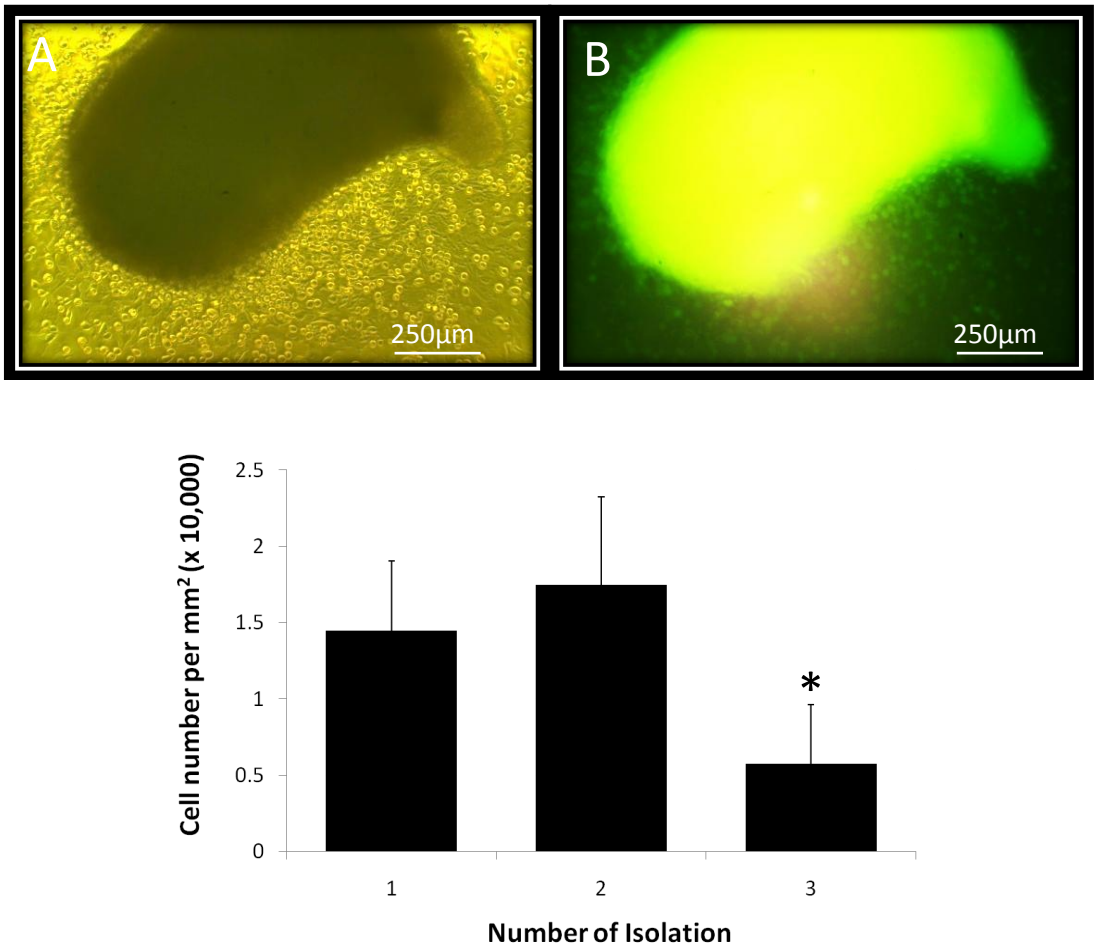

*Figure 3.2: Phase bright cells migrated from explants (A) created from one or two day-old neonatal Sprague Dawley-Tg(GFP)2BalRrrc neonatal rat heart were found to express green fluorescence protein (B). Explant-derived cells could be isolated several times (C) but the cell number decreased in the third harvest. Data are presented as mean ± SD (n=3). Statistical significance was analysed using one-way ANOVA, *P < 0.05 vs first isolation.*

3.4.2 Optimization of cardiosphere culture

After 4 days of EDC culture in CGM, cardiospheres formed had an average size of 50-100 µm. As illustrated in Figure 3.3, explant-derived cells plated on poly-d-lysine started to aggregate after 24 hours in CGM (Figure 3.3B) and formed cardiospheres after 4 days. EDCs formed a giant sphere in CGM if seeded at a high density (more than 60,000 cells per well). In contrast to published observations (99), cardiospheres formed through cell aggregation (Figure 3.3), but not by clonogenic amplification from a single cell. To optimize cardiosphere production, CGM serum concentrations, poly-d-lysine coating concentrations and cell density were evaluated.

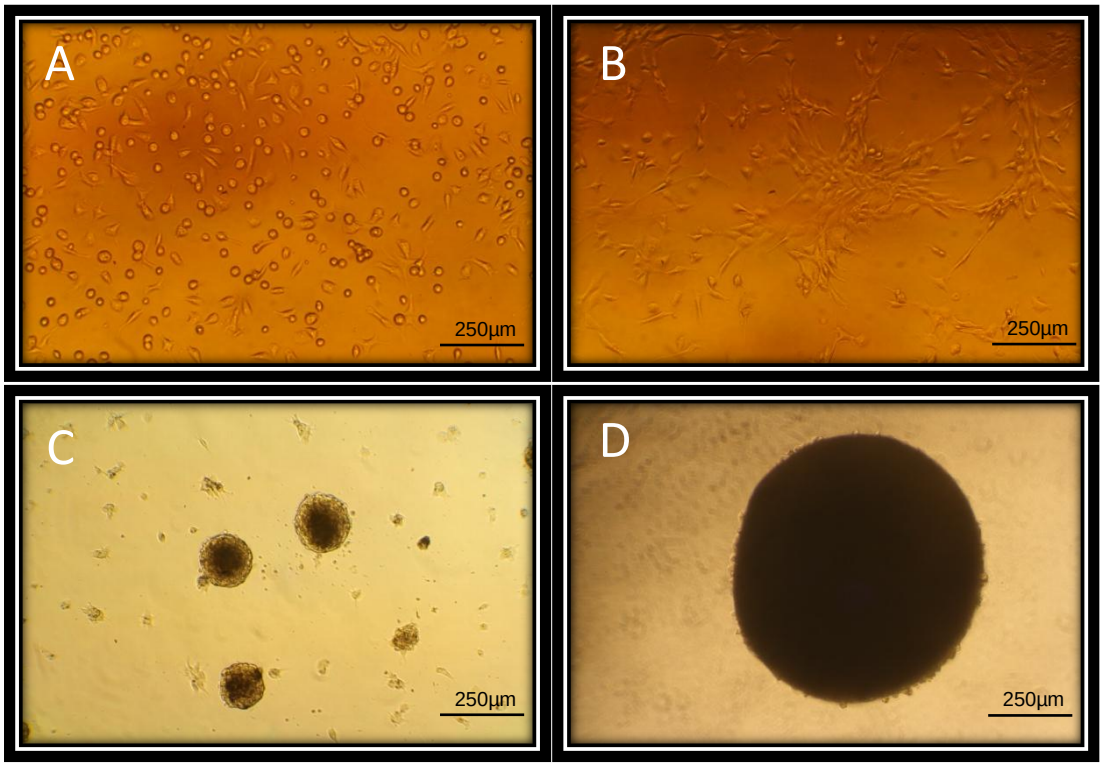

Figure 3.3: Cardiospheres were generated through cell aggregation. Representative images (n=3) were taken after plating EDCs on poly-D-lysine after 12 hours (A), 24 hours (B) and 96 hours (C). EDCs clumped and formed a giant sphere in CGM if seeded at a very high density (D).

3.4.2.1 Low serum concentration and poly-D-lysine coating concentrations produced more cardiospheres

Cardiosphere culture in CGM containing 7% serum on dishes coated with 33.3 µg/ml poly-d-lysine resulted in 283 ± 16 cardiospheres from 3 x 10^4 EDCs. Cardiosphere numbers increased to about 400 and 600, when cells were seeded in CGM containing 10% and 20% serum, respectively (Figure 3.4A), indicating that serum had a favourable effect on cardiospheres growth. Interestingly, when poly-d-lysine concentration was reduced to 16.7 µg/ml, a similar number of cardiospheres was obtained (539 ± 31), even when supplemented with only 7% serum. This suggests that low poly-D-lysine coating concentration may favour cell mobility and therefore requires lesser stimulation from serum to form cardiospheres, compared to that of high poly-D-lysine coating concentration.

Table 3.1: Summary of cardiosphere number after culturing using various serum and poly-D-lysine coating concentrations

Poly-d-lysine (µg/ml)	**Serum concentration (v/v)**	**Cell density Seeded**	**Cardiosphere number**
33.3	7%	30,000	283 ± 16
33.3	10%	30,000	392 ± 19
33.3	20%	30,000	591 ± 23
16.7	7%	30,000	539 ± 31

Data are presented as means ± SD (n=3)

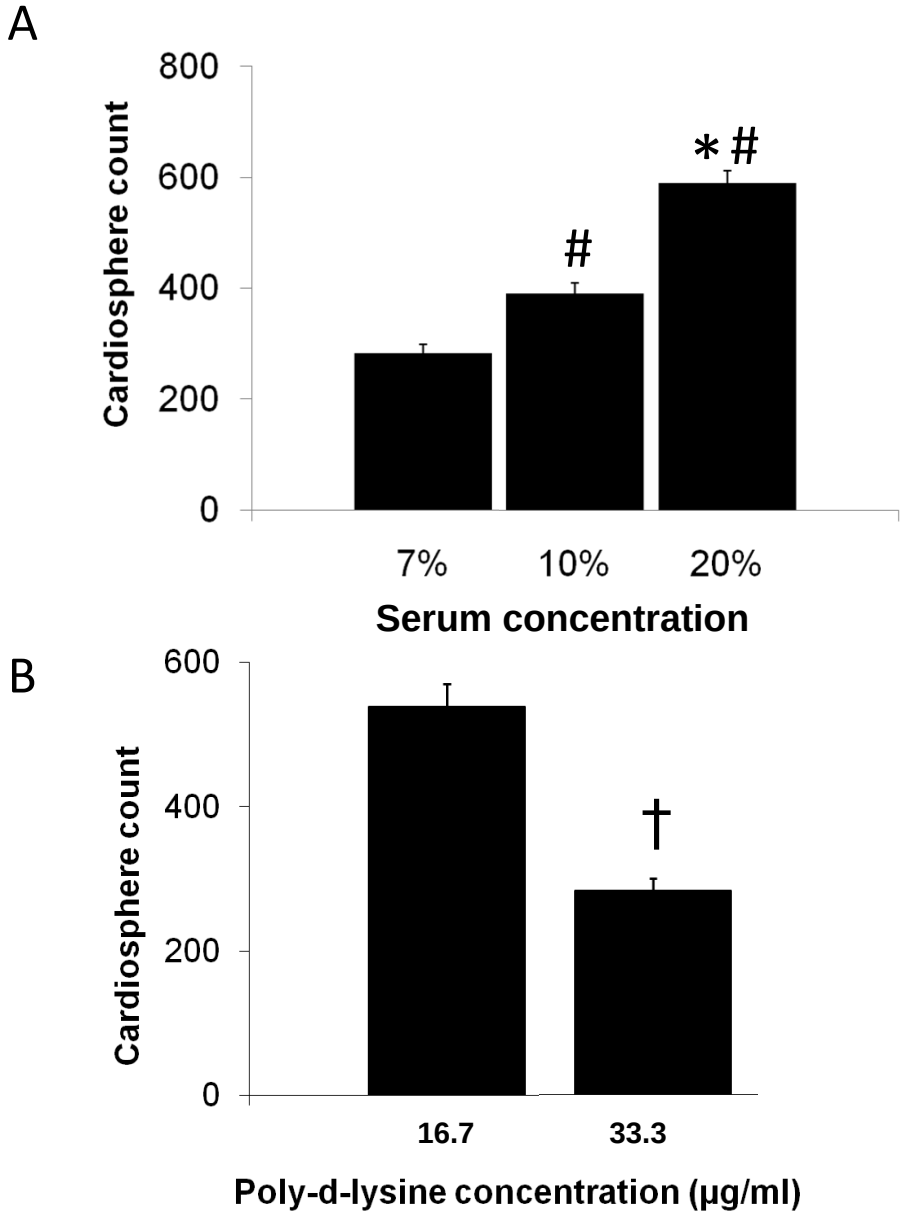

*Figure 3.4: (A) Cardiosphere formation depended on serum concentration. Statistical analysis was performed using ANOVA. # P < 0.05 versus 7% and * P< 0.05 versus 10% serum. (B) Cardiosphere growth dependence on different poly-d-lysine coating concentrations. †Significantly lower cardiosphere count in the well coated with 33.3µg/ml poly-d-lysine compared with 16.7 µg/ml. Data are presented as means ± SD, (n=3).*

3.4.2.2 Cell density and cardiosphere formation

Cardiospheres were grown from EDCs in CGM containing 7% serum and plated on 24-well plates coated with 16.7 µg/ml poly-d-lysine. The cardiosphere number was found to depend

on seeding density up to 3 x 10^4 cells. Most cardiospheres were generated with 3–5 x 10^4 cells, whereas more than 6 x 10^4 EDC resulted in cell clumping. When 1–2 x 10^4 EDC were seeded, fewer cardiospheres formed (Figure 3.5).

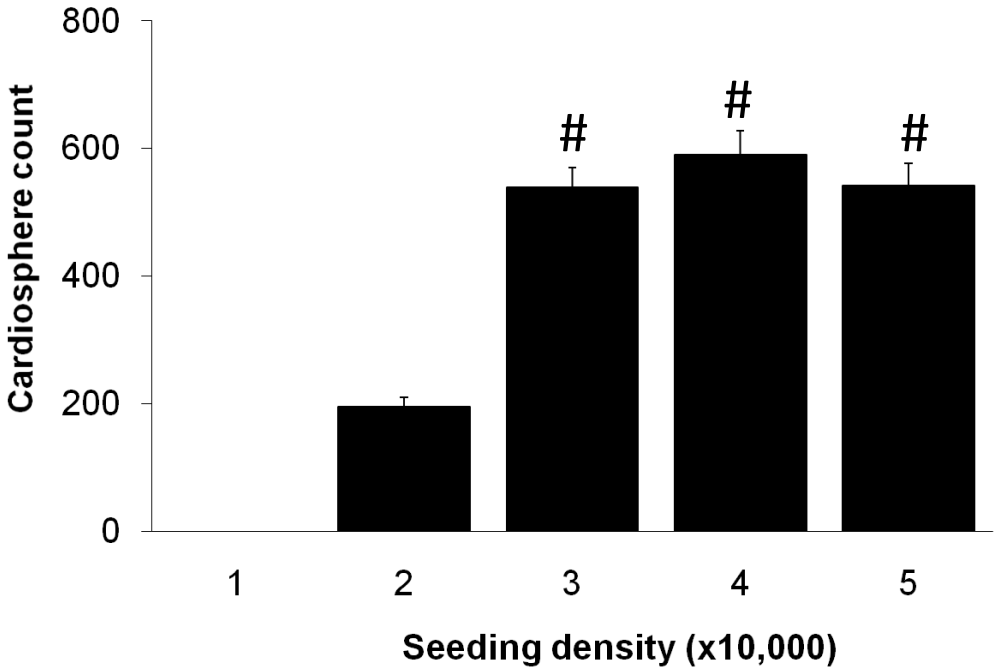

Figure 3.5: Cardiosphere formation depended on cell seeding density. Cardiospheres were grown from from EDCs in CGM containing 7% serum and plated on a 24 well plate coated with 16.7 µg/ml poly-D-lysine. One-way ANOVA showed no statistically significant difference between the number of spheres formed with cell seeding density between 30,000 and 50,000 cells. Values represent the means ± SD (n = 3). # Significant at P < 0.05 vs 20, 000 cells.

3.4.3. Characterization of cardiospheres and cardiosphere-derived cells

3.4.3.1 Cardiospheres as a source of c-kit expressing cardiac stem cells

The cardiospheres generated from 1 and 2 days old neonatal SD-Tg(GFP)2BalRrrc rat heart explants were fluorescent green (Figure 3.6A). However, the deriving CDCs did not show GFP expression (data not shown). Immunocytochemistry, performed using cardiospheres generated from 1 or 2 days old wildtype SD rat hearts, revealed that cardiospheres comprised $CD90^+$ mesenchymal cells and myocytes expressing troponin I (Figure 3.6 C and D). $C\text{-}kit^+$

cells migrated from the cardiospheres when seeded on fibronectin (Figure 3.6E). This suggests that the cardiospheres were rich in c-kit expressing cardiac stem cells and confirmed the validity of this method to selectively enrich and isolate cardiac stem cells without immuno-magnetic sorting.

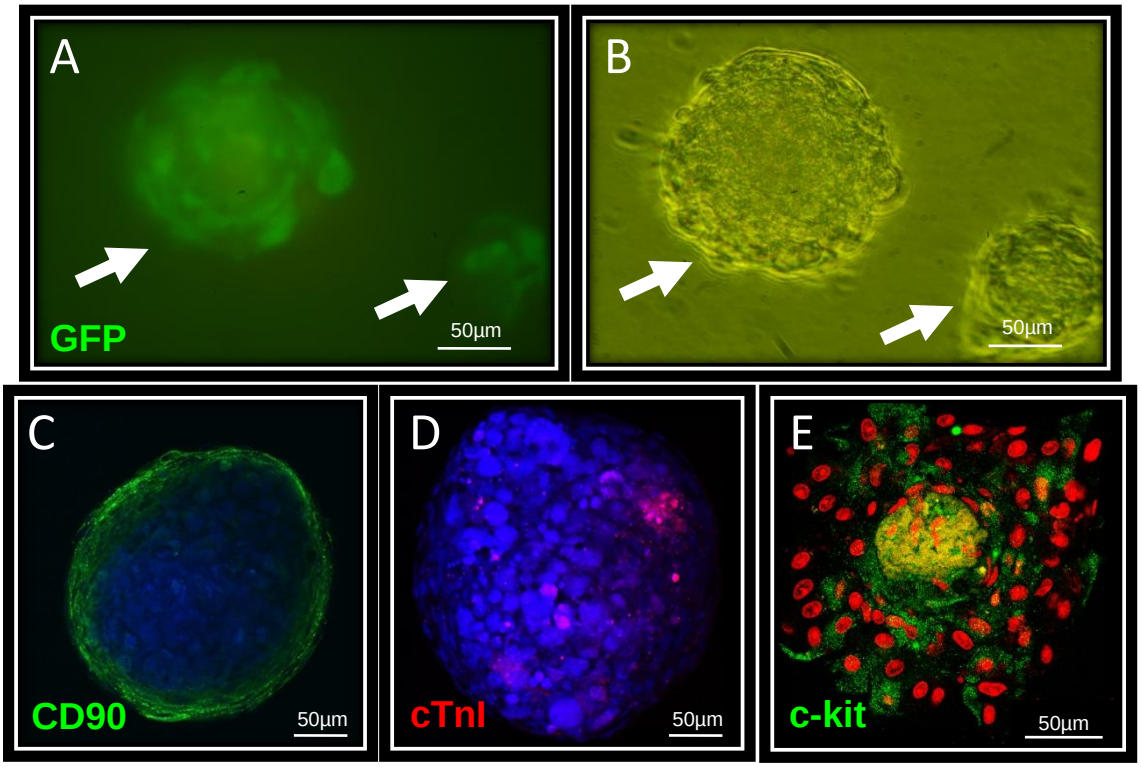

Figure 3.6: (A) Cardiospheres generated from EDCs, isolated from 1 or 2 days old SD-Tg(GFP)2BalRrrc neonatal rat hearts, were green under a fluorescence microscope (arrow). (B) Bright field view of the GFP-tagged cardiospheres. (C) Immunocytolabelling of cardiospheres showed that CD90 expressing cells (green, AlexaFluor 488) were located across the outer region of cardiosphere and a few cardiomyocytes (cTnI$^+$, red, AlexaFluor 546) cells were located in the inner region (D). Cells migrating from the cardiospheres were c-kit positive (green) (E). Nuclei are stained with DAPI (blue) or propidium iodide (red)

3.4.3.2 Cardiosphere-derived cell expansion and characterization

CDCs, generated from neonatal wildtype SD rat hearts, were expanded to reach > 90% confluence after 6-7 days. They had a heterogeneous morphology, ranging from very small (~15-20 µm), round cells to very large (~150-300 µm), elongated flat cells (Figure 3.7). However, the green fluorescent of CDCs cultured from SD-Tg(GFP)2BalRrrc rat hearts was lost in passage 2 CDCs (data not shown). The underlying reason was unknown, but it might

be due to photobleaching during CDC expansion. In addition, it is not known whether the GFP expression is present in these primitive cells.

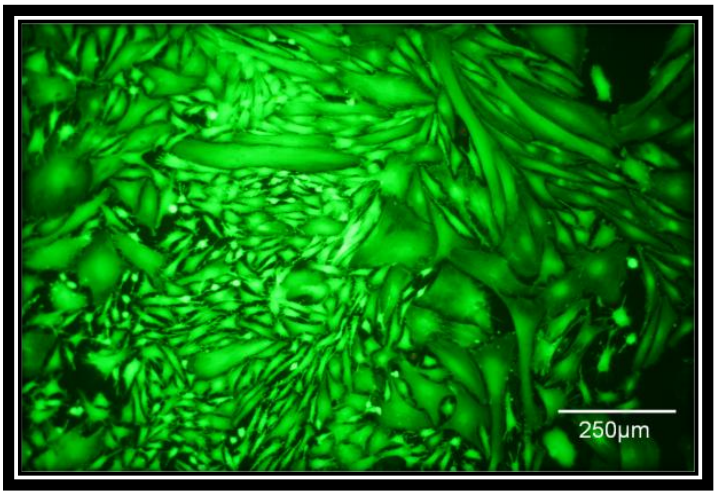

Figure 3.7: Passage 2 cardiosphere-derived cells, generated from 1 or 2 days neonatal wildtype SD rat hearts (stained with Calcein AM, green), were highly heterogeneous in size and shape.

3.4.3.3 CDCs were composed of cardiac progenitors and differentiated cells

Immunocytochemistry showed that passage 2 CDCs comprised cardiac stem cells (c-kit, Oct4, Sox-2, and klf-4), cardiac differentiating cells (Nkx2.5, GATA4), cardiac lineage committed cells (α-sarcomeric actin), and differentiated endothelial cells (von Willebrand factor), and smooth muscle cells (smooth muscle actin) (Figure 3.8). Flow cytometry detected 3% c-kit^{+} cells and 71% CD90+ cells in passage 2 CDCs, suggesting that most CDCs had a mesenchymal phenotype. Only 10.4% of the cells stained positive for discoidin domain receptor 2 (DDR2), a specific marker for cardiac fibroblasts (Figure 3.9).

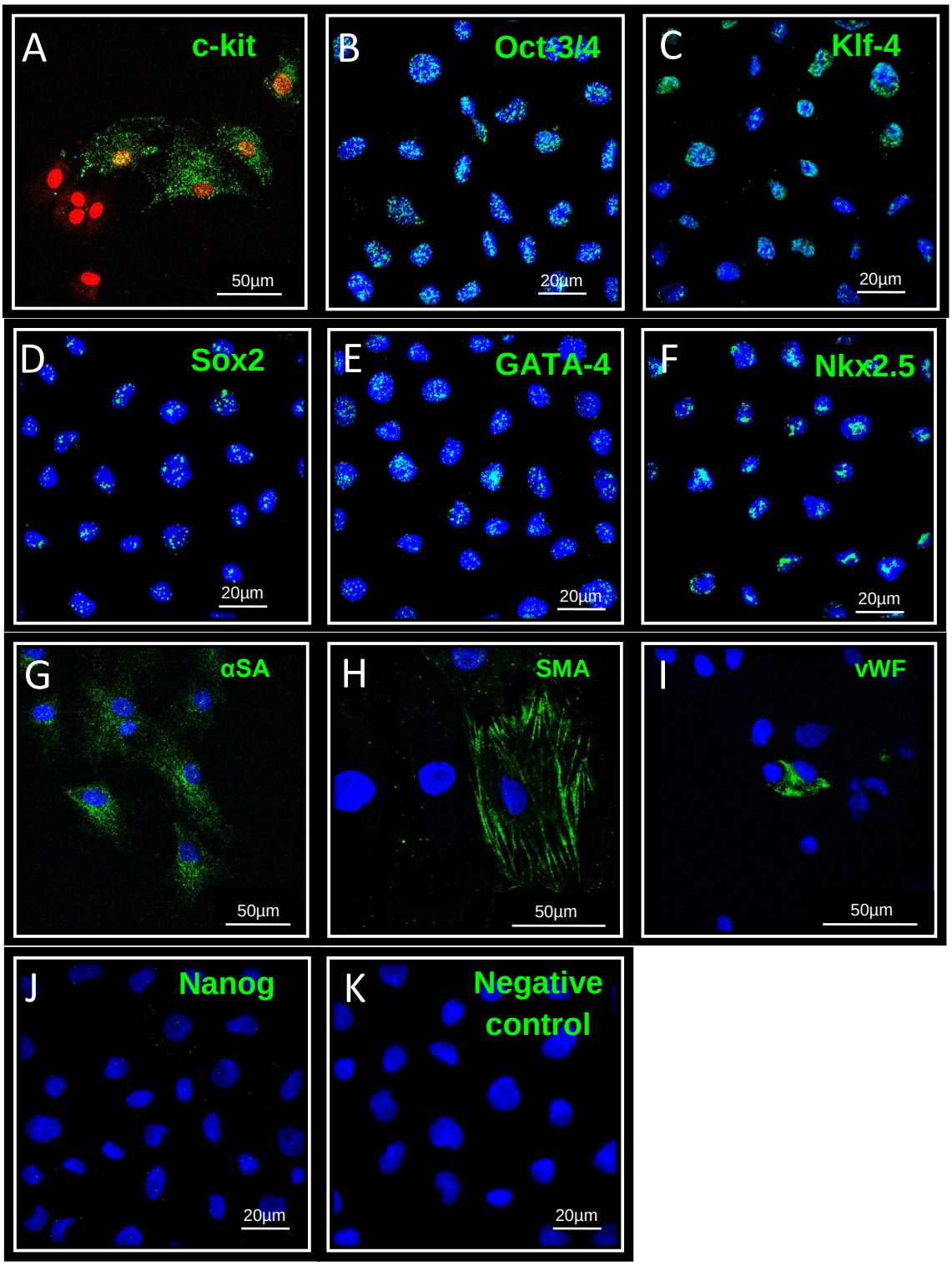

Figure 3.8: Characterization of passage 2 CDCs. Representative confocal images (of three independent experiments) showed that cardiosphere-derived cells (isolated from 1 or 2 days old neonatal wildtype SD rat hearts) represented a mixed cell population consisting of cardiac stem and progenitor cells expressing (A) c-kit , (B) Oct 3/4, (C) klf-4 and (D) Sox2, cardiac differentiating cells (E;GATA-4, F;Nkx2.5), cardiac lineage-committed cells (G;α-sarcomeric actin, αSA), cardiac smooth muscle cells (H;smooth muscle actin, SMA) and endothelial cells (I;von Willebrand factor, vWF). (J) However, CDCs did not express Nanog. (K) Negative controls were CDCs labelled with secondary antibody (AlexaFluor 488, green) without primary antibody. Nuclei were stained DAPI (blue) or propidium iodide (red).

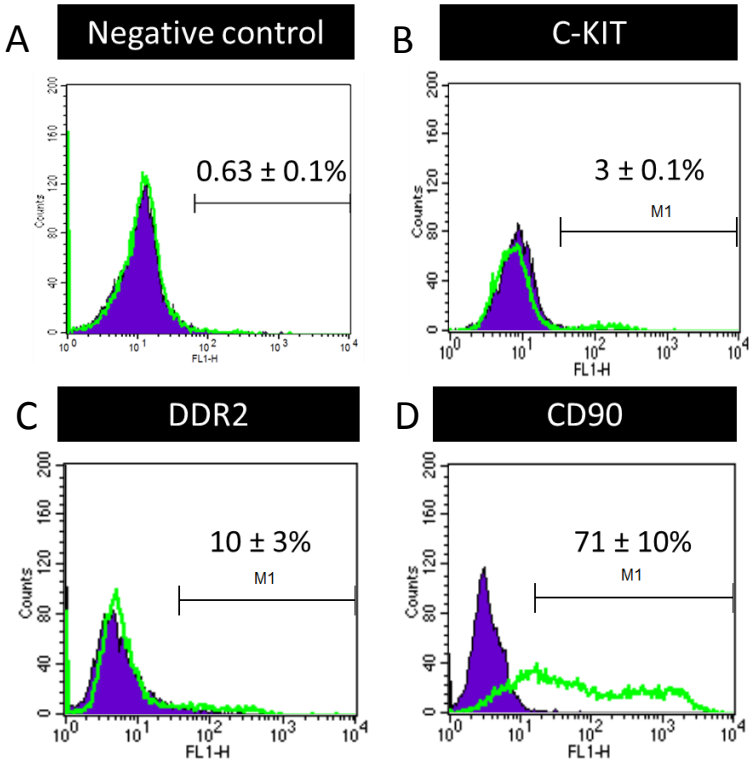

Figure 3.9: Characterization of passage two CDCs cultured from wildtype SD rat hearts using flow cytometry. (A) Negative controls were CDCs labelled only with secondary antibody without primary antibody (AlexaFluor 488). Passage 2 neonatal CDCs expressed (B) c-kit, cardiac stem cell marker, (C) DDR2, cardiac fibroblast marker, and (D) CD90, mesenchymal marker. Cells presented in region M1 are the positive populations; Blue histogram, the unstained controls. Green line, corresponding stained samples. Values represent mean ± SD of three independent experiments.

3.4.4 CDC glucose metabolism

The role of substrate metabolism in CSC proliferation has yet to be investigated. Alterations in cardiac substrate metabolism occur during ischemia and cardiac stem cells increase after myocardial infarction (79), suggesting that the environment during myocardial infarction, including metabolic substrate availability and utilization, could alter CSC proliferation. Here, the effects of glucose on the CDC metabolic phenotype and cell proliferation were evaluated.

3.4.4.1 CDCs expressed GLUT-1 but not GLUT-4

Western blot analysis revealed that neonatal CDCs did not express the insulin sensitive GLUT-4 protein, but expressed GLUT-1 (Figure 3.10)

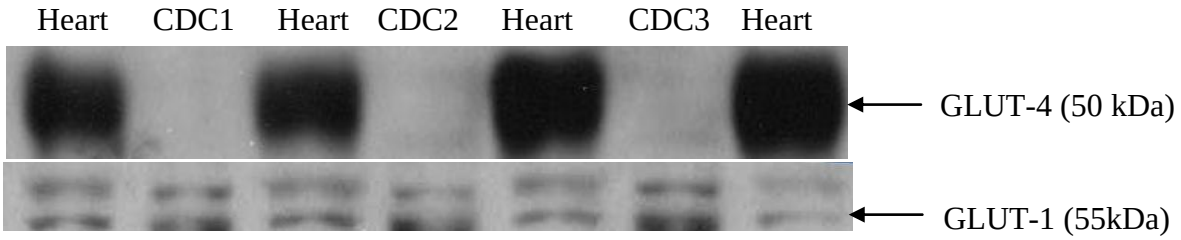

Figure 3.10: Western blot showing that CDCs express GLUT-1 but not GLUT-4 (n=3). Adult SD rat heart lysates were used as postiove controls. CDC1, cardiosphere-derived cells replicate 1; Heart, rat heart lysate

3.4.4.2 CDC proliferation was glucose dependent

The effect of different glucose concentrations was determined on CDC proliferation. Glucose concentrations in the media (formulated using DMEM without glucose and pyruvate supplementation) were measured in triplicate (analysis by Emma Carter) (Table 3.2).

Table 3.2: Glucose concentration in DMEM with 20% FBS (n=3).

Glucose concentration (mM)	Standard deviation (N=3)
0.6	0.1
11.7	0.3
22.8	0.5

After 4 days, the number of CDCs was significantly higher than other when treated with 22.8 mM glucose (Figure 3.11). By 8 and 14 days, CDCs fed with 11.7 mM and 22.8 mM glucose had proliferated significantly more than those cultured in 0.6 mM glucose.

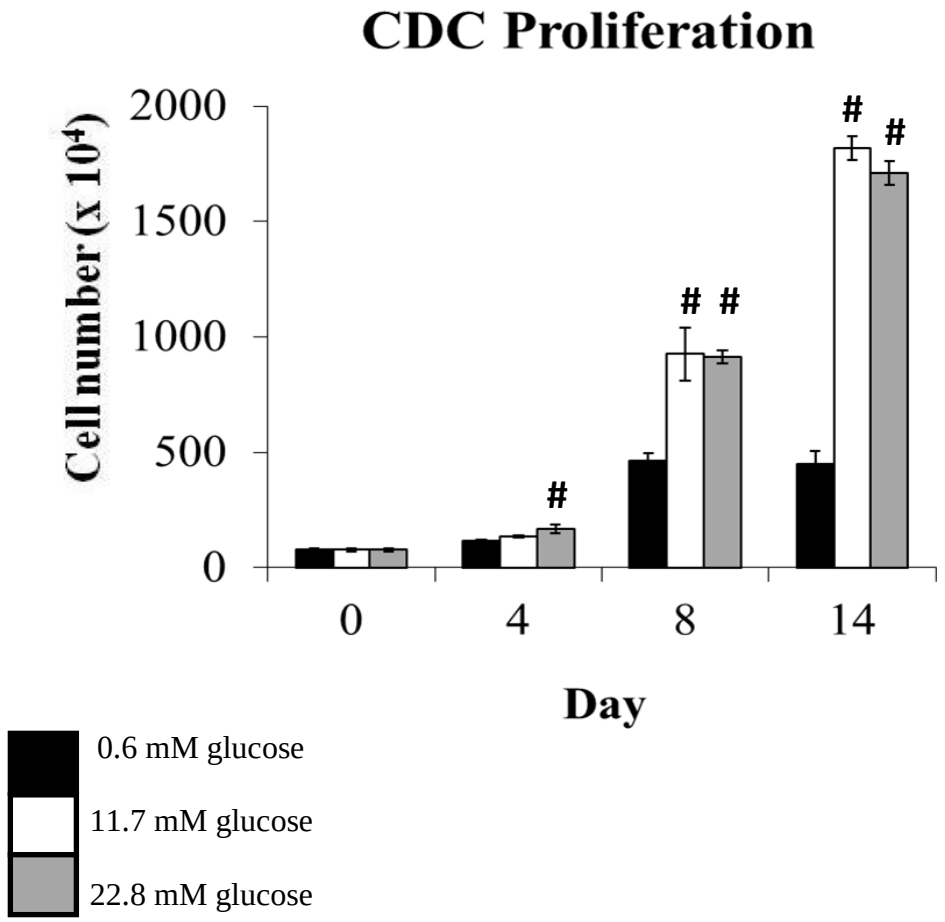

Figure 3.11: CDC proliferation at different glucose concentrations were assessed by plating passage 2 neonatal CDCs (from wildtype SD rats) at equal cell number (100 x 10^4) across each group at day 0. Cell number was calculated by manual counting using haemacytometer after trypsinization at day 4, 8 and 14. There was a significant difference in cell number between CDCs cultured in low glucose medium (0.6 mM) and those cultured in medium supplemented with 11.7 mM and 22.8 mM glucose. Values represent mean ± SD (n=4). Data were analysed using one-way ANOVA. # Significant difference at P < 0.05 compared with 0.6 mM glucose.

3.4.4.3 High glucose suppressed CDC PGC-1α and mitochondrial α-ketoglutarate dehydrogenase protein levels

PGC-1α protein levels were suppressed by 58% at 11.7 mM glucose, and by 93% at 22.8 mM glucose (Figure 3.12A). α-ketoglutarate dehydrogenase (αKD) is one of the Krebs cycle enzymes in the mitochondrion. Therefore, the αKD protein levels in the cells were examined as a measure of mitochondrial number. Low expression of α-ketoglutarate dehydrogenase was observed in CDCs at 22.8 mM, but not significant at 11.7 mM glucose (Figure 3.12 B). This indicates that high glucose concentrations decrease the mitochondrial content and thereby down-regulate oxidative phosphorylation in the cells.

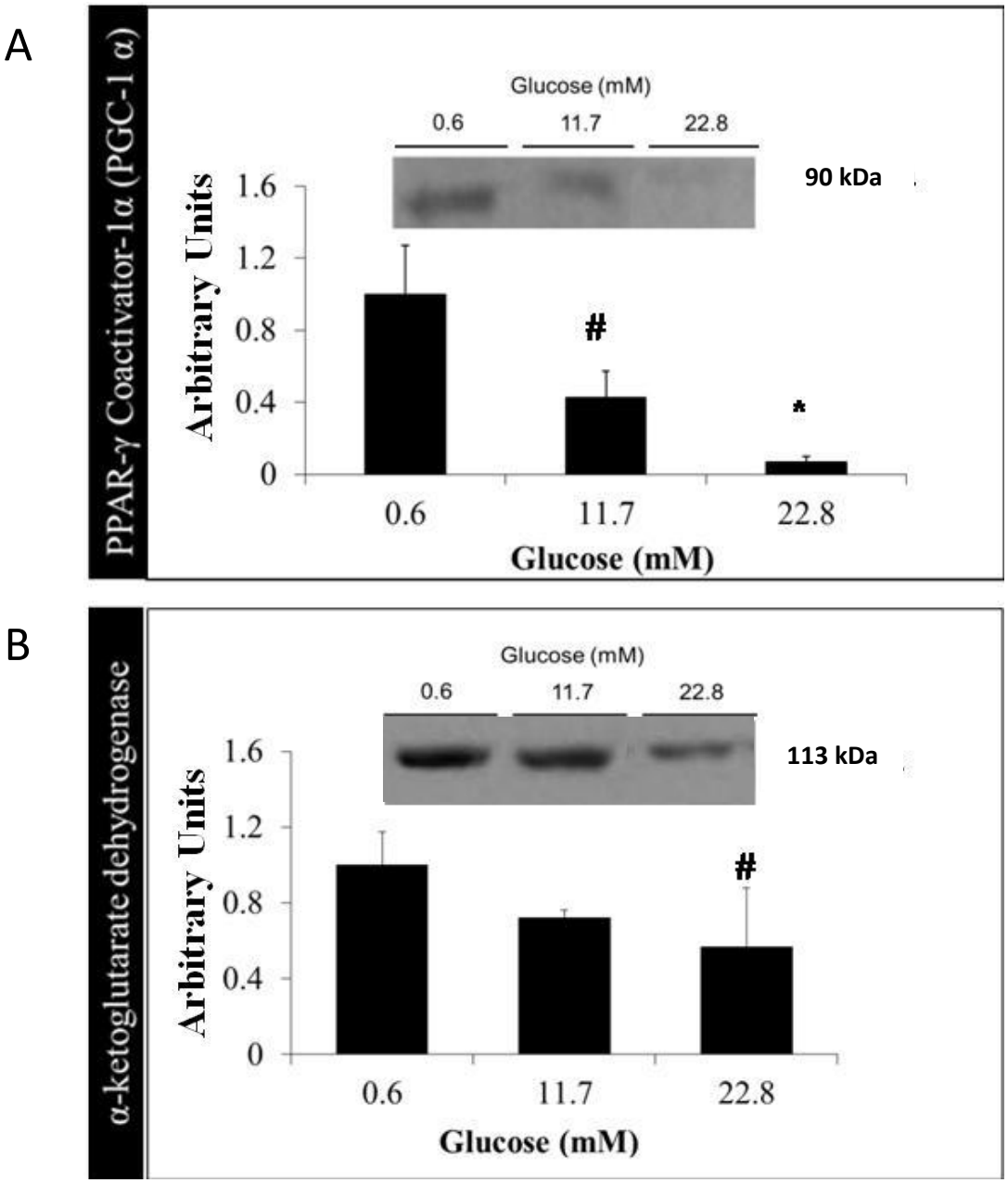

*Figure 3.12: Western blot analysis of (A) PGC-1α and (B) α-ketoglutarate dehyrogenase expression in passage 6 CDCs after culturing at 0.6 mM, 11.7 mM and 22.8 mM glucose for 14 days. Values represent mean ± SD (n=3). Data were analysed using one-way ANOVA. # P < 0.05 vs 0.6 mM glucose; * P < 0.01 vs 0.6 mM glucose.*

3.4.4.4 Glucose levels did not alter the relative CDC population

To examine whether the effect of different glucose concentrations was affecting CDCs as a whole or a particular cell population in CDCs, passage two neonatal wildtype SD rat-derived CDCs were cultured at 0.6 mM, 11.7 mM and 22.8 mM glucose for 14 days (to passage 6) and CDC c-kit$^+$ and CD90$^+$ cells were analysed using flow cytometry. No changes in the percentage of c-kit and CD90 expressing cells in CDCs (Figure 3.13) were observed, suggesting that the CDC phenotype remained unaltered by different glucose concentrations.

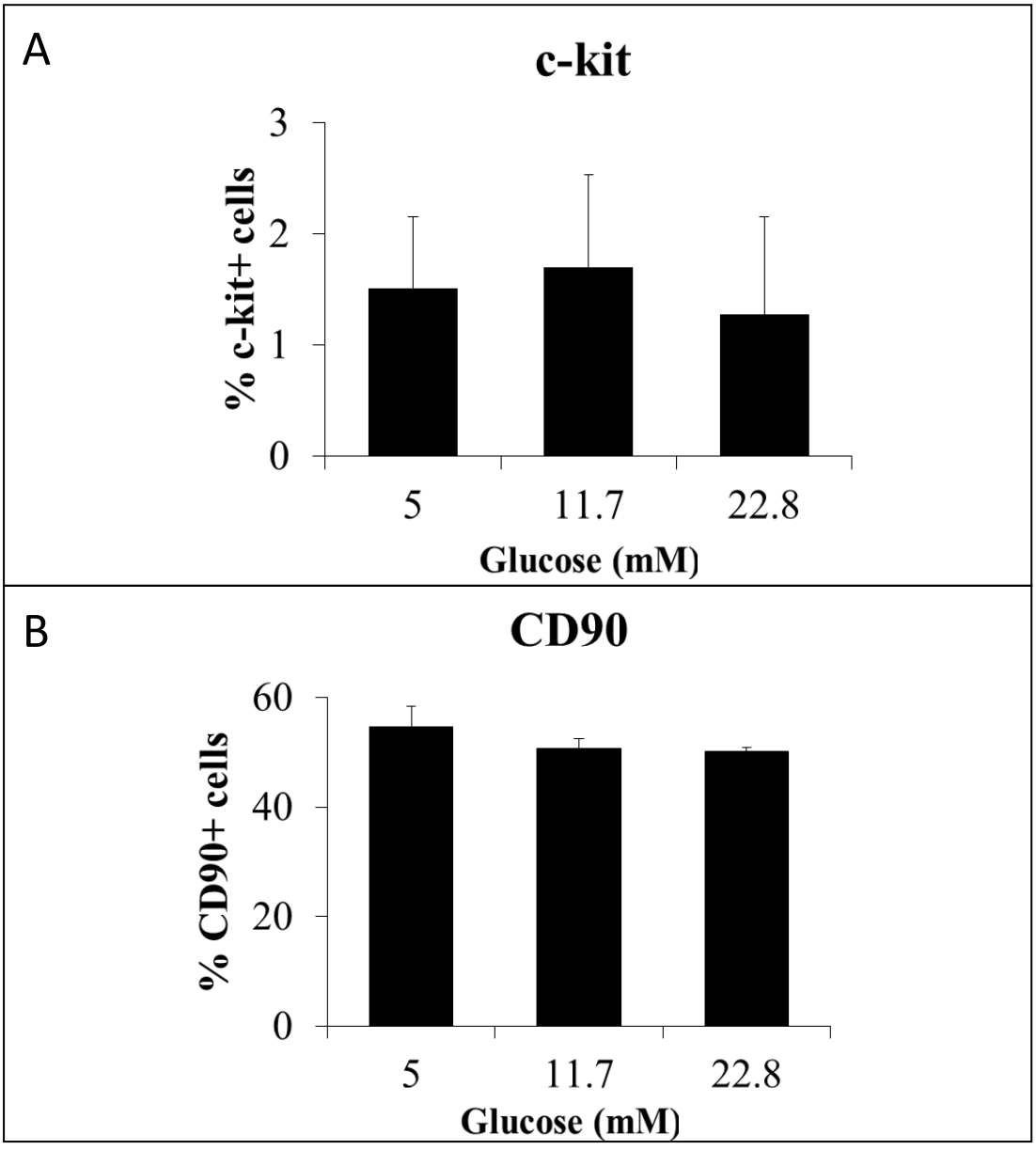

Figure 3.13: Flow cytometric analysis showed that the percentage of c-kit$^+$ (A) and CD90$^+$ (B) cells in passage 6 CDCs after culturing at 5 mM, 11.7 mM and 22.8 mM glucose for 14 days, remained unaltered by glucose concentration. Values represent mean ± SD (n=3). Data were analysed using one-way ANOVA.

3.4.5 CDC functional studies (in vitro)

3.4.5.1 CDCs were capable of cardiomyogenic differentiation

Passage 2 CDCs, generated from 1 or 2 days neonatal wildtype SD rat hearts, were induced to form cardiomyocytes by incubation with culture medium (*Appendix 1*) containing ascorbic acid and DMSO. After 5 days, 19 ± 6% cells stained positive for cardiac troponin I (Figure 3.14). No beating cells were observed.

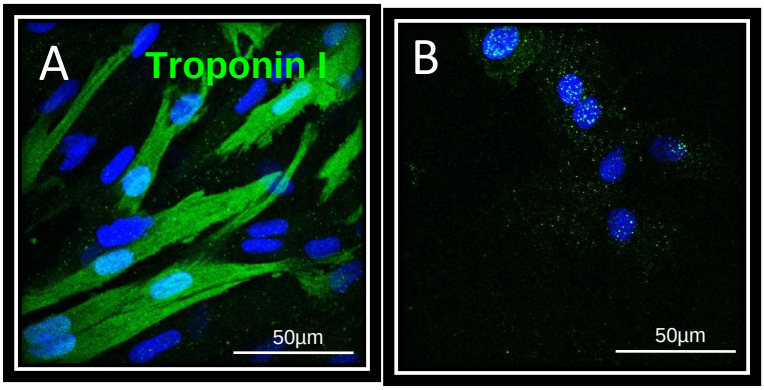

Figure 3.14: Immunocytochemistry showed that passage 2 CDCs differentiated to cardiomyocytes expressing cardiac troponin I (green, AlexaFluor 488) when induced with DMSO (A), whereas CDCs without DMSO did not (B).Nuclei were stained with DAPI (blue). Images are representative of three independent experiments.

3.4.5.2 CDCs viability and proliferation was unaffected by MPIO and CellTracker™ CM-DiI labeling

Labelling with MPIOs allowed cells to be tracked *in vivo* using MRI. Passage 2 neonatal CDCs (generated from SD-Tg(GFP)2BalRrrc rat hearts) labelled with MPIO and CellTracker™ CM-DiI retained the ability to form secondary cardiospheres (Figure 3.15). Proliferation of the labelled CDCs, measured by counting following staining for live and dead cells, was comparable with unlabeled cells. Cell viability after 3 days was not statistically different between the groups, measured using the MTT assay (Figure 3.16).

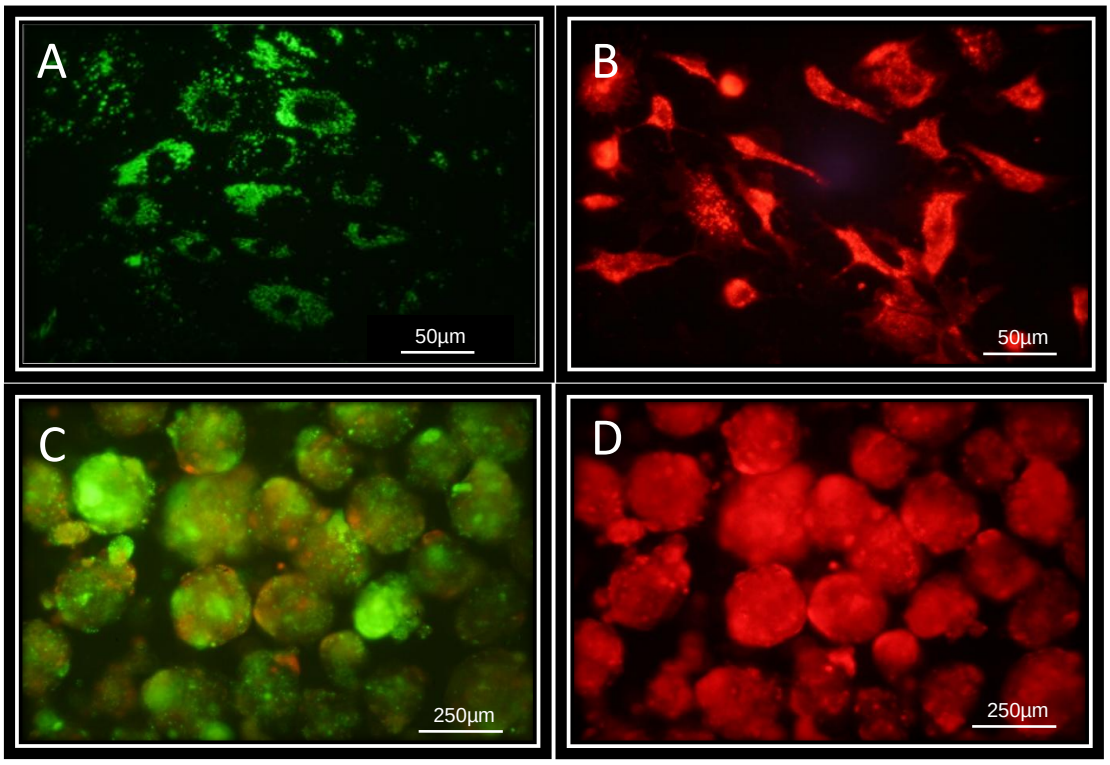

Figure 3.15: (A) Passage 2 CDCs generated from neonatal SD-Tg(GFP)2BalRrrc rat hearts were labelled with micron-sized particle of iron oxide conjugated with dragon green fluorescent particles (MPIO, green), and CellTracker™ CM-DiI (red) (B). The MPIO and CellTracker™ CM-DiI labelled-CDCs were able to form secondary cardiospheres at passage 3 (C and D).Images are representative of three independent experiments.

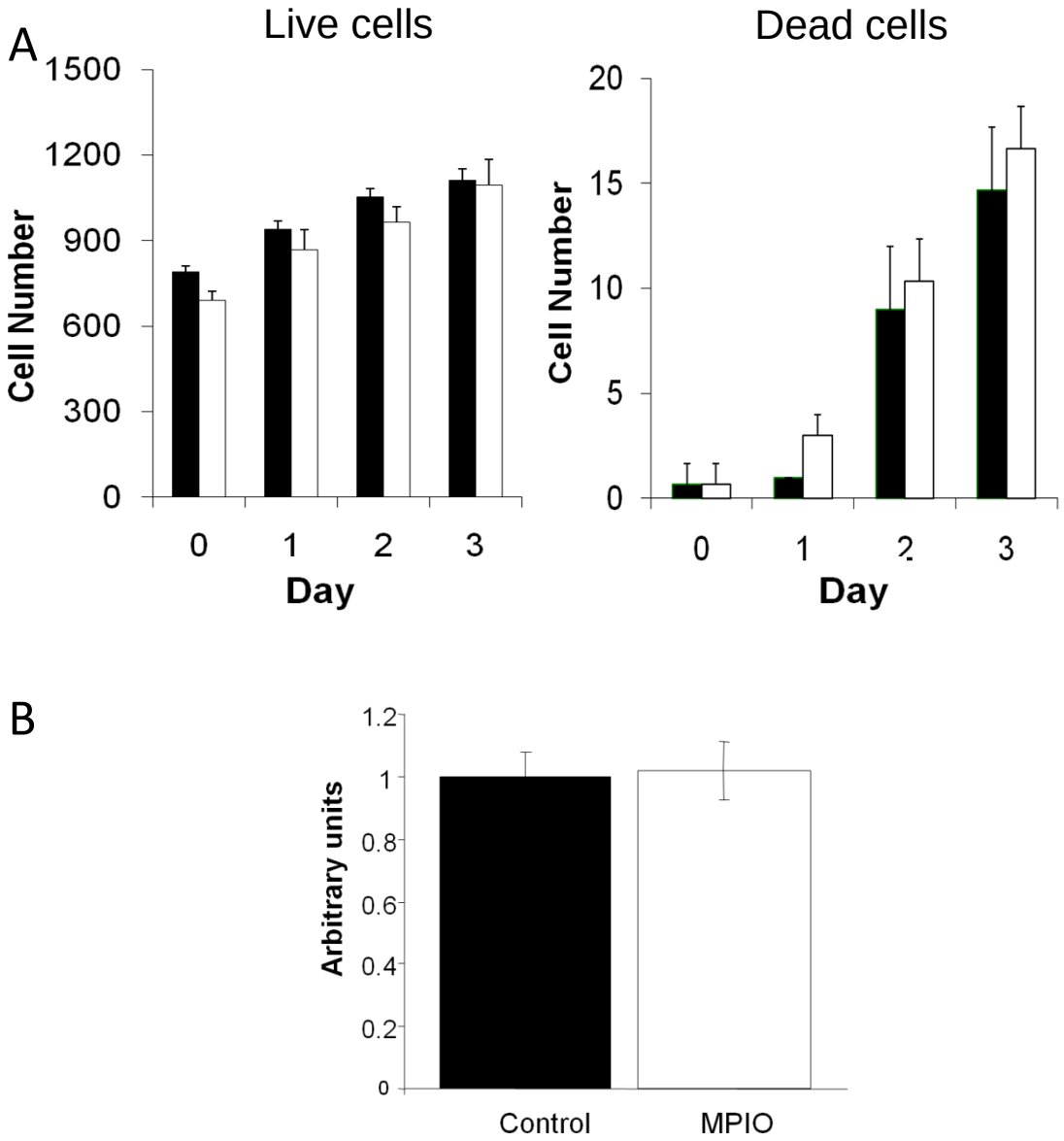

Figure 3.16: (A) Proliferation of iron particles (MPIO) and CellTracker™ CM-DiI labelled passage 2 neonatal CDCs (from SD-Tg(GFP)2BalRrrc rat hearts) was comparable with that of unlabelled cells. No significant difference in dead cell number was observed between labelled and unlabelled cells. (B) No difference in viability between MPIO labelled and unlabelled cells, measured using the MTT assay.Values represent mean ± SD (n=3). Statistical difference was analysed using student t-test.

3.4.6 CDC functional studies (in vivo)

To investigate the regenerative potential of CDCs *in vivo*, passage 2 CDCs, generated from neonatal SD-Tg(GFP)2BalRrrc rat hearts, were injected intramyocardially and intravenously to surgically infarcted female SD rats (200-250 g) (see *Chapter Two*). CDC engraftment and

heart function were measured over 16 weeks using MRI, and CDC cardiomyogenic differentiation *in vivo* was confirmed by immuno-histological staining.

3.4.6.1 CDCs ameliorated infarcted heart function

There was no statistical difference in ejection fraction between untreated controls, CDC-treated and sham hearts two days after myocardial infarction, although function was reduced. However, a sharp fall in ejection fraction was observed in untreated controls (to 52 ± 2%) and CDC-treated hearts (to 55 ± 2%) after two weeks, but not in shams (68 ± 1%). By six weeks, the ejection fraction in the CDC-treated group was 9% (significantly) higher than that of the untreated controls, and the difference persisted for up to 16 weeks (Figure 3.17).

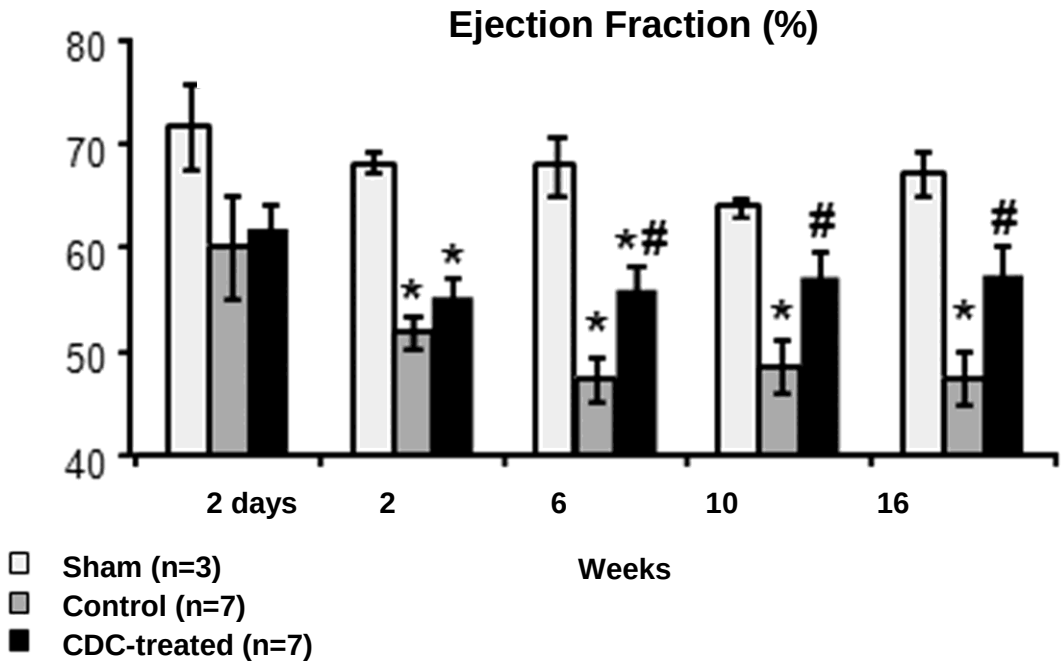

*Figure 3.17: Cardiac function. Rat left ventricular ejection fraction (LVEF) was measured using cardiac cine MRI. In sham operated animals (n=3), no changes in LVEF were observed over 16 weeks. Significant improvement in the ejection fraction of CDC-treated hearts was detected after 6 weeks and maintained after 16 weeks, compared with the untreated controls. Data are presented as mean ± SEM, and were analysed using ANOVA with post hoc t-test with Tukey corrections. * P < 0.05 vs sham. # P < 0.05 vs control. (work performed by Dr. Carolyn Carr and Dr. Daniel Stuckey)*

Wall thickness of the peri-infarct (myocardium adjacent to infarct where contraction was observed) and posterior regions of the myocardium were measured in a mid-papillary slice. Both control and treated groups had a thinner peri-infarct wall after two weeks (control 1.9 ± 0.2 mm, CDC-treated 2.2 ± 0.1 mm), compared with the initial thickness of 2.7 ± 0.2 mm and 2.8 ± 0.2 mm, respectively, at day 2 ($P < 0.05$). Peri-infarct wall thinning was ameliorated by the CDC treatment and becoming significantly thicker after 16 weeks, compared with the controls (2.5 ± 0.2 mm vs control 2.1 ± 0.0 mm, $P < 0.05$) (Figure 3.18).

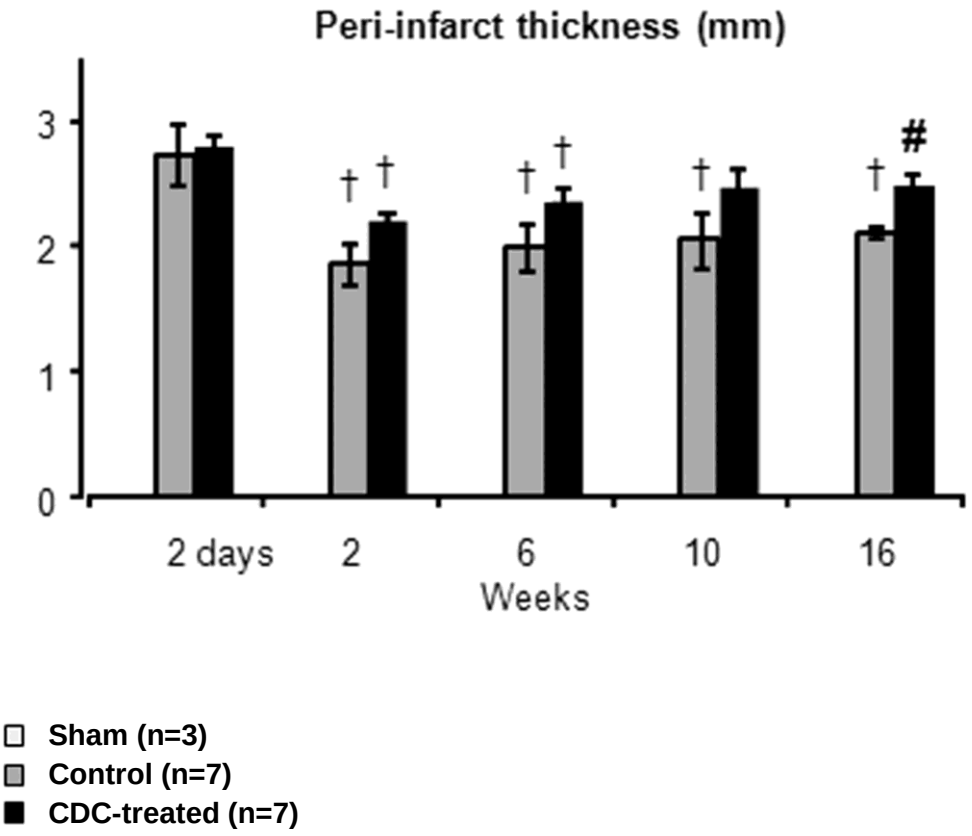

Figure 3.18: Peri-infarct thickness. Wall thickness of the peri-infarct and posterior regions of the myocardium were measured in a mid-papillary slice. Significant improvement in peri-infarct wall thickness in CDC-treated hearts was observed after 16 weeks. Values are presented in mean ± SEM and analysed using ANOVA with post hoc t-test with Tukey corrections. †$P < 0.05$ vs 2 days, # $P < 0.05$ vs control. (work performed by Dr. Carolyn Carr and Dr. Daniel Stuckey)

3.4.6.2 In vivo CDC differentiation

To investigate CDC retention and differentiation after injection, the treated hearts were isolated after 16 weeks, cryo-sectioned (performed by Suat Cheng Tan) and stained for cardiac troponin I (cTnI) to detect cardiomyocytes differentiation. High resolution confocal microscopy was used as the imaging modality to detect and confirm the staining of cTnI. This was because high resolution confocal microscopy utilized a laser with a narrow range of wavelengths for exciting specific fluorochromes, and a narrow bandpass filter, which permits detection of the emitted signal following fluorochrome excitation within a specific range of wavelengths, thus providing high detection specificity and sensitivity with low background. This is particularly useful in examining the colocalization of labelling for multiple fluorochromes, e.g. MPIO (green), CellTracker CM-DiI (red) and cTnI (costained with AlexaFluor 633) in individual cells.

Cells with MPIO and CellTracker™ CM-DiI labels that expressed cTnI (identified by cTnI staining) were quantified for the infarct and remote regions of the heart from at least 10 representative fields from 5 CDC-treated hearts. About 26 ± 9% MPIO and CellTracker™ CM-DiI labelled cells in the infarct area and 41 ± 11% in the remote region were co-localized with cardiac troponin I staining (Figure 3.19), indicating that CDCs were capable of cardiomyogenic differentiation after injection.

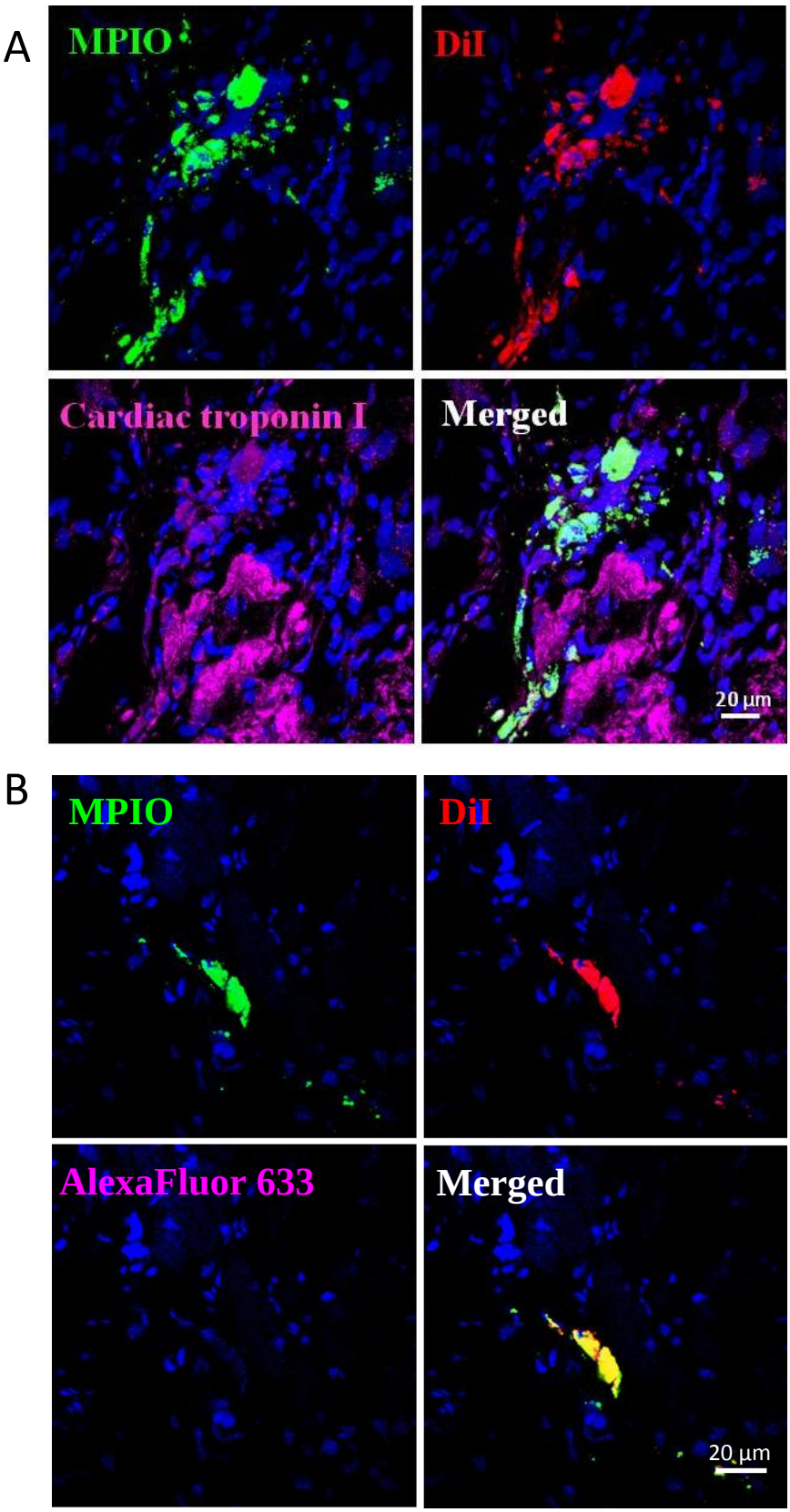

Figure 3.19 (A) In vivo CDC differentiation. Representative confocal images of the infarct region of five CDC-treated rat hearts showed that MPIO(green) and CellTracker™ CM-DiI-labelled (red) cells co-localised with cardiac troponin I staining (co-labelled with AlexaFluor 633), suggesting cardiomyogenic differentiation of transplanted CDCs in vivo. (B) Negative control with no primary antibody staining. Nuclei were stained with DAPI (blue).

It has been suggested that MPIO-labelled cells might not represent the donor cells, as MPIO released by dead donor cells may be taken up by the neighbouring host cells. Previous reports have also shown that some iron particles were identified in host macrophages (142, 143). However, $MPIO^{+}$ CellTracker™ CM-DiI $^{+}$ cells found in the CDC-treated heart (after 16 weeks) did not express CD68 (Figure 3.20), suggesting that the labelled cells were not macrophages. Hypointensity of MPIO observed during *in vivo* image acquisition matched signal void location in *ex vivo* images using MR microscopy (Figure 3.21).

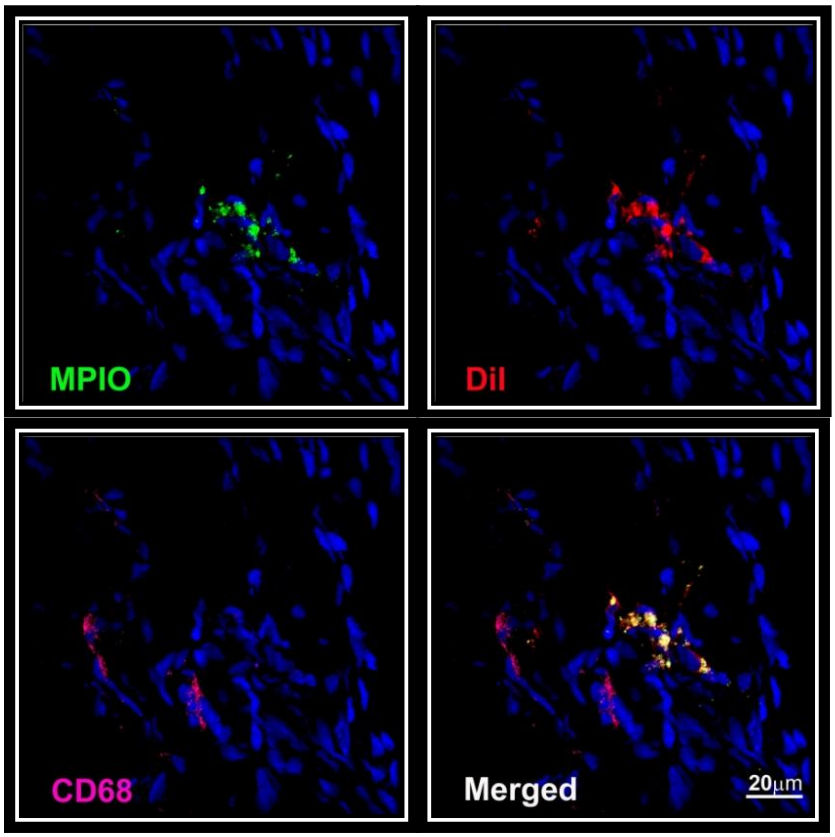

Figure 3.20: Immunostaining for macrophage. Representative confocal images of three CDC-treated rat hearts showed that $MPIO^{+}$ (green) *CellTracker™ CM-DiI $^{+}$ (red) cells present in the infarct area did not express CD68 (co-labelled with AlexaFluor 633). Nuclei were stained with DAPI (blue).*

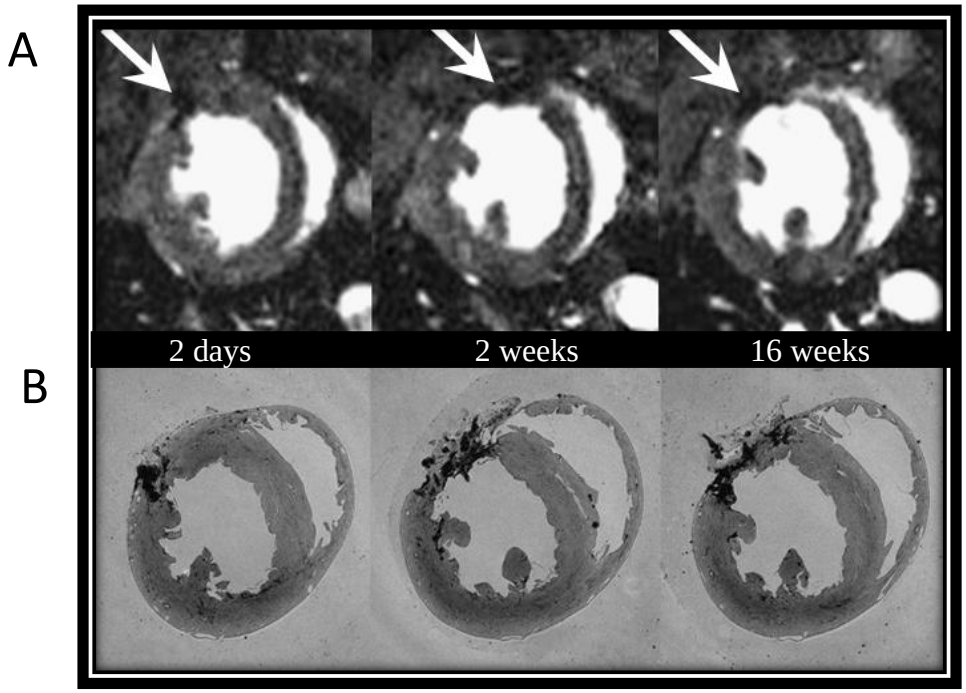

Figure 3.21: Colocalization of signal void and MPIO location in the CDC-treated hearts using in vivo and ex vivo MRI. Hypointense contrast (arrows) generated by MPIO-labelled CDCs was detected in the infarcted heart (n=7) using in vivo MRI (A) 2 days, 2 weeks, and 16 weeks after administration, which matched the signal void location seen in ex vivo MR images (B) of the corresponding heart (n=2). (work performed by Dr. Carolyn Carr and Dr. Daniel Stuckey)

3.5 Discussion

The identification of endogenous cardiac stem cells has raised interest in these cells for treating myocardial infarction. Isolation based on a single cell marker gives a homogenous population, but very low cell yield. Therefore, time-consuming extensive *ex vivo* expansion is required, which may compromise stem cell properties (144). Explant culture, followed by stem cell isolation and enrichment through the generation of cardiospheres may be a practical way to obtain sufficient cells in a short time period. Here, 5-6 x 10^6 EDCs were produced in 6 ± 1 days from one neonatal rat heart. Using the optimized protocol, by plating 3 x 10^4 cells/well of a 24 well plate coated with 16.7 µg/ml poly-D-lysine, in CGM containing 7% serum, a total of 9.6 x 10^4 cardiospheres were produced in 4 days. This produced eight 25 cm^2 flasks of cardiosphere-derived cells, which gave a total of 1.5 x 10^7 cells at the end of passage

1 after 6 ± 1 days (16 days in total starting from explant culture), a sufficient number of cells for therapy.

CDC culture, expansion and characterization

Cardiosphere growth is serum dependent (99), similar to other cell types (145), because the growth factors and hormones present in the serum are basic elements (but mostly unknown) required for cell proliferation. However, a high amount of bovine serum may risk the quality of stem cells (146), and may affect differentiation (147). Others have reported that a substantial reduction in total cardiosphere yield (1-2/cm^2) and prolonged culture time (7-10 days) were observed when a serum-free medium was employed (148). Here, a considerable increase in cardiosphere number (to about 284/cm^2, 568/well of a 24 well plate) was seen when serum concentration was double the published concentration (99). Although it can be argued that the differences in cell density (Table 3.3) disallow a direct comparison, these modifications produced more cardiospheres in 4 days than other protocols, showing it to be a more rapid protocol for generating cardiospheres.

Table 3.3: Cardiosphere growth conditions used by different groups

Reference	Cell type and origin	CGM serum (%)	Cell density	Growth area	Cardiosphere number	Cellular phenotype
(148)	Adult mouse/rat	0%	1-2 x 10^4 cells/cm^2	10cm^2	1-2/cm^2	Musashi-1, nestin
(99)	Adult mouse/human	0%	0.5-2 x 10^5 cells/ml	NI	Less than 50	c-kit$^+$, CD34$^+$, Sca-1$^+$, cTnI$^+$
(99)	Adult mouse/human	3.5%	0.5-2 x 10^5 cells/ml	NI	Less than160	c-kit$^+$, CD34$^+$, Sca-1$^+$, cTnI$^+$
(109)	Adult rat/human	3.5%	2 x 10^4 cells/ml	NI	NI	c-kit$^+$, CD34$^+$, CD31$^+$, CD90$^+$, cTnI$^+$
(149)	Neonatal rat/human	10%	0.5-2 x 10^5 cells/ml	NI	NI	c-kit$^+$, cTn$^+$, MHC$^+$,SMA$^+$, VT$^+$, vWF$^+$
Present study	Neonatal rat	7%	1.5 x 10^4 cells/cm^2	2 cm^2	~500-600	c-kit$^+$, CD90$^+$, cTnI$^+$

NI; not indicated. cTnI; cardiac troponin I. MHC; myosin heavy chain. cTn; cardiac troponin. SMA; α-smooth muscle actin. VT; vimentin. vWF; von WIllebrad factor.

Recently, Anderson and colleagues (2009) suggested that cardiospheres and CDCs were largely composed of cardiac fibroblasts and $CD45^+$ hematopoietic cells, with no cardiomyogenic potential (150). Although cultured from a similar source (neonatal rat cells), the results here contradict those of Anderson, as passage 2 CDCs expressed several pluripotent stem cell markers (Oct3/4, Sox-2 and Klf-4) and cardiac differentiation transcription factors (GATA4 and Nkx2.5), with very little or no expression of the hematopoietic marker ($CD45^-$). Furthermore, they were able to differentiate into cardiomyocytes. The discrepancy observed is most likely due to extensive modifications made by Anderson (109) to the culture protocol, stem cells being sensitive to *ex vivo* culture conditions. Improper handling of the cell preparation or variation of culture conditions will affect cell characteristics and function (151).

CD117 (c-kit), a stem cell factor receptor commonly expressed on hematopoietic stem cells (152), is used as a surface marker to identify the endogenous cardiac stem cells (28). Immunophenotyping of cells dissociated from cardiospheres showed that c-kit cells comprised about 30% of the cardiospheres (99, 149), which co-localized with replicating cells, indicated by BrdU incorporation, in the core region of the spheres (99). This suggests that cardiospheres are cellular aggregates that structurally provide a 3D, niche-like microenvironment that favours c-kit cell proliferation in the spheres (153). Smith was the first to report the expansion of cardiospheres as a source of cardiac stem cells, showing that 20% of the CDCs expressed c-kit, and approximately 40% were $CD90^+$ (Thy-1 antigen present in most mesenchymal cells). In contrast, we found that CDCs contained only 3 % c-kit cells, and that more than 70% expressed CD90, suggesting that they resembled a more mesenchymal phenotype, as also shown by Tateishi et al. (130). Despite these differences in CDC characteristics (Table 3.4), CDCs were still able to differentiate into cardiomyocytes *in vivo* and regenerate the injured heart.

Table 3.4: Phenotypic characterization of CDCs

Reference	Cell origin	c-kit	CD90	Other markers
(100)	Adult human	~20%	~40%	10% CD31, 5% CD34, ~99% CD105
(118)	Adult rat	~5%	~30%	1% CD31, >1% CD34
(154)	Adult human	7%	18%	99.9% CD105, 1% CD34, 0.62% CD31
Present study	Neonatal rat	3%	71%	10% DDR2

DDR2; Discoidin domain receptor-2.

CDC proliferation was glucose-dependent

Peroxisome proliferator-activated receptor-γ-coactivator-1α (PGC-1α) is a potent transcriptional coactivator that controls mitochondrial biogenesis and oxidative metabolism (155). A reduction in PGC-1α was observed in CDCs when cultured at high glucose concentrations (Figure 3.11), and coincided with a decrease in the mitochondrial enzyme, α-ketoglutarate dehydrogenase. This indicates that high glucose concentrations lowered the dependence of energy production on mitochondrial oxidative phosphorylation in CDCs, reported for other cell types (156). CDCs showed a metabolic phenotype which may result from the Warburg effect (157). The Warburg effect was first described in proliferating cancer cells (158, 159), which had a metabolic switch from mitochondrial oxidative phosphorylation to glycolysis for ATP generation under normoxia, with more than 90% of the glucose carbon converted to lactate. This aerobic glycolysis, or Warburg effect, was later found in other healthy proliferating cells (160), including ESCs (161). In quiescent cells, ATP production results from both glycolysis and oxidative phosphorylation. However, glucose metabolism is essential in proliferating cells to generate not only ATP, but intermediate precursors that are required for biosynthetic pathways, for example ribose for nucleotide synthesis (162). Even though only 2 molecules of ATP are generated per molecule of glucose through glycolysis, a high glycolytic flux in proliferative cells can generate an amount of ATP that exceeds the total ATP production from oxidative phosphorylation in the mitochondria (162). Instead of

utilizing the Krebs cycle to produce ATP, proliferating cells use Krebs cycle intermediates to synthesize lipids, proteins and nucleic acids. Unlike tumour cells, proliferating cells revert back to oxidative metabolism in the resting state (163). Thus, we observed that the Warburg effect was not permanent in CDCs *in vitro*, but could be reversed by altering the glucose levels in the culture medium.

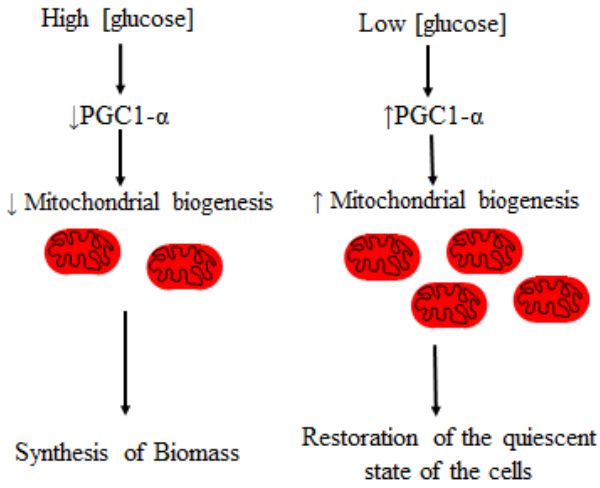

Figure 3.22: Schematic diagram of metabolic alterations in CDCs in response to different glucose concentrations in the culture medium.

MPIO labeling

Labelling cells with MPIO particles enabled verification of successful cell administration and retention non-invasively *in vivo* using MRI. However, the validity of this technique has been questioned, as the hypointense contrast detected using MRI could result from iron-nanoparticles that had been shed by stem cells and engulfed by macrophages (164, 165) or from blood clots (166). However, transplanted cells that were labelled with micron-sized iron particles, MPIOs, have been retained in the heart for 3 weeks (118), and remained detectable after 16 weeks (54, 114). In the present study, MPIO-labelled transplanted cells did not express CD68, confirmed that they were not macrophages.

Several studies have shown that CDCs improved ventricular ejection fraction (LVEF) after myocardial infarction (100, 167), in line with our study. Others showed no augmentation in LVEF with CDCs, but improvements were seen in hemodynamic function and infarct size (168). Here, deterioration in heart function observed in untreated infarcted rats was salvaged by transplanted CDCs and systolic wall thinning over 10 weeks was prevented by CDC treatment. A smaller infarct size and an increase in vascular density were observed in the CDC-treated hearts. These benefits were likely ascribed to direct regeneration through cell differentiation and through secretion of paracrine factors that led to neoangiogenesis and recruitment of endogenous cardiac stem cells (167, 169).

In summary, the work in this chapter was to develop a method to increase cardiosphere production and a more rapid method of generating CDCs. The modifications in culture conditions described in the present study enabled culture of 1.5×10^7 of CDCs in 16 days. The modifications were included as part of the standard protocol (Figure 3.23) in culturing CDCs for all experiments described in the later part of this thesis. Immunophenotyping revealed that CDCs contained a mixture of stem cells and differentiated cells, and were capable of differentiation into cardiomyocytes *in vitro* and *in vitro*. MPIO labelling allowed cell tracking *in vivo* using MRI without compromising cell properties and function. CDCs improved ventricular ejection fraction after myocardial infarction in rat and the benefit persisted for at least 16 weeks.

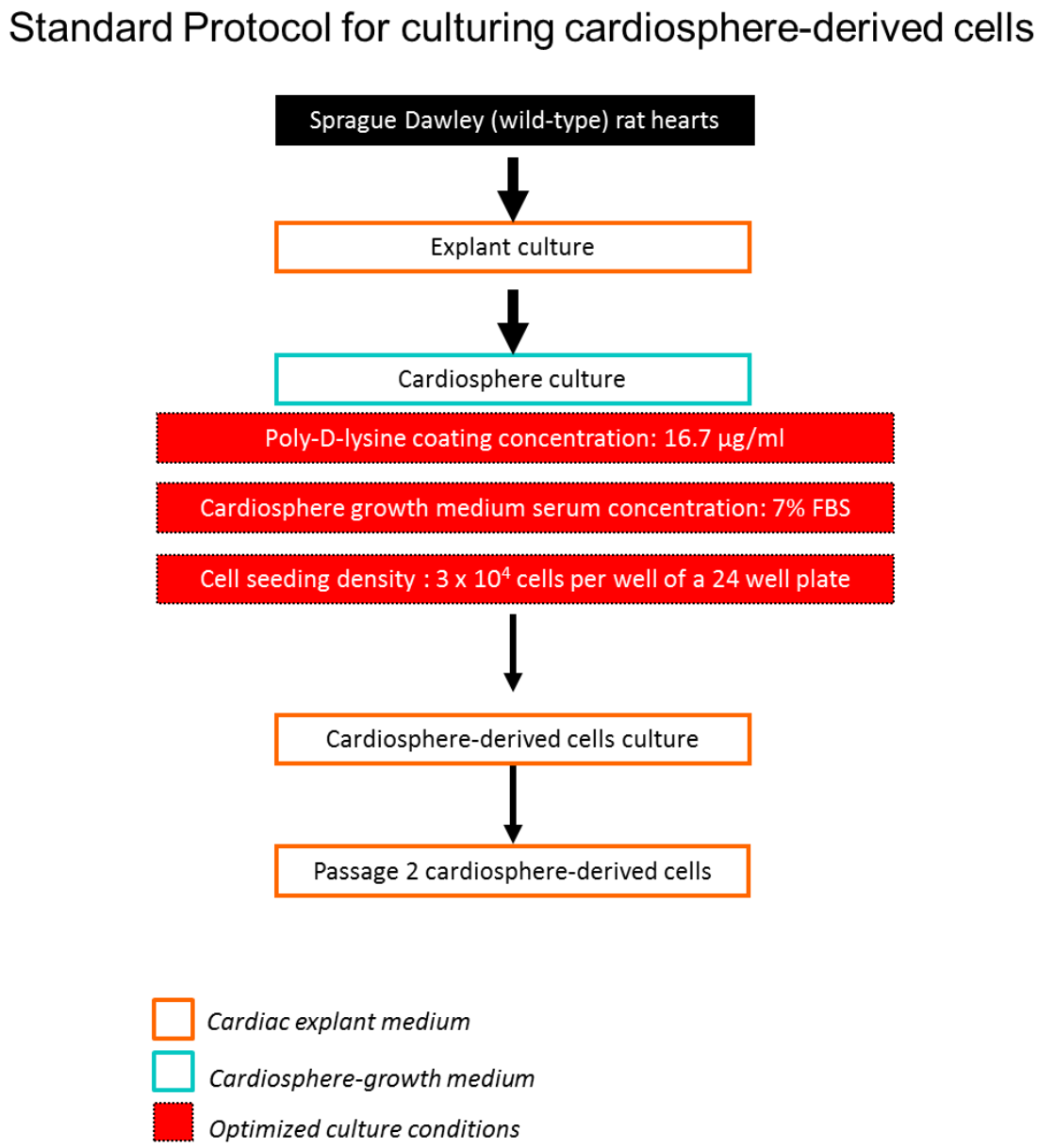

Figure 3.23: Flow diagram showing the standard protocol which was established after culture modifications.

Study limitations

There were a few limitations in the experimental design described in this chapter. Firstly, the heart tissue from neonatal (1 or 2 day-old SD rats) was used as the starting material for explant culture and optimization experiments. This may preclude direct comparisons of total cell yield and time required for *in vitro* expansion with the published data, which used the

tissue from adult heart for explantation. In addition, a faster rate of explant cell migration and proliferation was observed when compared with 5 weeks SD rat heart explants (data not shown). Therefore, the rate of cardiosphere formation, and the optimal culture conditions described in this chapter, may not apply to the explant cells derived from adult heart tissue. Furthermore, isolating cardiac-derived stem cells from human infants would raise ethical and safety concerns, which could prevent the transfer of the protocols to the clinic when culturing CDCs from human tissues, in the longer term.

Secondly, the immunolabelling for characterizating the CDC phenotype did not include quantification of labelled cells. This may be useful to identify the proportion of stem cells to differentiated cells in the populations and help to monitor culture events that may change the cell identity, e.g. spontaneous stem/progenitor cell differentiation. Future investigations would include quantification of labelled cells, which could be achieved by performing flow cytometry on fixed cells. As for flow cytometry experiment, analysis was performed without using a live cell gating strategy. Although a non-specific secondary antibody was used as a negative control in addition to unstained cells, live cell gating would aid in excluding the dead cell population that may potentially give rise false positive staining in the analysis due to internalization and binding of unspecific antibodies.

Chapter 4

Optimization of culture conditions to increase c-kit^{+} cells from explant tissue for cell therapies

4.1 ABSTRACT

Although cardiosphere-derived cells (CDCs) at passage two were functionally competent, their therapeutic effect may be limited by the low proportion of c-kit$^+$ cells. Therefore, two approaches were used to increase the number of c-kit$^+$ cells in CDCs, using hanging drop culture for generation of cardiospheres and varying the extracellular matrix (ECM) for cell expansion. Flow cytometry revealed that EDCs contained a small population of c-kit$^+$ cells (~4-7%), which do not decrease over multiple isolations. The first isolation of EDCs contained about 22 ± 4% of CD90-expressing mesenchymal cells and this increased significantly to 37% and remained at that level after the second isolation. It was found that phase bright cells did not form cardiospheres, or express c-kit after clonal amplification. The hanging drop culture method produced cardiospheres with increased levels of c-kit$^+$ cells than the poly-D-lysine-coated and low-bind bacterial grade culture dishes. EDC migration, CDC proliferation and clonogenicity, cardiosphere number and the proportion of c-kit$^+$ cells in EDCs and CDCs were examined after culturing on fibronectin, laminin, gelatine and collagen I and IV. Collagen IV enhanced EDC migration and produced the highest proportion of c-kit$^+$ cells (10 ± 4%) in explant culture. CDCs became more adherent, highly proliferative and contained more clonogenic cells on collagen IV compared with other matrices, yet contained a low number of c-kit$^+$ cells. Nevertheless, expansion on collagen IV, with cardiosphere culture in hanging drops, increased the number of c-kit+ CSCs to 11%. In contrast, collagen I produced a high proportion of c-kit$^+$ cells (9 ± 2%) in CDCs, but showed poorer cell migration and produced fewer cardiospheres and clonogenic cells compared with collagen IV. In conclusion, the optimal culture protocol employed collagen IV for EDC and CDC culture and expansion, with hanging drop culture to generate cardiospheres.

4.2 INTRODUCTION

Endogenous cardiac stem cells are responsible for intrinsic heart repair and myocyte turnover, and have the potential to regenerate injured myocardium. However, the endogenous stem cell-repair system fails after myocardial infarction. This is caused by a substantial depletion in resident cardiac stem cell (CSC) number (170) and other factors that possibly limit the self-renewal, proliferation and differentiation capability of the remaining viable stem cells (171). Therefore, CSC isolation and *ex vivo* expansion is needed to generate sufficient cells to replace CSC loss and reconstitute the infarcted myocardium.

Tissue explantation is one of the best methods to isolate and expand cardiac stem cells, and has been employed in a recent clinical trial (CADUCEUS). CDCs are cultured from the explant derived cells (EDCs) via the formation of cardiospheres, with a c-kit$^+$ cell selection and enrichment step (99), before amplification to the number necessary for therapy (100). *Chapter 3* described an efficient method to culture cardiosphere-derived cells (CDCs) in 16 days, with a significant improvement in cardiac function *in vivo* after treating with CDCs. However, the 3% c-kit expression in the CDC population raised concerns, as c-kit$^+$ cells may be pivotal for the therapeutic effect of CDCs. Therefore, the degree of c-kit$^+$ cell amplification from explant-derived cells (EDC) to CDCs was studied, as was methods for augmenting the c-kit$^+$ cell numbers by defining the cardiosphere culture method and the effect of extracellular matrix proteins.

Different culturing methods for cardiospheres have been proposed. Cardiospheres have been cultured from rat, mouse, pig and human, using poly-D-lysine coated plates, which gave high level of c-kit$^+$ cells (10-20%) (99, 100, 109), although discrepant observations exist (172). Others generated cardiospheres using a low-bind bacterial grade culture dish, but this resulted in only 0.8% c-kit$^+$ cells (130). This suggests that modifications to the culture method could

change cell identity. To date, no direct comparison has been made between methodologies to evaluate the impact of the modifications on the cardiospheres and c-kit$^+$ cells. Hanging drops create surface tension and allow cells to aggregate. They have been employed in the culture of embryoid bodies from embryonic stem cells (ESCs) (173) and to promote ESC cardiomyogenic differentiation. Here, hanging drop culture was compared with culture in two-dimensional poly-D-lysine-coated and low-bind bacterial culture dishes, to grow cardiospheres and evaluate the number of c-kit$^+$ cells in passage two CDCs.

Stem cell expansion *in vitro* may compromise stem cell properties and potential (174). A broad consensus has been reached that the fate of stem cells is determined by the surrounding microenvironment, in which stem cells reside (175). This specialized microenvironment, or niche, dictates the undifferentiated state of stem cells by coordinating self-renewal and differentiation of the cells (176). One of the important niche components for stem cells is the extracellular matrix, which provides not only the structural and mechanical support for the cells, but also modulates cells through several biochemical signalling pathways (177). Many studies have shown that cell-ECM interactions significantly influence stem cell self-renewal, migration, proliferation and differentiation *in vitro* (178-181). Therefore, mimicking one aspect of the stem cell niche, by determining the preferred extracellular matrix to regulate and control stem cell self-renewal and differentiation *in vitro*, may provide useful information for establishing an ideal culture condition for long term expansion of competent stem cells.

Cardiosphere generation selects and enriches c-kit$^+$ cells from the explant-derived cells without antibody sorting (99). However, as also shown by others (153, 182), it was found that the level of c-kit$^+$ cells in CDCs was ~3% at passage two and comparable to that found in EDCs. Although the loss of c-kit expression apparently did not affect the efficacy of the

CDCs in treating the injured heart, it is possible that low level of c-kit$^+$ cells in CDCs may limit the regenerative potential of CDCs.

Previous reports have documented that levels of fibronectin, collagen type I and type IV increase during myocardial infarction (183), which coincides with the activation of c-kit$^+$ cardiac stem cells (78); whereas laminin, fibronectin and collagen IV have been proposed to be the extracellular matrix found in the putative niche for c-kit$^+$ cardiac stem cells (153, 184, 185). To improve the cardiosphere culture method, and obtain a higher level of c-kit$^+$ cells in passage two CDCs, collagen I and IV, fibronectin, laminin and gelatin were tested to determine whether c-kit$^+$ cells in CDC can be preserved after two passages in culture.

Previously in *Chapter 3*, neonatal rat heart tissue was used as the starting material for isolating explant-derived cells. However, as the use of heart tissue from infants is not applicable for the use in clinic. In order to establish a clinically transferable culture protocol for CDCs, all experiments described in this chapter were performed using CDCs isolated from 5-week-old SD rat hearts.

4.3 METHODS

The study design described in this chapter is illustrated in a simplified flow diagram (Figure 4.2 - 4.4). Specific experimental methodologies are described below.

4.3.1 EDC characterization

Cells were characterized using immunofluorescence staining and quantification of labelled cells was performed using flow cytometry. The procedures were performed according to the protocols described in *Chapter 2*.

4.3.2 Phase bright cell isolation and cardiosphere formation

Heart explants were cultured from 5-week old rats. Phase bright cells, budding from explant tissue, were collected by several washes with phosphate buffered saline (PBS). Collected phase bright cells were centrifuged and induced to form cardiospheres, as described in *Chapter 2*.

4.3.3 Explant migration

Heart explant tissues were plated on 60 mm petri dishes, coated with either 10 µg/ml fibronectin from bovine plasma (F1141, Sigma), 10 µg/ml laminin from Engelbreth-Holm-Swarm murine sarcoma (L2020, Sigma), 1% w/v type A gelatine from porcine skin (G1890, Sigma) , 100 µg/ml collagen I from calf skin (C8919, Sigma) or 10 µg/ml collagen IV from Engelbreth-Holm-Swarm murine sarcoma (C0543, Sigma), according to the manufacturer's protocol. Images of explants with migrating cells were taken after 5 days in culture (Figure 4.1). The maximum distance of cell migration in the explant culture was measured (in mm) from at least 8 plated explant tissues for each matrix, using imageJ.

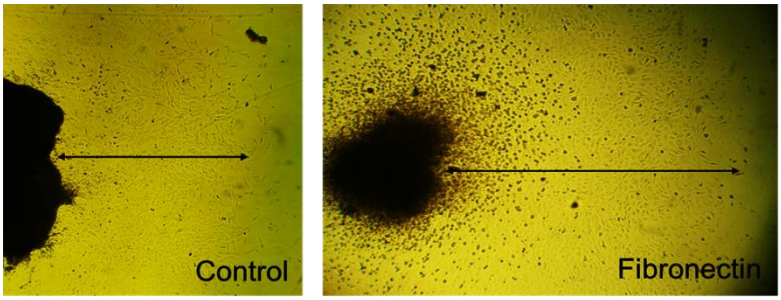

Figure 4.1: Representative images of an explant with migrating cells growing on an uncoated petri dish (control, left) and on fibronectin (right). The maximal distance of cell migration after 5 days in culture was measured using imageJ.

4.3.4 Cell adhesion and proliferation

Passage two CDCs (500) were seeded into each well of a 96-well plate coated with fibronectin, laminin, gelatine, collagen I or collagen IV. Cells seeded in the uncoated wells served as the control. After two hours, non-adherent CDCs were removed by multiple washes with PBS and the number of adherent CDCs were assessed using Alamar®Blue. CDC proliferation was measured at day 0, day 1, day 2 and day 3 using Alamar®Blue, according to the protocol described in *Chapter 2*.

4.3.5 Clonogenic assay

Passage two CDCs, which had been cultured under the standard protocol using fibronectin, were expanded on fibronectin, gelatine, laminin, and collagen I and IV for two passages. The passage 4 CDCs were then plated at a single cell per well (n = 5) and the total number of wells containing colonies was calculated after 2 weeks. About 6 of the wells with single-cell derived colonies were randomly selected, trypsinized and expanded in a 6-well plate to confirm the proliferation of the colony-forming cells. CDC clonal efficiency was calculated as described in *Chapter 2*. The difference of the clonal efficiency of CDCs cultured on different ECMs was analysed using one-way analysis of variance (ANOVA) with Tukey post hoc test.

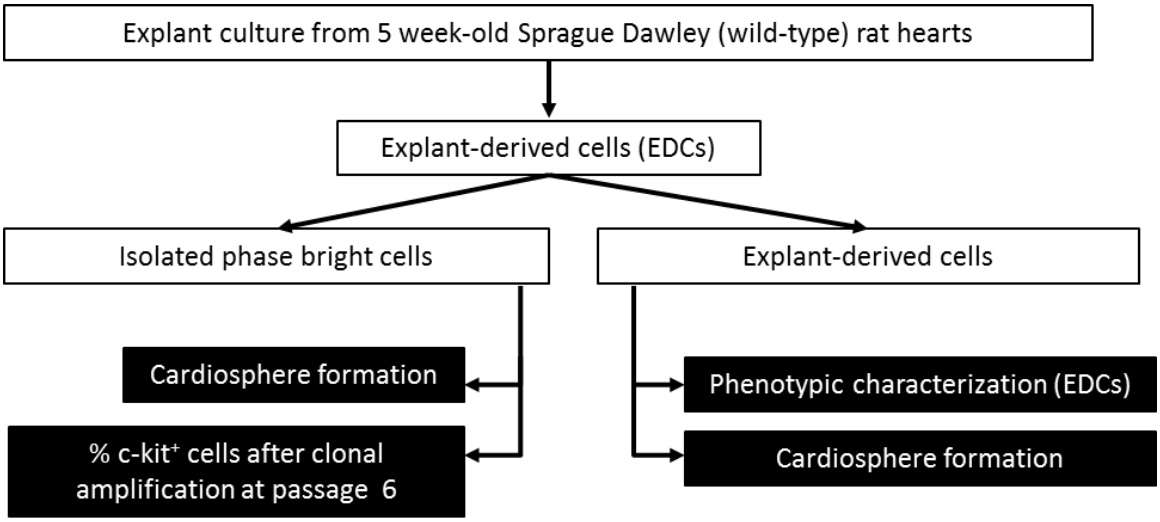

Figure 4.2: Flow diagram showing the experimental design for characterizing explant-derived cells.

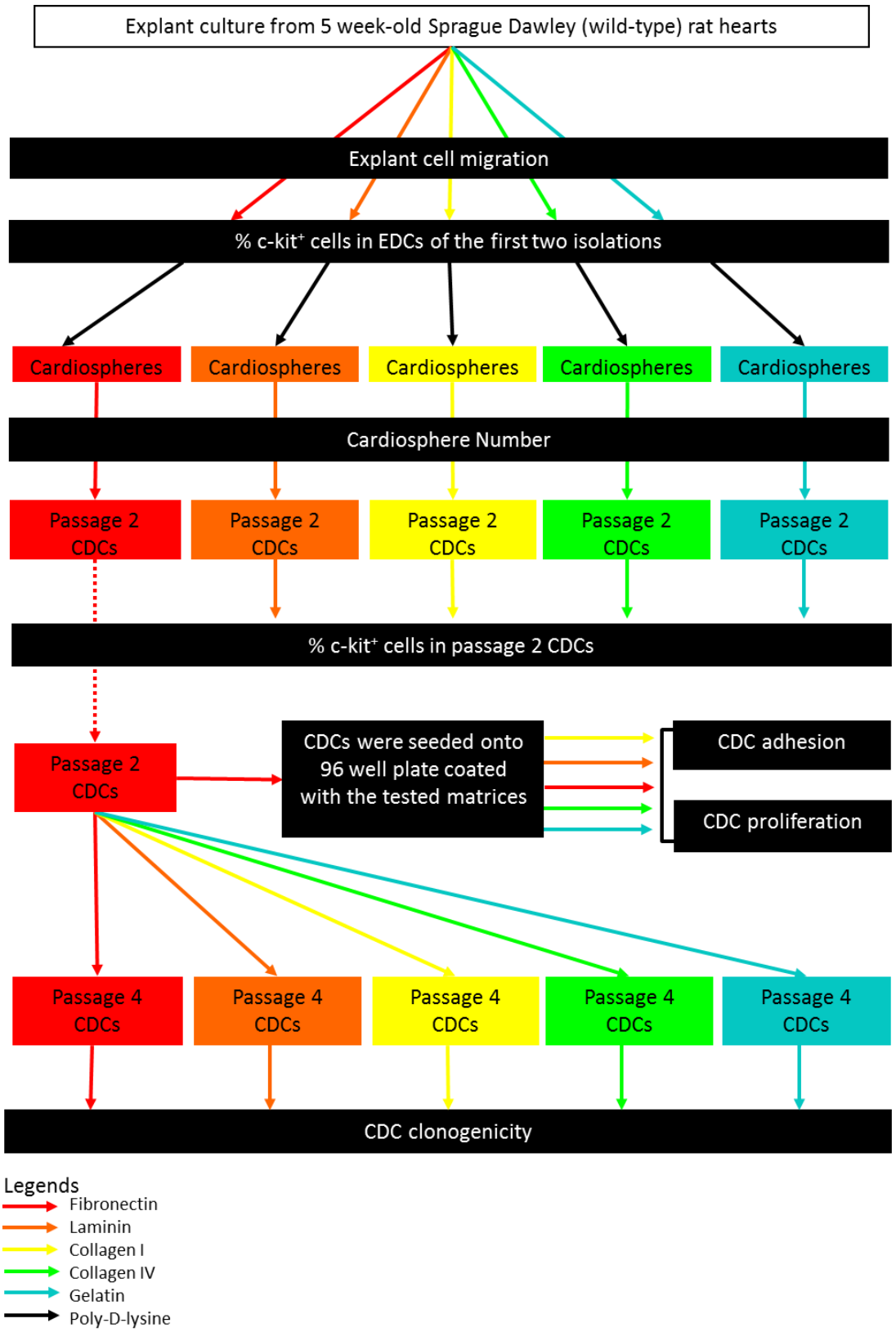

Figure 4.3: Flow diagram describing the experiment design for identifying the optimal extracellular matrices to be used in culturing CDCs.

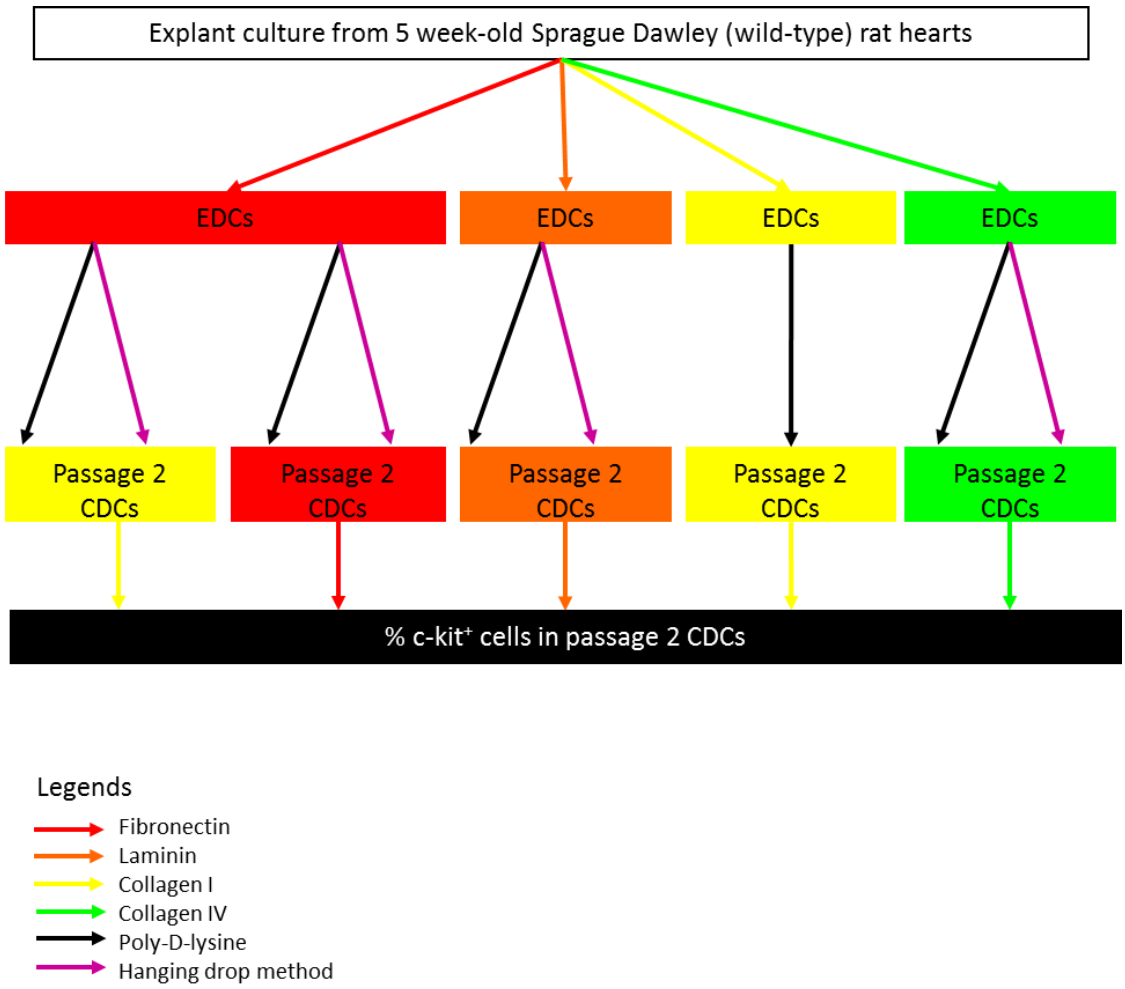

Figure 4.4: Flow diagram showing the study design to examine the percentage of c-kit$^+$ cells in CDCs following the incorporation of hanging drop culture and the selected extracellular matrices.

4.4 RESULTS

4.4.1 Characterization of explant-derived cells

Explant-derived cells (EDCs) contain both non-adherent phase bright cells and adherent stromal-like cells. To characterize EDCs, migrated EDCs were isolated from heart explants every 7 days, up to 4 times. Immunofluorescent-labeling showed that adherent EDCs contained cells expressing von Willebrand factor (vWF), which is an endothelial cell marker (Figure 4.5). EDCs consistently expressed c-kit and CD90 (Figure 4.6). No significant difference in the amount of c-kit+ cells (~4-7%) was observed between isolations. The percent of $CD90^{+}$ cells in the first EDC isolation was 22 ± 4%, but this significantly increased to 38 ± 5% in the second isolation, to remain constant for the third (38 ± 3%) and the fourth isolation (37 ± 4%).

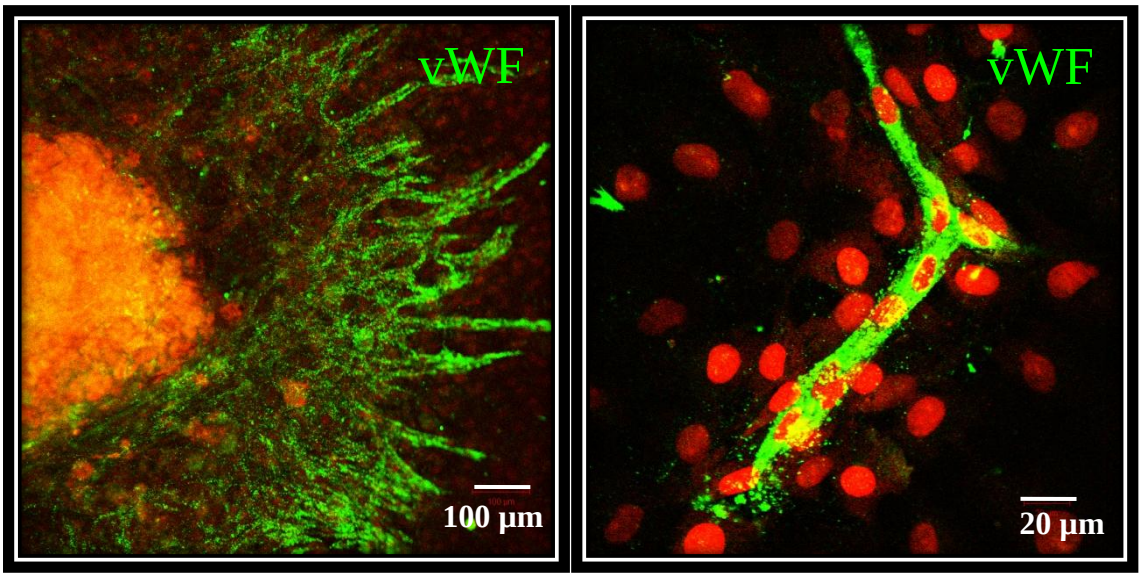

Figure 4.5: Representative confocal images of explant-derived cells (n=3) labelled for (A) vWF-expressing cells (green, AlexaFluor 488) migrating from the explant. (B) Magnified image of vWF expressing EDCs.

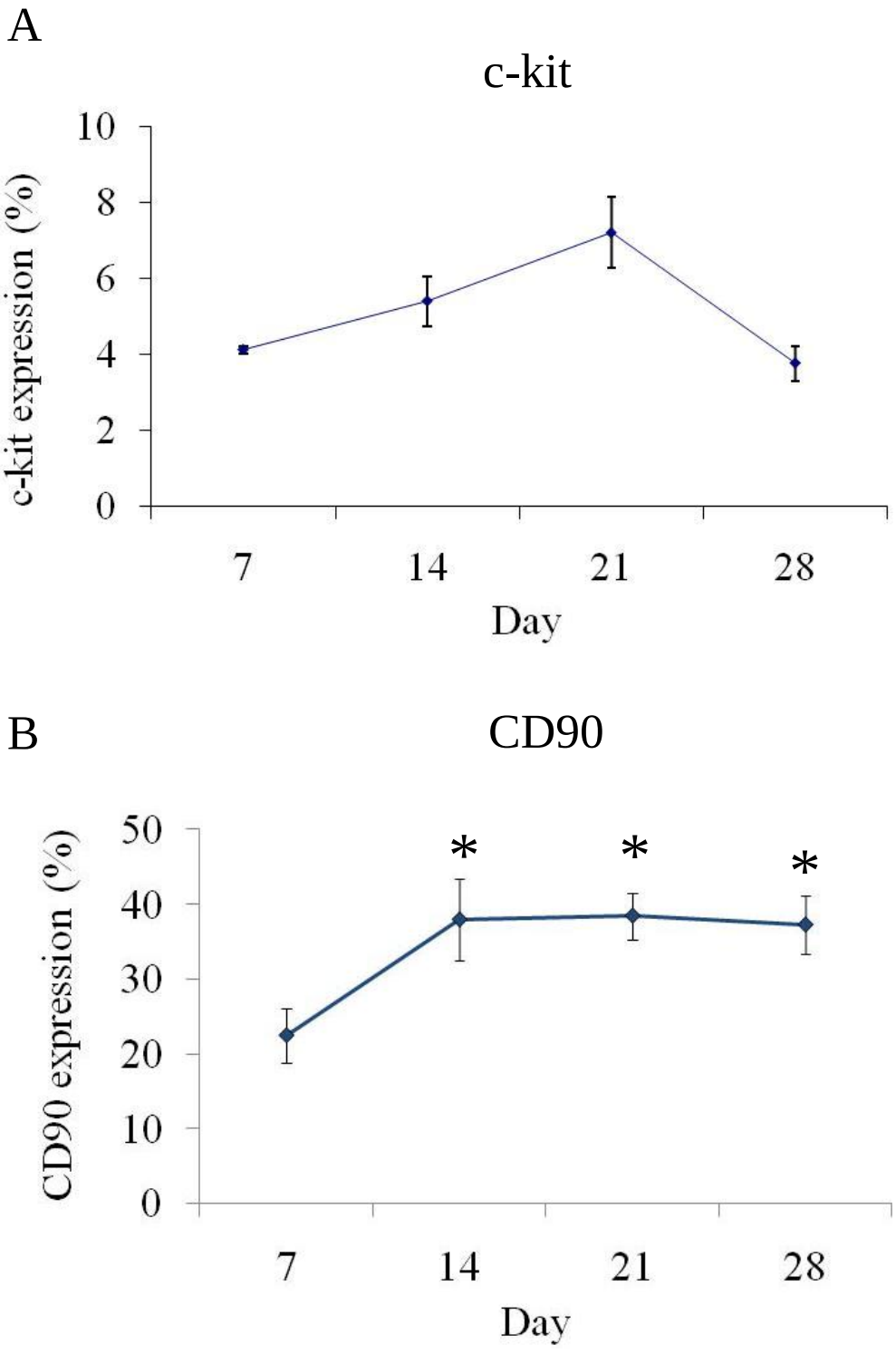

*Figure 4.6: EDCs isolated from 5-week old SD rat heart explants (n=4) were characterized for c-kit (A) and CD90 (B) expressing cells at day 7, 14, 21 and 28.Data are presented as mean ± SD. Statistical analysis were performed using one-way ANOVA. * P < 0.05 vs day 7.*

Phase bright cells are a loosely adherent subpopulation of explant-derived cells. These cells can be isolated by gently washing explant dishes with PBS. The yield of phase bright cells from the explant culture was generally low (< 10,000 cells/60 mm dish). To investigate whether the phase bright cells were the main source of cardiosphere-forming cells, phase bright cells were isolated by three gentle washes of the explant dish after 7 days using PBS, and then incubated with CGM, according to the protocol described in *Chapter 3*. Only one cardiosphere formed from 90,000 plated phase bright cells (Figure 4.7).

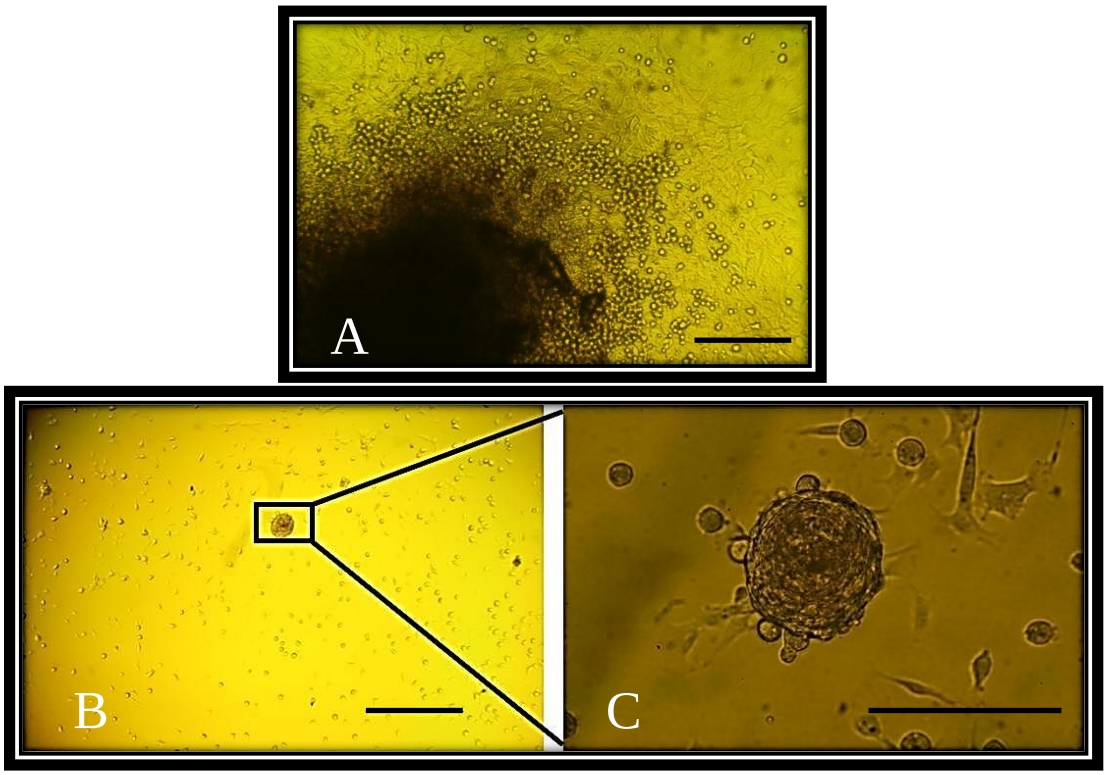

Figure 4.7: Rat heart explants (from 5 weeks old SD rat) were plated on fibronectin and cultured in CEM for 7 days. Representative images from three independent heart explant cultures were taken at day 7. (A) Phase bright cells are round, bright in appearance, semi-attached and a subpopulation of explant-derived cells on top of adherent stromal-like cells. (B) The majority of the phase bright cells did not form cardiospheres (n=3). (C) Cardiospheres generated from phase bright cells had a similar morphology to those derived from explant-derived mixed-population cells. Scale bar = 250 µm

To determine whether c-kit^{+} cells in EDCs were from the phase bright cell (PBC) population, PBCs were tested for c-kit expression. Due to the extremely low number of cells that could be isolated from explant culture, amplification of the cells was needed to provide sufficient cells

for flow cytometry analysis. However, in order to reduce the possible contamination by a non-stem cell population, PBCs were amplified based on cell clonogenicity, a stem cell feature which has also been reported in c-kit^{+} cardiac stem cells (28). Freshly isolated, phase bright cells were collected and plated in a T75 culture flask coated with fibronectin to allow cell growth, but at a very low density (approximately 3-5 cells/ cm^{2}). This allowed only the clonogenic cells to be amplified, whilst the number of quiescent cells remained unchanged in the flask. After 7 days, amplified phase bright cells formed colonies throughout the culture flasks, while quiescent cells remained adhered individually without sign of proliferation (Figure 4.8). Then, colony-forming cells were trypsinised and plated at one cell per two wells on a 96-well plate. Wells containing a cell colony were trypsinized and cells were expanded on a culture dish to passage 6, and analysed for c-kit. However, none of them (out of 4 randomly selected colonies) were c-kit^{+} (Figure 4.8E).

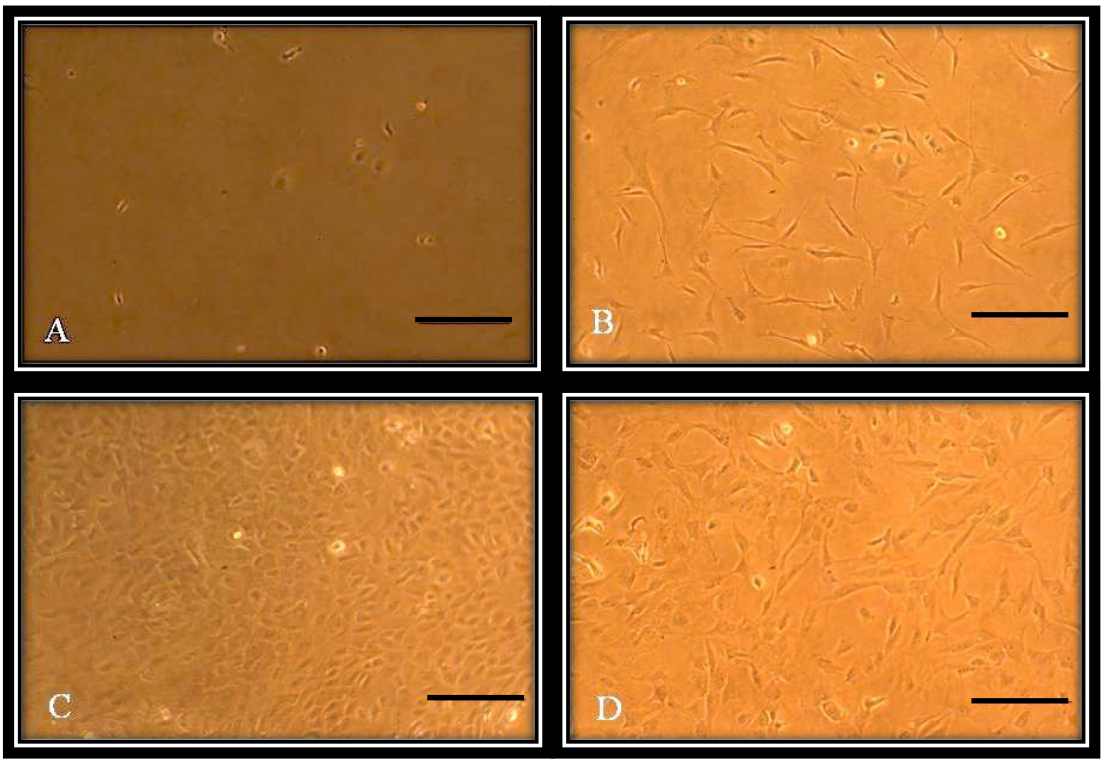

E

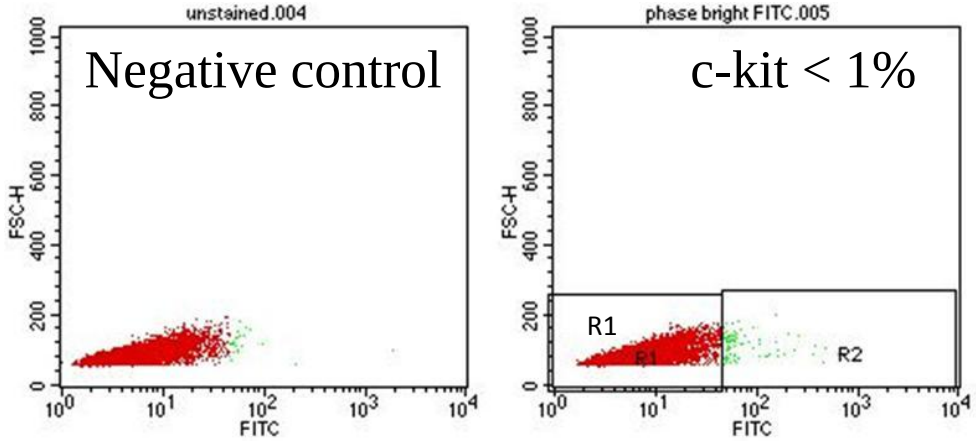

Figure 4.8: Cell colonies, with distinct morphology, formed from phase bright cells when plated at low density (3-5 cells/cm^2) after 20 days, which were (A) small round, non-proliferative quiescent cells (B) elongated, spindle-shaped cells, (C) round and amplifying cells, and (D) stromal/fibroblast like cells. (E) Flow cytometry analysis of passage 6 phase bright cells showed that they did not express c-kit (n=4). Region R1 gated the negative population and region R2 gated the positive. Scale bar = 250 µm

4.4.2 Optimizing cardiosphere growth: evaluation of the cardiosphere culture method

4.4.2.1 The effect of trypsin digestion on cardiosphere number

Trypsin digestion of EDCs during isolation could affect cardiosphere production. EDCs were cultured from three 5-week-old rats. Isolation of EDCs was performed using 0.05% trypsin at day 7. Times of trypsin incubation (2 and 5 minutes) were tested and the dissociated cells were induced to form cardiosphere in CGM for 4 days. The number of cardiospheres generated was calculated by an experimentally-blinded investigator (performed by Lien-Cheng Hsiao). A reduction in cardiosphere number was observed after 5 minutes of trypsin treatment, compared with that of 3 minutes (Figure 4.9). This indicates that 5 minutes of trypsin treatment may have caused disruption to EDC surface proteins and interrupted cardiosphere formation.

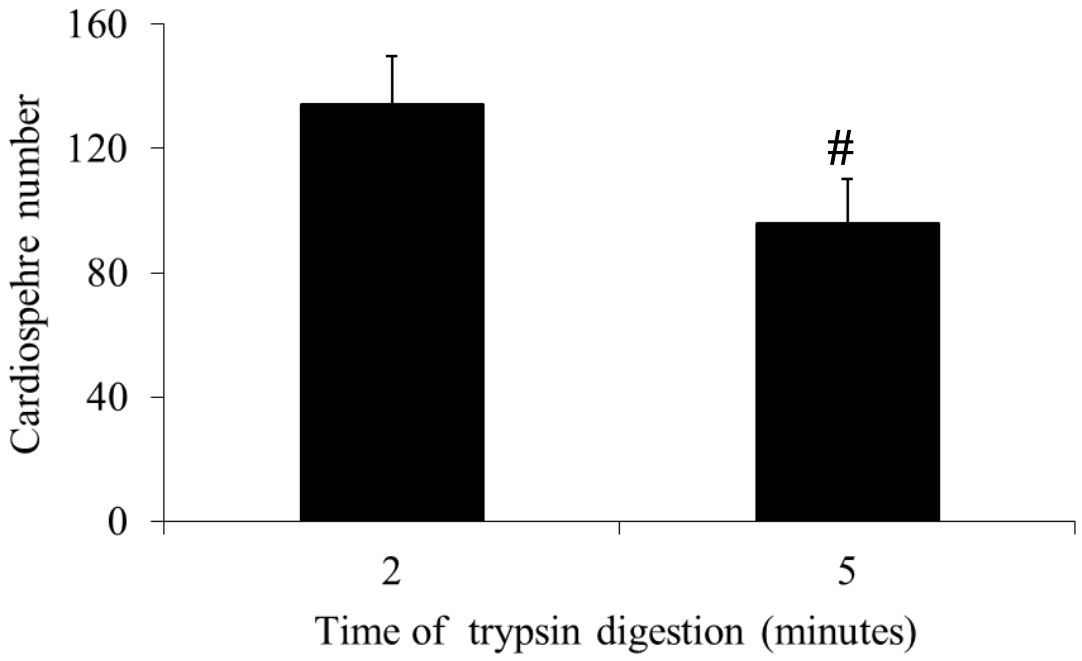

Figure 4.9: Cardiospheres were generated from five independent 5-week old SD rat heart explants using the standard method described in chapter three. Cardiosphere number decreased after trypsinization for 5 minutes. Data are presented as mean ± SD. Statistical analysis was performed using student t-test. # $p<0.05$ compared to 2 minutes.

4.4.3.2 Hanging drop technique in culturing cardiospheres

To examine whether altering the method to grow cardiospheres could increase the number of c-kit^{+} cells, EDCs were plated using the hanging drop technique or on uncoated bacterial-grade petri dish. EDCs formed smaller cardiospheres when plated on the bacterial grade culture dish, compared with those formed on poly-D-lysine coated plates. However, the size of cardiospheres cultured using the hanging drop technique showed a direct relationship with the cell density seeded per drop (Figure 4.11). An EDC density of 1000 cells per 25 µl CGM or more produced more than one cardiosphere (Figure 4.10). Phase bright cells cultured using hanging drops gathered together, but were not adherent to each other, and did not form cardiospheres (Figure 4.12).

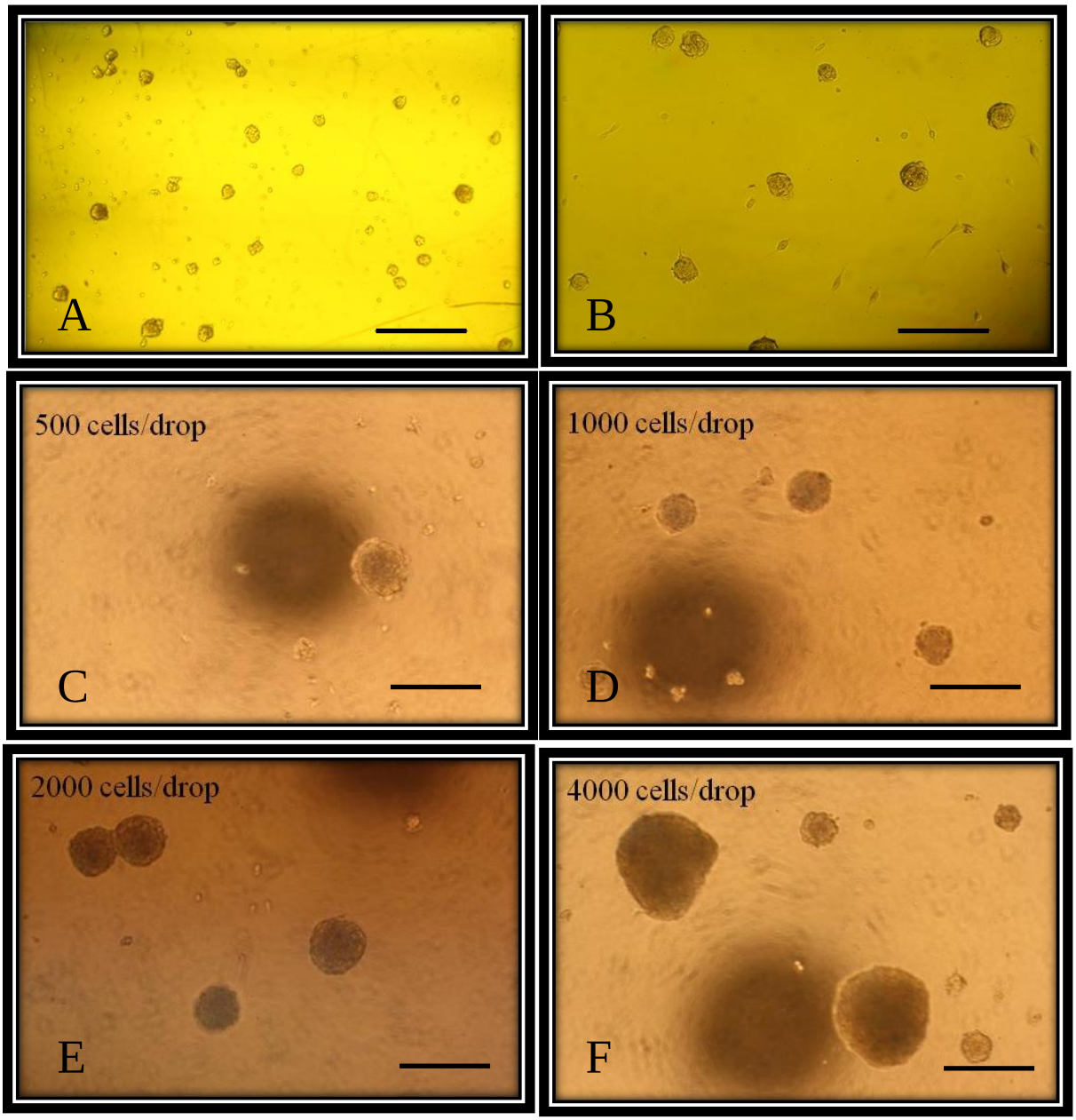

Figure 4.10: Representative images of cardiospheres cultured using different methods from three independent experiments. (A) Cardiospheres produced on bacterial grade petri dishes (1 x 10^5 cells/ml) showed relatively small sizes on low-bind culture dishes. (B) Cardiospheres cultured on poly-d-lysine using standard protocol. (C) Culturing of cardiospheres using the hanging drop technique with cell density of (C) 500, (D) 1000, (E) 2000, and (F) 4000 cells per 25 µl CGM shows that cardiosphere size increased with increasing cell densities. Scale bar = 250µm

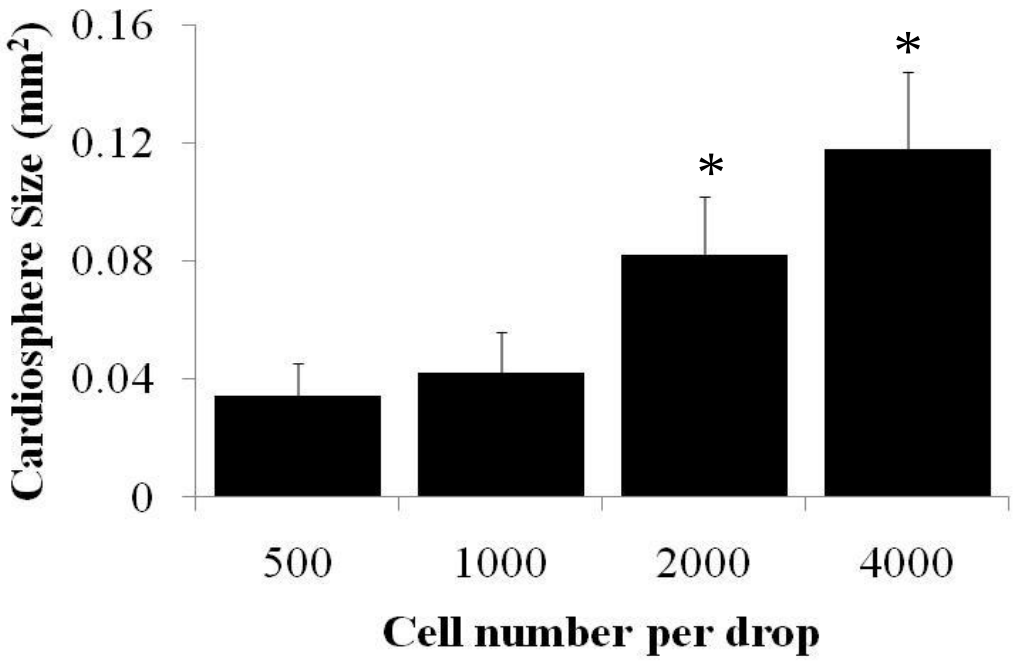

Figure 4.11: Cardiospheres were cultured in hanging drops at different cell densities. Representative images were taken while cardiospheres were still in hanging drops 3 days after plating. Cardiospheres (n=20) size were calculated using imageJ. Size of the cardiospheres generated using the hanging drop method increased with cell density.Data are presented as mean ± SD. Statistical analysis was performed using one-way ANOVA. P < 0.01 vs 500 cell per drop.*

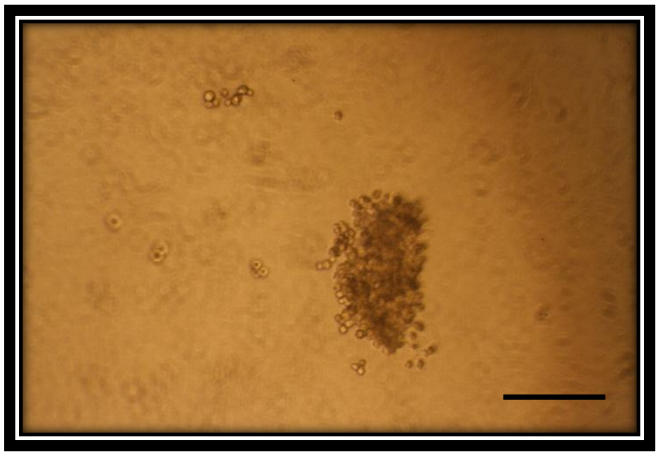

Figure 4.12: Non-adherent phase bright cells were isolated from the explant culture through washing with phosphate buffered saline (PBS) without trypsinization. Representative images of three independent experiments were taken at day 3 after phase bright cells were plated in hanging drops (500 cells per 25 µl). Phase bright cells did not form cardiospheres when cultured using the hanging drop technique. Scale bar = 250µm

Cardiospheres produced on bacterial grade petri dishes, poly-D-lysine (1 x 10^5 cells/ml) or by hanging drop (plated at 500 cells/25 µl droplet) were expanded in monolayers on fibronectin. C-kit expression was determined in the expanded cardiosphere-derived cells at passage two using flow cytometry. Hanging drop-derived cardiospheres gave more c-kit$^+$ cells in passage two CDCs (9 ± 3%) than that on poly-D-lysine (3 ± 1%) or bacterial grade petri dishes (2 ± 1%) (Figure 4.13).

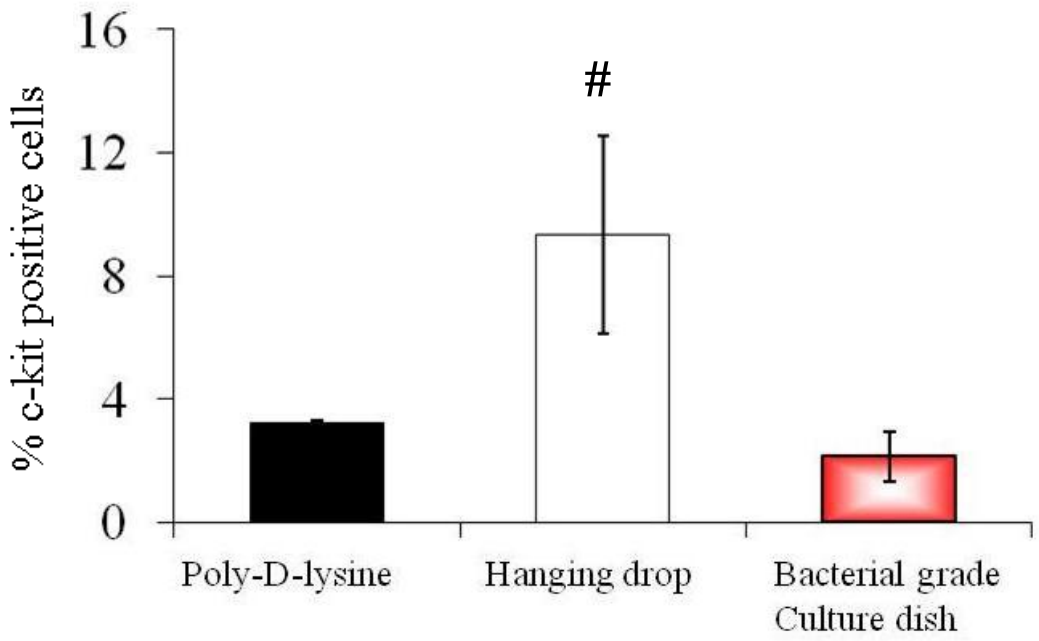

Figure 4.13: Percentage of c-kit$^+$ cells in passage two CDCs were analysed using flow cytometry after culturing cardiospheres on bacterial grade petri dishes (1 x 10^5 cells/ml), poly-D-lysine (as described in the standard protocol) or by hanging drop (plated at 500 cells/25 µl droplet) and expanded in monolayers on fibronectin. Hanging drop-derived cardiospheres produced higher c-kit$^+$ cells in passage two CDCs. Data are presented as mean ± SD (n=3). Statistical analysis was performed using one-way ANOVA. # $P < 0.05$ compared with poly-D-lysine.

To examine whether HD-CSp of different sizes contained c-kit expressing cardiac stem cells, cardiospheres generated from different cell densities were grown on fibronectin coated coverslips for 24 hours and immuno-labelled for c-kit. Confocal microscopy revealed that cardiospheres of all sizes contained c-kit expressing cells (Figure 4.14).

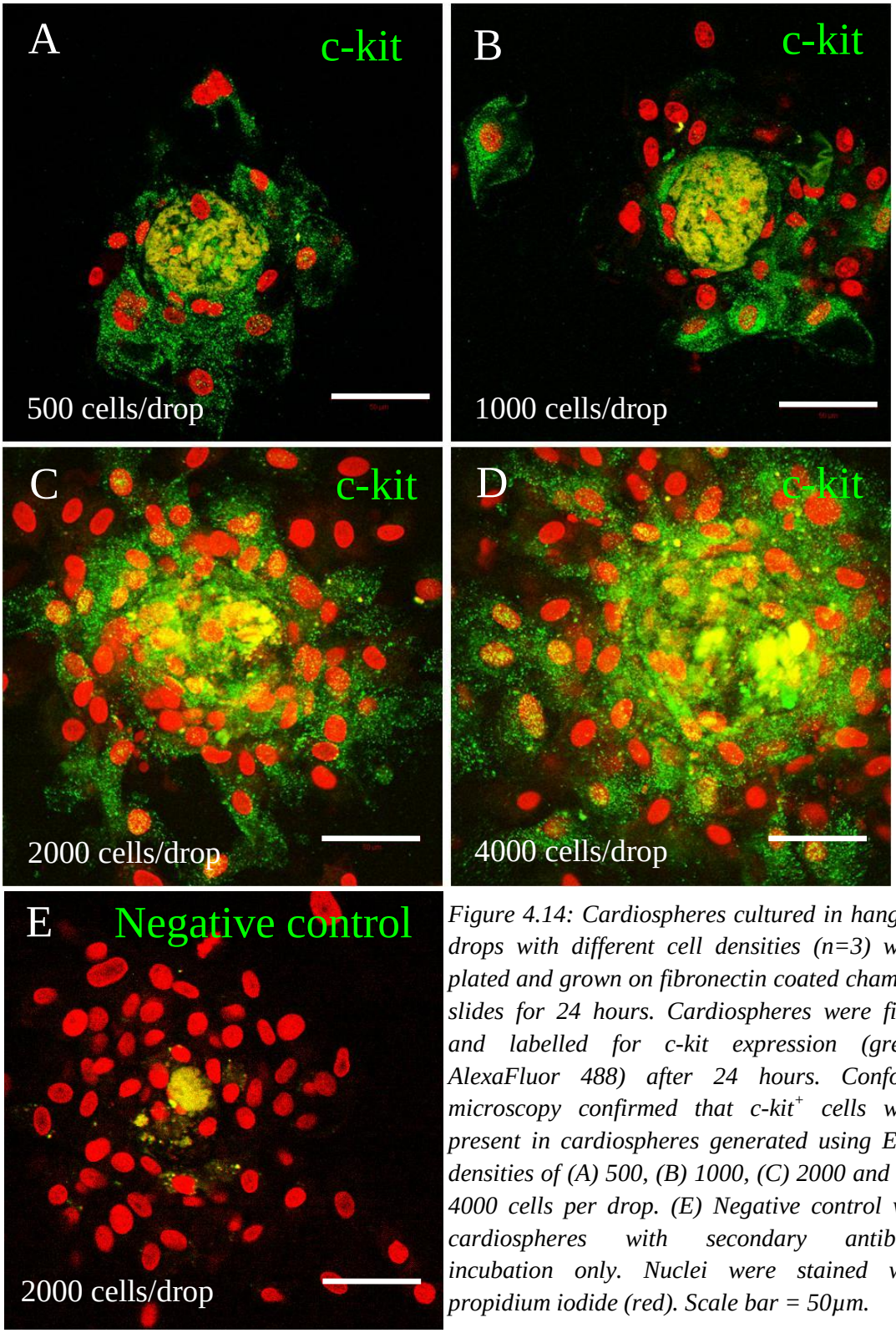

Figure 4.14: Cardiospheres cultured in hanging drops with different cell densities (n=3) were plated and grown on fibronectin coated chamber slides for 24 hours. Cardiospheres were fixed and labelled for c-kit expression (green, AlexaFluor 488) after 24 hours. Confocal microscopy confirmed that c-kit^{+} cells were present in cardiospheres generated using EDC densities of (A) 500, (B) 1000, (C) 2000 and (D) 4000 cells per drop. (E) Negative control was cardiospheres with secondary antibody incubation only. Nuclei were stained with propidium iodide (red). Scale bar = 50µm.

In a series of z-stack confocal microscopy images, with 0.9 µm for each slice interval, the c-kit$^+$ cells (green) could clearly be distinguished from the unstained cells among the cells that migrated from the cardiosphere (Figure 4.15). This confirmed that the cardiosphere-derived cells were rich in c-kit$^+$ cells.

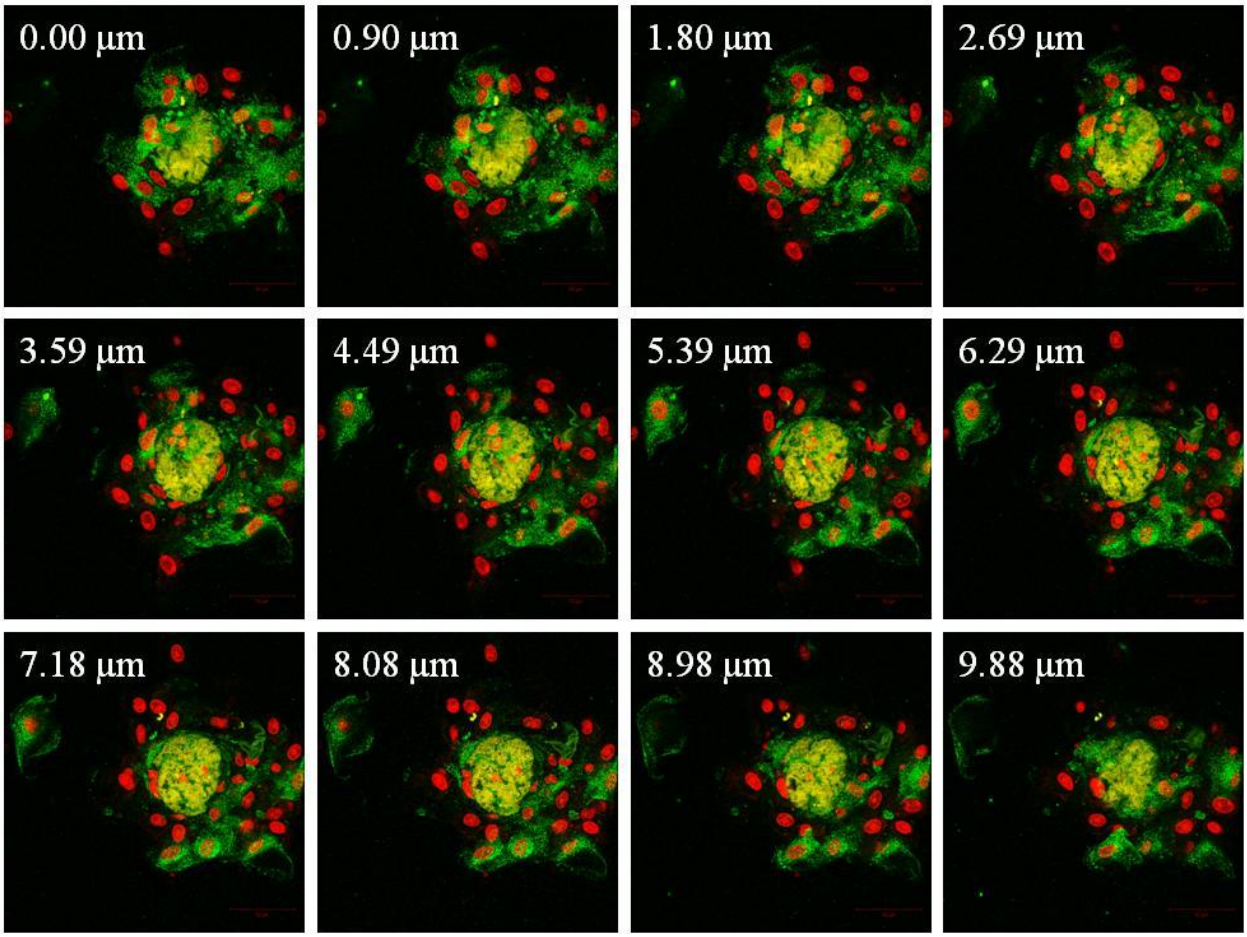

Figure 4.15: A series of z-stack images of cardiospheres plated on fibronectin. Green staining (AlexaFluor 488) represents c-kit, and red propidium iodide stained cell nuclei.

4.4.3 The effect of extracellular matrix on CDC expansion

4.4.3.1 Explant-derived cell migration was optimal on fibronectin, laminin and collagen IV

Heart explants were cultured on fibronectin, gelatin, laminin, and collagen I and IV. Explants plated on the uncoated petri dish served as the control. The maximal distance cells migrated from the explants was significantly further on fibronectin, laminin and collagen IV (2.1 ± 0.3 mm, 1.8 ± 0.2 mm and 2.1 ± 0.4 mm, respectively), compared with the control (1.2 ± 0.3 mm) (Figure 4.16).

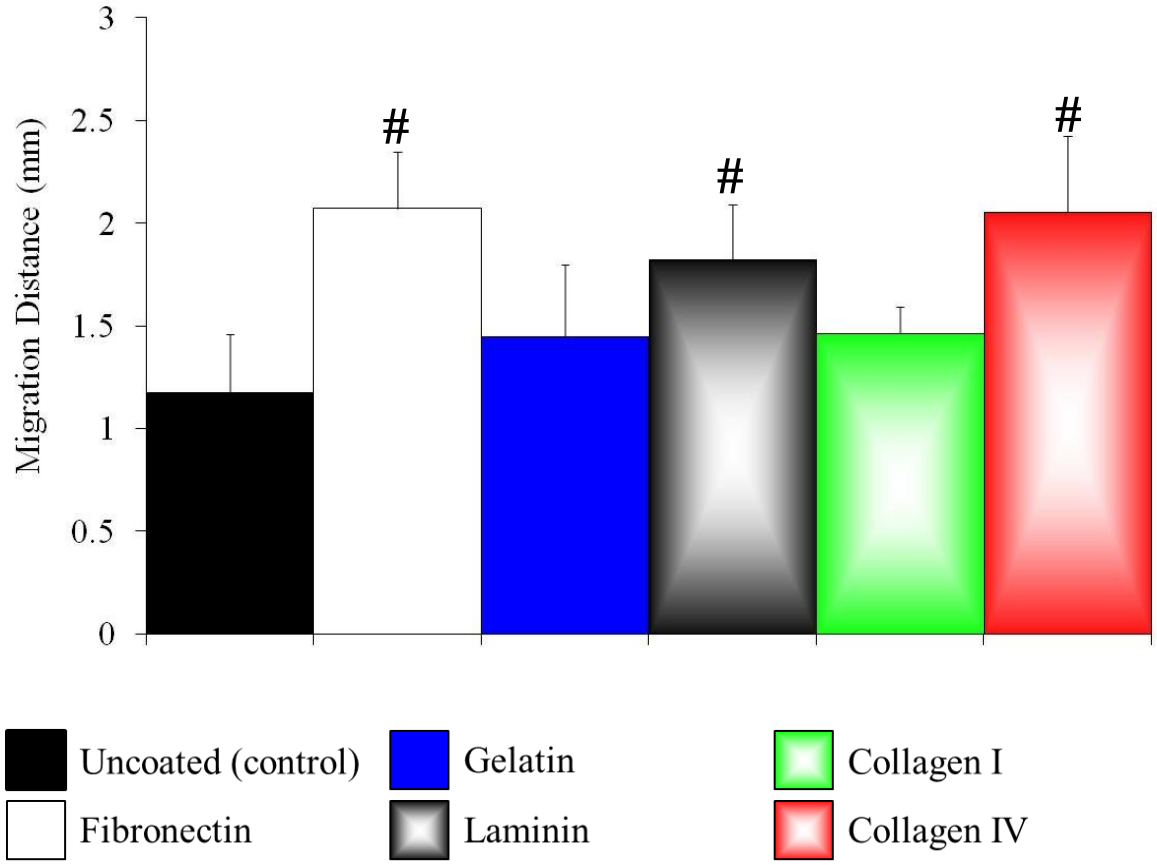

Figure 4.16: Heart explants (from 5-week-old SD rats) were plated on fibronectin, gelatin, laminin, and collagen type I and IV. Representative images of explants with migrating cells were taken after 5 days in culture. Maximal distance of explant-derived cell migration was measured from randomly selected explant tissues for each matrix after 5 days, using imageJ. Migration of EDCs on uncoated culture dish served as the control. Data are presented as mean ± SD (n=4). Statistical analysis was performed using one-way ANOVA. # $p < 0.05$ vs control.

4.4.3.2 Explant-derived cells contained more c-kit$^+$ cells when cultured on collagen IV

Fibronectin, gelatin and collagen I consistently produced CDC populations containing 2-4% of c-kit$^+$ cells, comparable to those found with the control. However, a significantly higher number of c-kit$^+$ cells was obtained during the first isolation of EDCs that were cultured on laminin and collagen IV (11 ± 6% and 10 ± 4%), compared to the controls (2 ± 1%) (Figure 4.17A). This difference was maintained in the second EDC isolation. Cells cultured on collagen IV also generated more c-kit$^+$ cells than those cultured on fibronectin, the recommended ECM for heart explants (99, 186).

4.4.3.3 The number of c-kit$^+$ cells was unrelated to the cardiosphere number

As the ECMs influenced the number of c-kit$^+$ cells in EDCs, we tested the resulting EDCs for their cardiosphere-forming capability to see if the number of c-kit$^+$ cells in EDCs altered cardiosphere number. EDCs cultured on fibronectin produced a significantly higher number of cardiospheres (198 ± 50 vs control 152 ± 19, $P < 0.05$), whereas those cultured on laminin and collagen I generated significantly fewer cardiospheres than the control (Figure 4.17B), suggesting that cardiosphere production is independent of the number of c-kit$^+$ stem cells present in the EDCs.

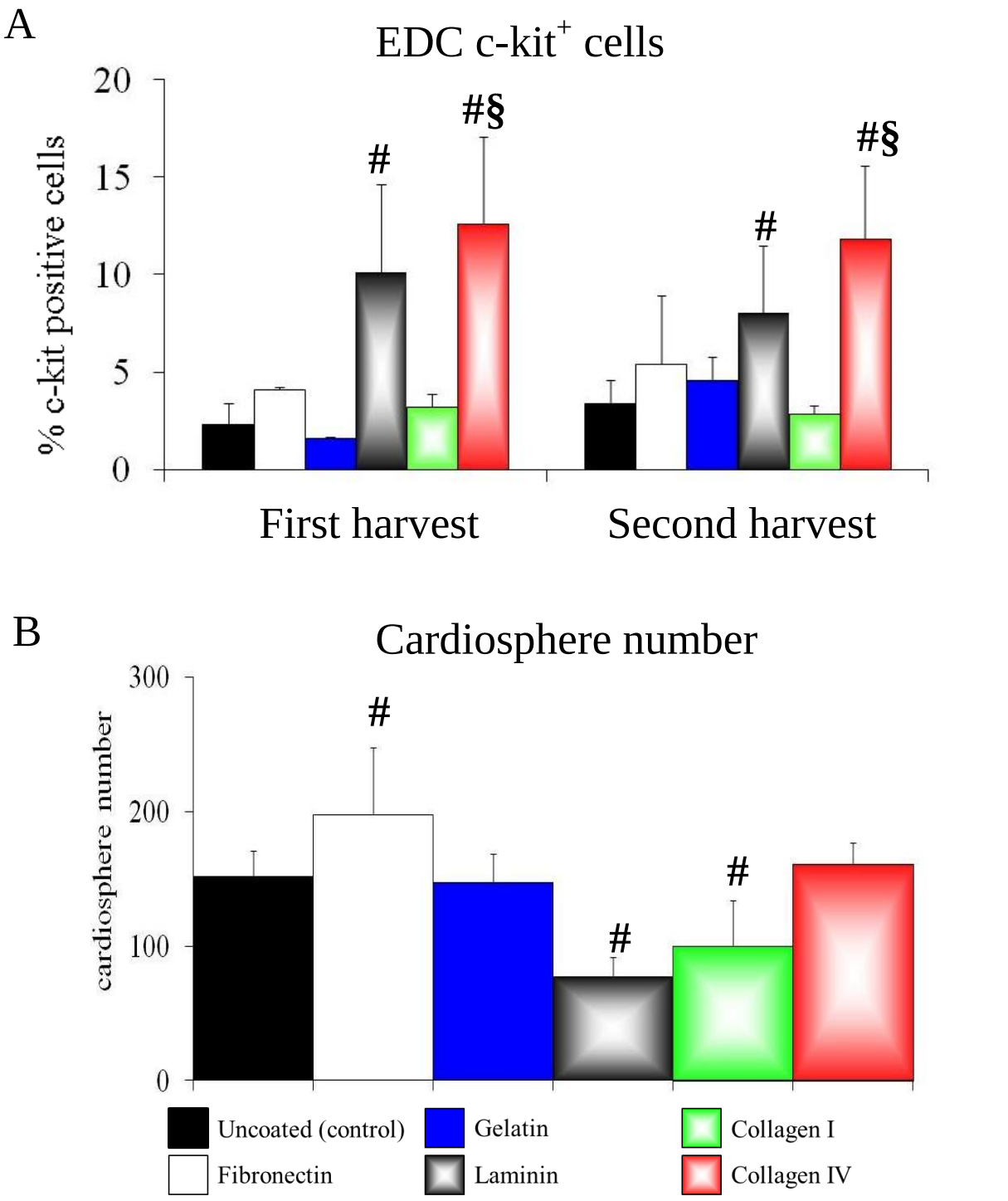

Figure 4.17: EDCs were isolated from 5-week-old SD rat (n=4) heart explants after 7 days. The percentage of c-kit$^+$ cells in EDCs were analysed using flow cytometry. (A) A significantly higher number of c-kit$^+$ cells was obtained during the first isolation of EDCs that were cultured on laminin and collagen IV. (B) EDCs were induced to form cardiospheres using the standard protocol, and cardiosphere number was counted (n=4). EDCs cultured on fibronectin produced a significantly higher number of cardiospheres but there was a significantly lower cardiosphere yield from EDCs cultured on laminin and collagen I, compared with uncoated control. Data are presented as mean ± SD. Statistical analysis was performed using one-way ANOVA. # $P < 0.05$ vs control; § $P < 0.05$ vs fibronectin.

4.4.3.4 Collagen I produced CDCs with the highest level of c-kit$^+$ cells.

When CDCs were expanded as a monolayer, type I collagen produced significantly more c-kit$^+$ cells (9 ± 2%), whereas fibronectin, gelatin, laminin and collagen IV produced a comparable number of c-kit$^+$ cells in passage two CDCs (around 2–4%) (Figure 4.18).

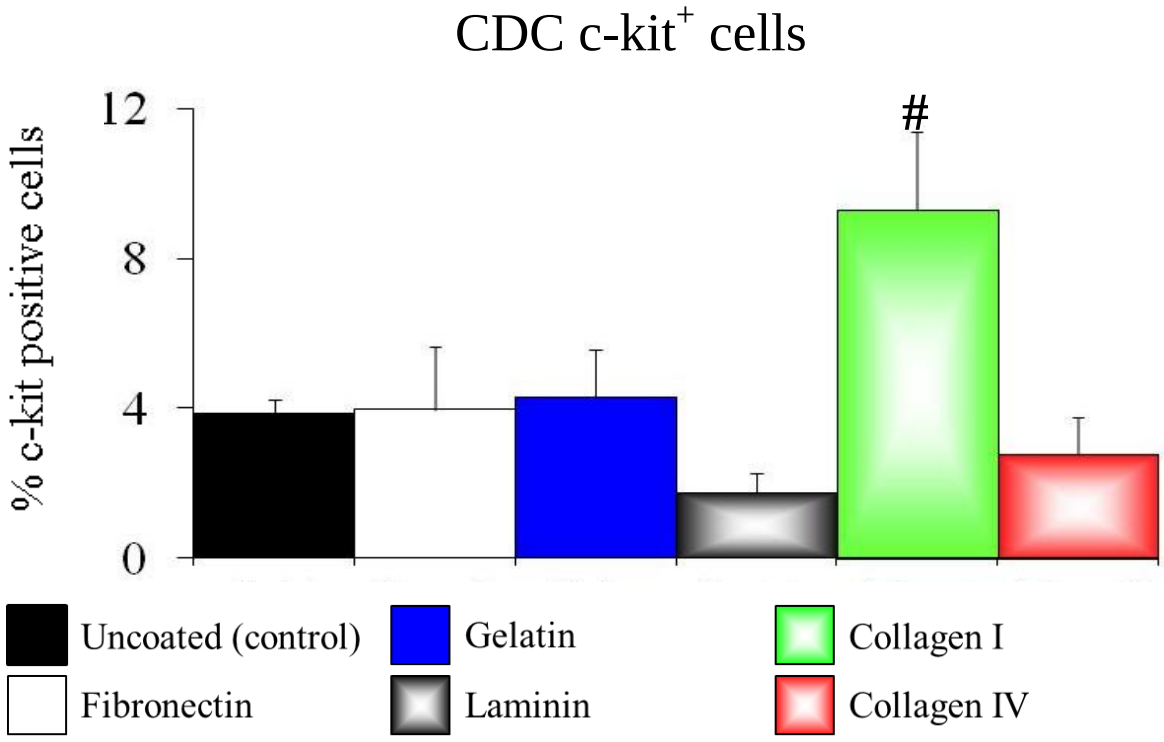

Figure 4.18: Flow cytometry analysis of c-kit$^+$ cells in passage 2 CDCs after culturing on different extracellular matrices showed that type I collagen produced significantly more c-kit$^+$ cells. Data are presented as mean ± SD (n=4). Statistical analysis was performed using one-way ANOVA. # P < 0.001 vs control.

4.4.3.5 Collagen IV enhanced CDC adhesion and proliferation

The number of CDCs adhering to the matrix was tested on all matrices using Alamar®Blue. Non-adherent cells were removed using three PBS washes. Adherent cells were incubated for 2 hours with Alamar®Blue under the standard cell culture conditions and fluorescent intensities were normalized to control. The number of adhered cells was significantly reduced on gelatine, but increased on laminin and collagen I and IV, compared with control and fibronectin (Figure 4.19A). Furthermore, CDC proliferation was significantly increased on fibronectin, laminin and both collagen I and IV after day 1, compared to the controls. Wells coated with gelatine contained significantly fewer cells at day 0 due to poor cell-matrix adhesion, but proliferated to a level comparable to control by day 2 (Figure 4.19B). Futhermore, CDC proliferation was better on collagen I and IV than on fibronectin. However, the collagen IV significantly enhanced CDC proliferation over all other matrices at day 4, suggesting that collagen IV would be the best ECM for CDC expansion.

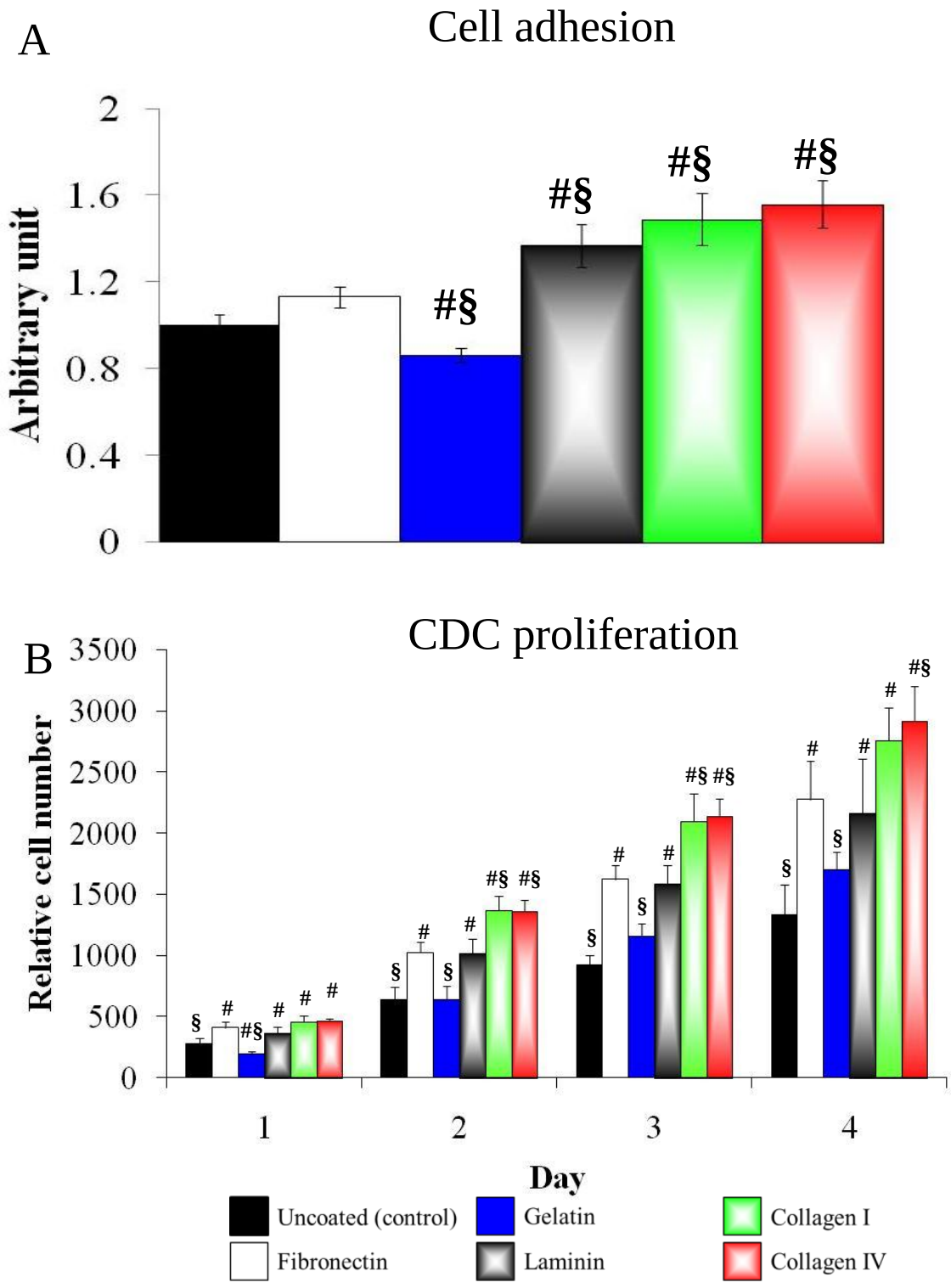

Figure 4.19: CDC adhesion and proliferation. Passage 2 CDCs which were cultured using the standard protocol were seeded at 500 cells per well of 96 well plate pre-coated with fibronectin, gelatin, laminin, collagen I and collagen IV. (A) Passage 2 CDCs exhibited a lower adhesion to gelatin, and favoured laminin and collagen I and IV after two hours incubation at 37°C. (B) CDCs showed the fastest rate of proliferation on collagen IV at day 4. Data are presented as mean ± SD (n=5). Statistical analysis was performed using one-way ANOVA with Tukey post hoc test. # P < 0.05 vs control; § P < 0.05 vs fibronectin.

4.4.3.6 Clonal efficiency

To examine the effect of ECM on CDCs, clonal efficiency and c-kit expression after cultured on various ECMs were evaluated. Fibronectin, laminin and collagen IV contained a higher number of clonogenic cells at passage 4, compared with control CDCs grown on uncoated culture flasks (55 ± 6%, 51 ± 9%, and 56 ± 8% vs 34 ± 7%, respectively) (Figure 4.20).

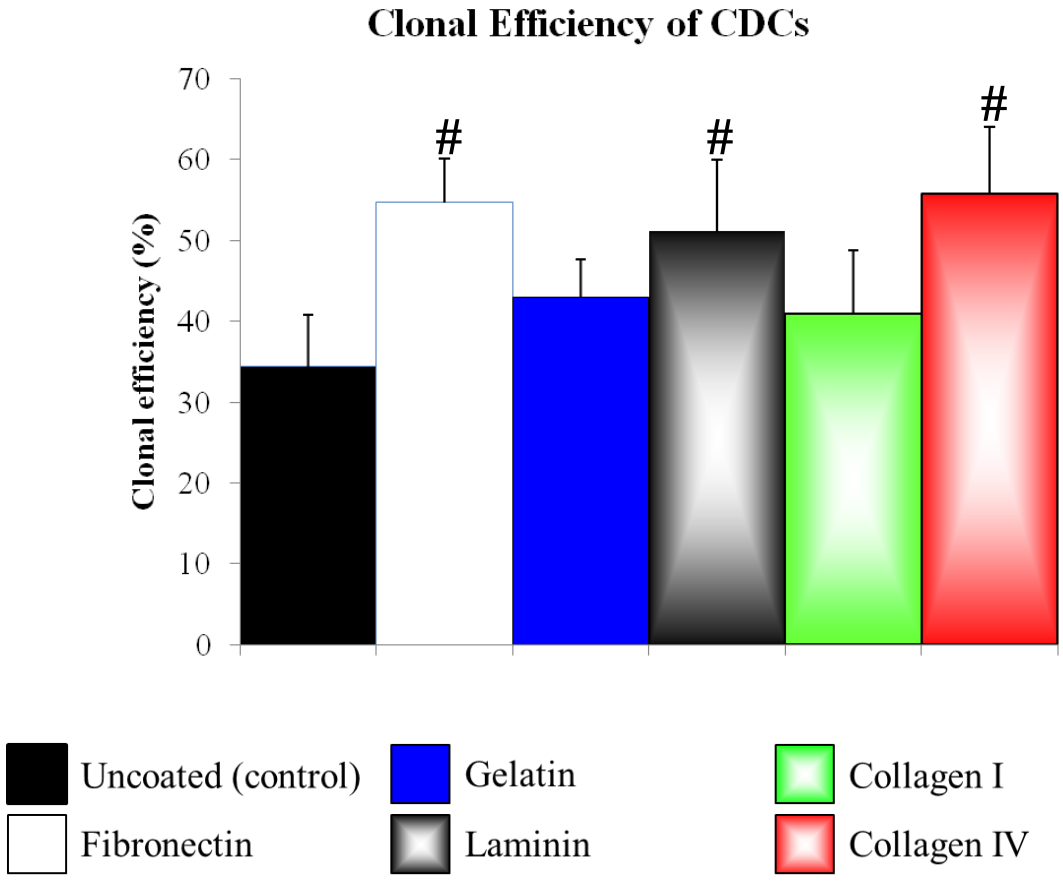

Figure 4.20: Passage 2 CDCs cultured using standard protocols were expanded on all tested ECMs to passage 4. Clonal efficiency of passage 4 CDCs were assessed by plating a single cell per well of a 96-well plate (n=5). The total number of wells containing colonies was calculated after 2 weeks. Data are presented as mean ± SD. Statistical analysis was performed using one-way ANOVA with Tukey post hoc test. # P < 0.05 vs control.

Table 4.1: Summary of the c-kit expression in EDCs and CDCs

ECM	C-kit level		Changes in c-kit level
	EDCs (1st isolation)	CDCs (Passage 2)	
Control	2 ± 1%	4 ± 0.4%	+ 2%*
Fibronectin	4 ± 0.1%	4 ± 2%	ND
Gelatine	2 ± 0.1%	4 ± 1%	+ 2%**
Laminin	11 ± 6%	2 ± 1%	- 9%*
Collagen I	3 ± 1%	9 ± 2%	+ 6%**
Collagen IV	10 ± 4%	3 ± 1%	- 7%*

*ND; no difference, *P < 0.05, **P < 0.001; significant difference between c-kit+ level in EDCs and CDCs using unpaired T-test.*

Sumarizing the changes of the c-kit+ cell number from EDCs to CDCs, collagen I was the only ECM that significantly increased c-kit$^+$ cells in CDCs (Table 4.1). However, collagen I gave poor cell migration and lower c-kit expression during explantation. Therefore, fibronectin was used to boost EDC migration and thus shortened the explant culture time, but collagen I was used for CDC expansion. However, the c-kit$^+$ level did not significantly change (6 ± 1%) with this modification (Figure 4.21), neither did it when hanging drop culture was incorporated (8 ± 3%).

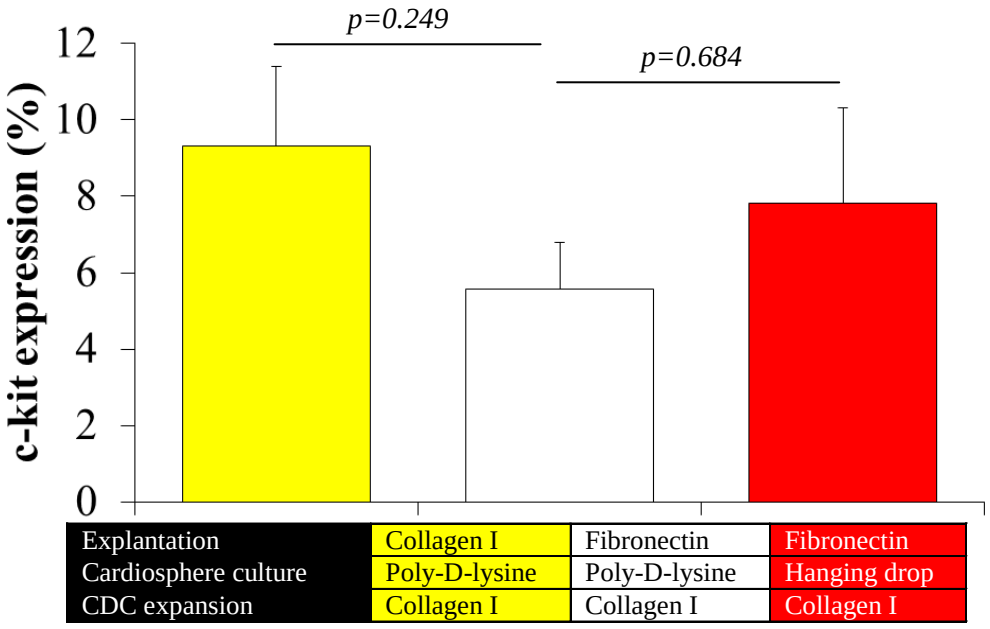

Figure 4.21: The percentage of c-kit$^+$ cells in passage two CDCs using different combinations of ECM and cardiosphere culture methods were analysed using flow cytometry. Data are presented as mean ± SD (n=3). Statistical analysis was performed using one-way ANOVA with Tukey post hoc test.

Fibronectin, laminin and collagen IV improved explant cell migration, which decreased the EDC culture period, but the number of c-kit$^+$ cells on these matrices was low when the resulting cardiospheres were expanded to passage two CDCs. When hanging drops were used to produce cardiospheres, a significant increase in the number of c-kit$^+$ cells from the cardiospheres was observed from cells cultured on fibronectin (9.3 ± 3.2%) and collagen IV (11.2 ± 0.4%), but not on laminin (Figure 4.22). Futhermore, type IV collagen provided superior enhancement to CDC adhesion and proliferation, compared with fibronectin.

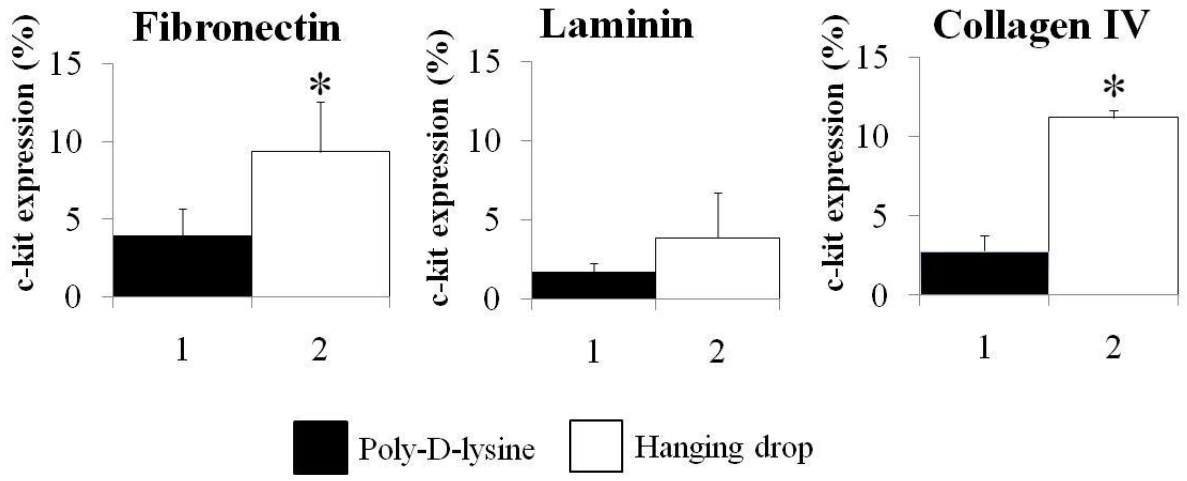

*Figure 4.22: Hanging drop culture augmented c-kit$^+$ cells in passage two CDCs cultured using fibronectin and collagen IV, but not laminin. Data are presented as mean ± SD (n=3). Statistical analysis was performed using student t-test. * P < 0.005 vs poly-D-lysine.*

Taken together, collagen IV produced the highest number of c-kit+ cells from heart explant and improved CDC adhesion and proliferation, and this was the best ECM for rapid cell expansion. Low c-kit$^+$ cells in passage 2 CDCs after expansion on collagen IV could be improved by integrating hanging drop culture to grow cardiospheres. In summary, a final optimized culture protocol for explant-derived cells and CDCs was established, with collagen IV being the ECM for explant culture and CDC expansion, and the hanging drop method

replacing the 2D system using poly-D-lysine for culturing cardiospheres. A final optimized protocol is illustrated in a flow diagram in Figure 4.23.

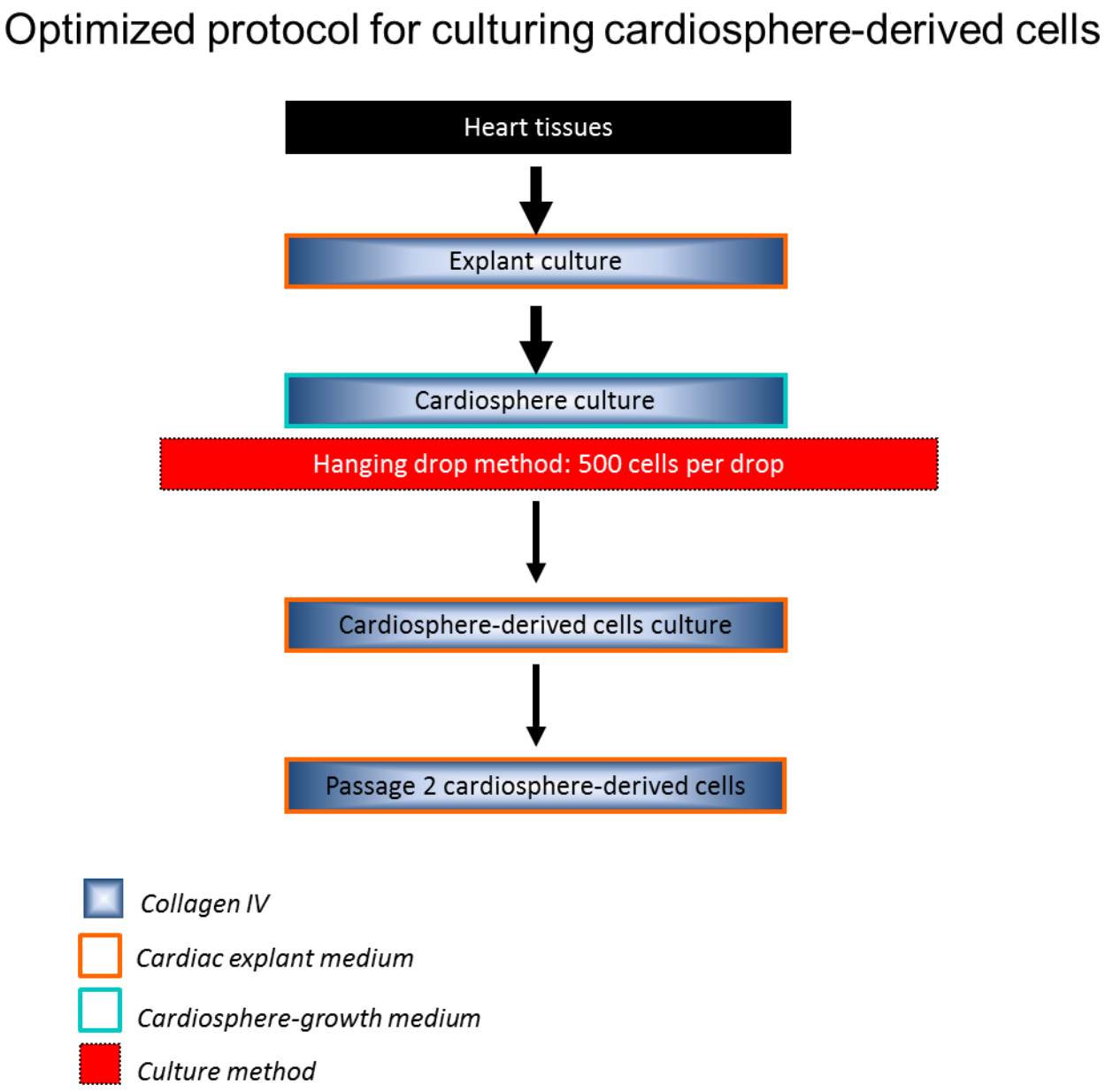

Figure 4.23: Flow diagram showing the final optimized protocol proposed to isolate and culture heart explant-derived cells and cardiosphere-derived cells.

4.5 DISCUSSION

Explant-derived cells

This study demonstrated that c-kit expressing cells can be isolated from EDCs at least 4 times, in agreement with other studies (99, 187). Davis et al. (2010) suggested that EDCs expressed the cardiac stem cell marker c-kit, ATP-binding cassette sub-family G member 2 (ABCG2), which is a cardiac side population marker, and stage-specific embryonic antigen-1 (SSEA-1), which is a pluripotent stem cell marker. These cells were able to differentiate into cardiomyocytes and endothelial cells and improved cardiac function after myocardial infarction (187). However, as observed here, they also showed that the proportion of c-kit$^+$ cells was low, and that cardiosphere formation to augment c-kit$^+$ cell number was still required.

Explant-derived phase bright cells

Phase bright cells are a subpopulation of cells derived from the heart explants. They appear bright under a light microscope and loosely reside on top of the adherent stromal-like cell monolayer. Thus, phase bright cells can easily be collected through multiple washes with PBS, leaving fibroblast-like cells adhered to the culture plate. Reports have shown that phase bright cells are able to form cardiospheres, and express several stem cell markers, including c-kit (99, 149, 188), and stem cell antigen-1 (sca-1) (86, 182) (Table 4.2). Conversely, Shenje and coworkers observed a substantial reduction in phase bright cell number in the explant culture after performing retrograde perfusion of the heart, and suggested that phase bright cells were the hematopoietic elements that resided in the heart circulation system (189). However, Davis and colleagues attributed the difference in their findings to the extensive modifications made in the culture conditions which Shenje employed in their study (109). Here, freshly isolated phase bright cells could not form cardiospheres. However, these cells could be clonogenically amplified, and underwent infinite propagation. Unfortunately, none

were found to express c-kit. As the c-kit expression of clonally amplified phase bright cells was evaluated after 6 passages, it may be that the discrepancy was attributed to the different stages at which the cells were analysed, as several studies have demonstrated that a longer cell expansion time *in vitro* could lead to loss of c-kit expression (182, 190). It is possible that the phase bright cells expressed other stem cell markers, such as Sca-1, but the experiment was limited by antibody availability for rat cell labelling. Further evaluation of the cells for other stem cell properties such as multi-lineage differentiation may be required to define the 'stemness'of the cells.

Table 4.2: Summary of the characteristic of heart explant-derived phase bright cells from other laboratories

Reference	Cell source	Stem cell marker(s)	Expression of other marker(s)
(189)	12 week old C57B16 mice	c-kit – Sca-1–	GATA4+, MyoD-, SMA-, ANF-, Nkx2.5-, Vimentin+, ASA+, vWF-, NG2-
(150)	Neonatal rat	c-kit–	CD45+
(188)	Neonatal Lewis rat	ABCG2+, c-kit+	Cmet+, CXCR+, Flt-1+, IGF-1R+
(182)	L2G85 Transgenic mice	Fresh isolation: 40.0 ± 5.5 % Sca-1+ After sub-culturing: 95% Sca-1	Mesenchymal markers: CD29+, CD90+, CD44+, CD106 +
(149)	SD rat and human biopsies	Human and rat: 30% c-kit	vWF+, SMA+, KDR+, Nkx2.5, GATA4+
(86)	2-month-old mouse	Sorted Sca-1 population from phase bright cells containing 19.8% c-kit, 6.5% CD34,	GATA4+, histone H3+

SMA; smooth muscle actin. ANF; atrial natriuretic factor. ASA; α-sarcomeric actin. vWF; von Willebrand factor. CXCR-4; C-X-C chemokine receptor type-4. cMet; proto oncogene encoding hepatocyte growth factor receptor. IGF-1R; insulin-like growth factor-1 receptor. KDR; kinase insert domain receptor. Sca-1; stem cell antigen-1.

Cardiospheres

This study showed for the first time that the method used for cardiosphere culture influences the level of c-kit$^+$ cells in passage two CDCs. The hanging drop method gave superior c-kit$^+$ cell enrichment, and larger cardiospheres (120-150 μm^2) were produced by increasing the cell density to 4,000 cells per 25 μl. It has been shown that the size of cardiospheres is directly related to the expression of vascular endothelial growth factor (VEGF) (191), a signal protein that plays a crucial role in angiogenesis (formation of new blood vessels from existing vessels) and neovascularisation (formation of new microvasculature). A larger sphere size would create a lower oxygen tension in the middle of the cardiospheres, and promote up-regulation of oxygen susceptible hypoxia-inducible factor-1α (HIF-1α), an upstream regulator of VEGF transcription (192, 193). In addition, cardiosphere c-kit expression was unaffected by the size, and therefore it is possible that larger cardiosphere size may provide CDCs with greater therapeutic effects than cells derived from the smaller cardiospheres.

Extracellular matrix

There are three types of ECM that may be found in the niche for c-kit$^+$ cardiac stem cells. Urbanek and colleagues demonstrated that α-4 integrin, a receptor that mediates cell-matrix adhesion, is consistently expressed in lin$^-$ c-kit$^+$ CSC, but not in early lineage-commited cells, which coexpress GATA4 and MEF2C. (184). Evidence showed that α-4 integrin colocalized with the α-2 chain of laminin and fibronectin, which suggests that fibronectin and laminin may be the matrices that help to maintain the undifferentiated state of c-kit$^+$ cardiac stem cells. Castaldo et al. (2010) demonstrated that cardiac c-kit$^+$ cell activation is coupled with α-6 integrin and laminin-1 (185), while Li et al. (2010) suggested that collagen IV is present in the core of cardiospheres, which recaptitulate the niche-like enviroment for c-kit$^+$ cells (153). In

short, fibronectin, laminin-1 and collagen IV are all candidates to be the niche matrices for c-kit$^+$ cardiac stem cells.

Here, fibronectin, laminin and collagen IV improved explant cell migration compared with other matrices, with more c-kit$^+$ cells found in EDCs cultured on collagen IV than fibronectin. When the EDCs from these three matrices were induced to form cardiospheres and expanded to passage two CDCs, they yielded fewer than 5% c-kit$^+$ cells. Nonetheless, a higher number of clonogenic cells were found in cultures grown on fibronectin, laminin and collagen IV than on uncoated control plates. The underlying mechanism that contributes to this observation is unclear, but judging from the CDC clonal efficiency, fibronectin, laminin and collagen IV are all suitable for CDC expansion.

Hanging drop method

The hanging drop method produced a higher percentage of c-kit$^+$ cells in the cardiosphere-derived cell population. Although the underlying mechanism is not clear, the short culturing time necessary to form cardiospheres within the hanging drop, with the aid of gravity, could possibly be an advantage. Previously in *Chapter 3*, cardiospheres were found to form through EDC aggregation, regardless of the method used. However, EDCs plated on poly-D-lysine took a longer time (3 days) to form cardiospheres; whereas the hanging drop method induced cardiosphere formation within a day (Figure 4.24). This indicates that the time the c-kit$^+$ cells are maintained within cardiospheres, which provides a niche-like microenvironment that favours stem cell maintenance, is longer using the hanging drop method (3-4 days) than in cardiospheres cultured on poly-D-lysine (1-2 days), assuming that both source of cardiospheres are collected on day 4. It may be that the cardiospheres formed on poly-D-lysine culture would possess similar characteristics to those in hanging drops if they were cultured for a longer time period. However, the short culture time is an added advantage to

using hanging drop method. Nonetheless, evidence is needed to compare the characteristics between the two sources of cardiospheres, in terms of the paracrine secretion profile, the number of c-kit$^+$ cells produced, the regulation of the stemness genes, and the therapeutic benefits *in vivo*.

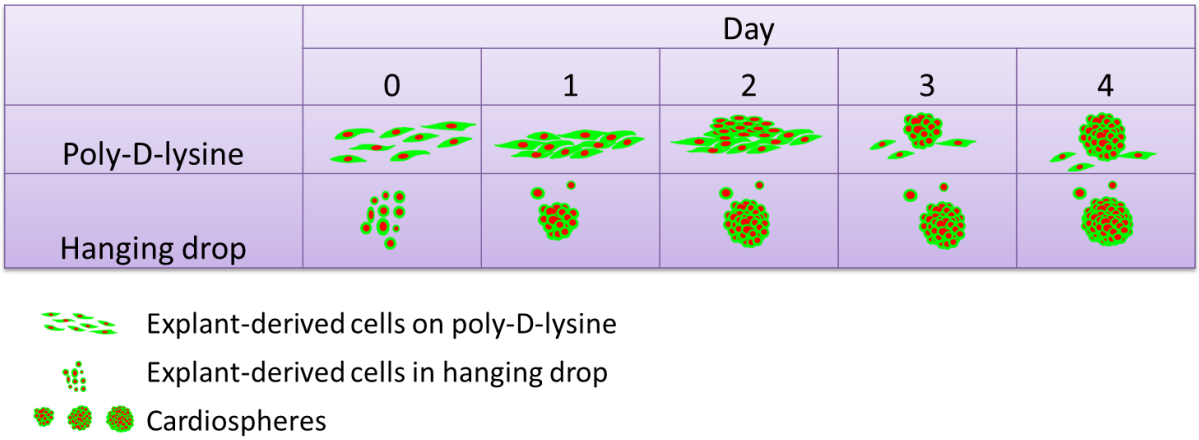

Figure 4.24: EDCs plated on poly-D-lysine took a longer time (3 days) to form cardiospheres; whereas the hanging drop method induced cardiosphere formation within a day, indicating that the time the c-kit$^+$ cells live and proliferate in the niche-like microenviroment in cardiospheres is longer using hanging drops and thus these contain more c-kit$^+$ cells than the cardiospheres cultured on poly-D-lysine (if both were isolated on day 4).

The initial rationale of growing cardiospheres using poly-D-lysine was to remove contaminating cardiac fibroblasts from explant-derived cells (99). It is possible that the proportion of the cardiac fibroblasts in the cardiospheres generated in hanging drops is higher than in those cardiospheres growing on poly-D-lysine, despite the fact that some non-sphere-forming cells were consistently present in hanging drop culture. Therefore, the culture method could be refined further by incubating EDCs in a plastic culture flask for few hours to remove fast-adherent fibroblastic cells before proceeding to creating the hanging drops. Nevertheless, the possible role of cardiac fibroblasts in stem cell maintenance in cardiospheres has yet to be identified.

The scalability and applicability of the use of hanging drop method for culturing human cardiospheres has been questioned. Assuming that a millions EDCs are isolated from heart explants, the standard protocol requires only 34 wells of 24 well plates coated with poly-D-lysine for culturing cardiospheres, with the hanging drop method, about 100 drops could be fitted in a 150 mm petri dish, and so a total of 20 petri dishes are required to plate 1000,000 EDCs (with a cell seeding density of 500 cells/25 µl). However, EDC-containing drops could be plated using an automated multichannel pipette, in which case plating the drops is relatively rapid. For large scale expansion, a better customized petri dish which would allow more drops to be plated in each plate could be made to reduce the total number of plates required.

With regard to the total cardiosphere yield, approximately 3400 cardiospheres could be generated using the standard protocol (an estimated figure based on the assumption that 100 cardiospheres are produced per every 30,000 cells plated), while only 2000 cardiospheres could be generated using hanging drops (assuming that only one cardiosphere is formed per drop). However, the culture time and the stemness quality of the cardiospheres may be better with the hanging drop method as discussed before, although more evidence is required to support this.

Table 4.3: Calculation to estimate the number of plates required for each culture method and the total cardiosphere yield.

Culture method	Number of explant derived cells	Cell density	Number of well or drop required	Number of plate required	Number of cardiospheres generated	Total cardiospheres
Poly-D-lysine (Standard)	1000000	30,000 cells/well of 24 well plate	33 wells	1 ½ units of 24 well plate	100 per well of 24 well plates	3300
Hanging drop (Optimized)	1000000	500 cells per 25 µl drop	2000 drops	20 units of 150 mm petri dish	1 per drop	2000

Although the standard protocol produced more cardiospheres and CDCs than reported in the literature (99, 100), the percentage of c-kit$^+$ cells was low. Furthermore, from the same number of EDCs, cardiosphere yield was lower using the optimized protocol, and so was the resulting CDC number. However, the percentage of c-kit+ cells was higher using the optimized protocol. Therefore, the total number of c-kit$^+$ cells in passage 2 CDC did not differ between the two protocols. As CDCs would be administrated in an aliquot of a specified number of CDCs, those cultured from the optimized protocol would contain a better cell distribution with a higher proportion of c-kit$^+$ cells in CDCs than those from the standard protocol.

Future work

The interactions between cells and extracellular matrix are established through the integrins, cell surface receptors which comprise two subunits (α and β). Integrin binding triggers intracellular signals that regulate cell proliferation, migration and differentiation (194). Therefore, future experiment would include analysing the relevant integrin expression in CDCs cultured on collagen IV using the extracellular matrix and adhesion molecules PCR Array (Qiagen, UK), and may also include mapping the underlying signalling pathways that contributes to the observations reported in this chapter, for instance the focal adhesion kinase (195) and the platelet-derived growth factor (196) signalling pathways. In-depth examination of the effect of collagen IV on the supporting cells such as CD90$^+$ mesenchymal cells would also help to identify the changes in paracrine secretory profile or cell phenotype, which could be important in stem cell maintenance in culture. Furthermore, although CDCs cultured using the optimized protocol contained a higher percentage of c-kit$^+$ cells and showed better cell migration, adhesion and proliferation on collagen IV, *in vivo* evidence regarding cell retention, proliferation and cardiomyocytes differentiation capability in the infarcted heart, and resulting improvement in cardiac function, are required in order to further validate the optimized culture protocol.

In conclusion, c-kit^{+} cells were consistently present in the explant-derived cells. Phase bright cells were clonogenic, but did not form cardiospheres, nor did they express c-kit, although the loss of c-kit expression may have resulted from long-term *ex vivo* expansion. Hanging-drop culture can generate cardiospheres with increased c-kit^{+} cell enrichment compared with culture on the two-dimensional poly-d-lysine or the bacterial grade non-adhesive culture dishes. Collagen IV was the best ECM to be used in CDC culture and expansion, as it improved cell migration, adhesion, proliferation and clonal efficiency. Although the level of c-kit+ cells in passage two CDCs on collagen IV was low, this could be improved by employing hanging drop method to culture cardiospheres.

Chapter 5

Magnetic resonance agent labelling of cardiosphere-derived cells for positive contrast detection at 11.7 T

5.1 ABSTRACT

Stem cell therapy is a promising approach to treat myocardial infarction. Tracking stem cells *in vivo* can provide insights into cell engraftment and survival after administration. *In vivo* MRI can be used to non-invasively track transplanted cells, pre-labelled with contrast agent. However, the sensitivity of detection depends on the paramagnetic contrast agent employed for labelling. Iron is the most commonly used contrast agent for stem cell labelling, which yields T2 and T2* enhancement, and manifests as hypointensity in MR images. However, hypointensities seen in an MR image could also be due to artefacts or an endogenous source of signal disruption (such as blood clot), and may not necessarily represent the donor cells. Quantification of transplanted cells *in vivo* based on signal dropout can therefore be difficult, making a positive contrast agent preferable. Gadolinium-based contrast agents generate hyperintensity on an MR image. Here, gadolinium-DTPA (Gd-DTPA) and gadonanotubes were used to label cardiosphere-derived cells and phantoms, which were studied at 11.7 T. Gd-DTPA labelling did not affect CDC viability and cardiosphere-forming capability. Successful *ex vivo* quantification of Gd-DTPA-labelled CDCs was achieved by performing T1 mapping. However, Gd-DTPA had low sensitivity (1.4×10^5 cells/mm^2), which may limit its usefulness for *in vivo* tracking. Gadonanotubes were non-toxic to CDCs, but were unstable in solution after two months storage at room temperature, yielding cytotoxic breakdown products. In addition, our high field study at 11.7 T showed gadonanotubes to have a dominant T2 effect on T1-weighted images, which produced hypointensities in MRI, indicating that gadonanotubes are not suitable for positive contrast detection at high field.

5.2 INTRODUCTION

The true test of stem cells for cardiac therapy is the ability to improve *in vivo* cardiac function. Most reports from clinical trials, however, documented modest improvement in global function (197, 198) with augmented regional perfusion (199) and one study reported that global benefits did not sustain a few years after cell therapy (200). These conflicting observations are confounded by a lack of knowledge of cell location and behaviour *in vivo* after transplantation. Thus, more information concerning cell fate after injection is needed in order to define the best route of administration to give optimal cell integration and retention in the infarcted myocardium, as well as to assess the relationship between the survival of transplanted cells and the observed functional benefit.

Studies have demonstrated MRI as a safe and non-invasive imaging modality that can be used for *in vivo* cell tracking (54, 201). To visualize donor cells in MR images, cells are pre-loaded with a paramagnetic contrast agent, a substance that disturbs local magnetic fields and consequently the neighbouring proton spins, to create a difference in signal intensity in MRI. Iron oxide particles are the most widely used T2/T2* contrast medium in stem cell tracking (202). These iron oxide particles shorten transverse (T2) proton relaxation time, and thus can be visualized as hypointensities in MR images. With advances in MRI technology, many studies have demonstrated that a single cell can be identified, *in vitro and in vivo*, with iron oxide labelling (203, 204). In addition to serving as a contrast medium for MRI detection, labelling cells with iron particles can facilitate cell homing and engraftment in the target tissue by magnetic targeting (118), or be used to re-isolate the labelled cells for post-engraftment cell fate examination (114).

However, there are limitations to the use of iron oxide particles in tracking stem cells as they may be retained in dead cells and taken up by macrophages (164, 165). This may lead to an

overestimation of cell engraftment. In addition, regional signal loss can also occur as a consequence of other endogenous sources of signal interference, for example, the presence of hemosiderin in cardiac haemorrhage (166). Moreover, it is difficult to correlate signal dropout with the number of injected cells, and thus it is not possible to accurately measure cell retention. Hence, an agent that gives positive, instead of negative, contrast may be preferable.

Positive contrast appears bright on an MR image and can easily be distinguished from cardiac MR artifacts, which commonly manifest as a signal loss. Gadolinium-based contrast agents are characterized by the ability to shorten longitudinal (T1) proton relaxation time, which enhances signal intensity. Gadolinium-diethylene triamine penta-acetic acid (Gd-DTPA) was the first gadolinium-based T1 contrast agent approved by the US Food and Drug Administration (FDA) (205). The gadolinium ion (Gd^{3+}) alters proton relaxation when in contact with water molecules, and thus enhances signal intensity in T1-weighted images. It has been used in many clinical MR applications, such as angiography (206), or in determining the necrotic region in the infarcted myocardium (207). However, only a few studies have employed Gd-DTPA for cell tracking, and most studies used a clinical MR system (1.5 T) (208, 209). No study has reported using Gd-DTPA in tracking stem cells at a high magnetic field of 11.7 T.

Recently, Sitharaman and coworkers synthesized a gadolinium-based contrast agent by loading Gd^{3+} ion clusters into a carbon nanotube, which successfully masked the toxicity of free Gd^{3+} ions, and greatly enhanced the T1-weighted signal (210). These gadonanotubes (Gd^{3+}_n@US-tube) outperformed Gd-DTPA by nearly 40-fold at 1.5 T. Gadonanotubes used to label bone marrow mesenchymal stem cells showed MR signal enhancement at 1.5 T, without affecting the stem cell phenotype, cell viability or decreased function (119). Thus,

high biocompatibility and signal enhancement suggest that gadonanotubes hold promise as an alternate contrast agent for stem cell labelling and tracking.

Here, two gadolinium-based contrast agents, Gd-DTPA (Magnevist™) and gadonanotubes (Gd^{3+}@US) were tested for cell labelling and positive contrast detection at 11.7 T.

5.3 GADOLINIUM-DTPA (MAGNEVIST™) AS A LABELLING AGENT FOR POSITIVE CONTRAST DETECTION AT 11.7 T

5.3.1. METHODS

Cell labelling

Passage 2 and 3 CDCs cultured using standard protocol were used in this study. Gd-DTPA (25 mM) was loaded into CDCs using the calcium-phosphate precipitation method (see *Chapter 2*). Proliferation and cardiosphere-forming capability of labelled CDCs were compared with unlabelled CDCs.

Phantom study

An MR phantom is an *in vitro* model used to mimic the *in vivo* environment of cells labelled with MR contrast agent for MR imaging. MR imaging and phantom studies were performed by Dr Philip Lee. All MR images were acquired in a vertical plane using a T1-weighted gradient recalled echo sequence (T1W-GRE), unless stated otherwise. The imaging parameters of the T1W-GRE were as follows: repetition time (TR) 4.5 ms; echo time (TE) 1.709 ms; flip angle 10^{o}. The field-of-view (FOV) and matrix size were 25.6 x 60 mm and 256 x 256, respectively. A region-of-interest (ROI) of 4 mm^2 was used on each MR image to measure signal intensity.

In vitro cell quantification

To correlate signal intensity and cell number, Gd-DTPA-labelled cells were serially diluted with unlabelled cells to yield a total of 1 x 10^6 cells. The size of the cell pellet was around 14 mm^3. MR images were generated using a mixed inversion recovery spin echo (IR-SE) sequence (TR = 2500s, TE = 6 ms, matrix size = 256 x 256, field of view (FOV) = 25.6 x 60

mm). Signal intensity were measured at a region-of-interest (ROI) of 4 mm^2, with inversion times of 11.44 ms, 50 ms, 100 ms, 200 ms, 300 ms, 400 ms, 500 ms, 600 ms, 700 ms, 800 ms, 900 ms, 1050 ms, 1200 ms, 1500 ms, and 2400 ms. Signal intensities were normalized to unlabeled cells and plotted against inversion time (TI) to calculate longitudinal relaxation time (T1) by fitting *Equation 1* using Microsoft Excel Solver.

$$\mathbf{M_z = M_0 (1 - 2e^{-TI/T_1})} \text{…….. } \textbf{\textit{Equation 1}}$$

M_z = longitudinal (z) magnetization at the time of TI, M_0 = initial longitudinal magnetization before the induction of 180^O pulse.

5.3.2 RESULTS

5.3.2.1 Gadolinium-diethylenetriamine penta-acetic acid (Gd-DTPA) labelling and CDC function

CDCs were transfected with 25 mM Gd-DTPA using calcium-phosphate precipitation. Labelled CDCs showed a higher signal intensity than the unlabelled cells on T1-weighted images, confirming successful Gd-DTPA loading (Figure 5.1). There was no difference in cell proliferation and cardiosphere-forming capability between Gd-DTPA-labelled CDCs (Gd-DTPA-CDCs) and unlabelled cells, suggesting that the labelling did not alter cell function (Figure 5.2).

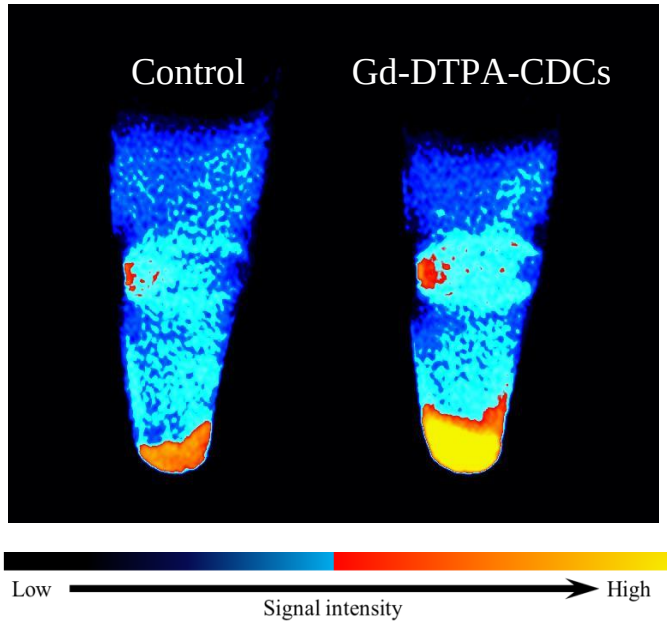

Figure 5.1: CDCs were labelled with Gd-DTPA using calcium-phosphate precipitation. Labelled cells were pelleted at the bottom of a 1.5 ml eppendorf tube and topped with 2% agarose in DMEM/F12 medium. Representative T1-weighted MR images showed that Gd-DTPA-CDCs produced higher signal than the unlabelled CDCs (control) (n=2).

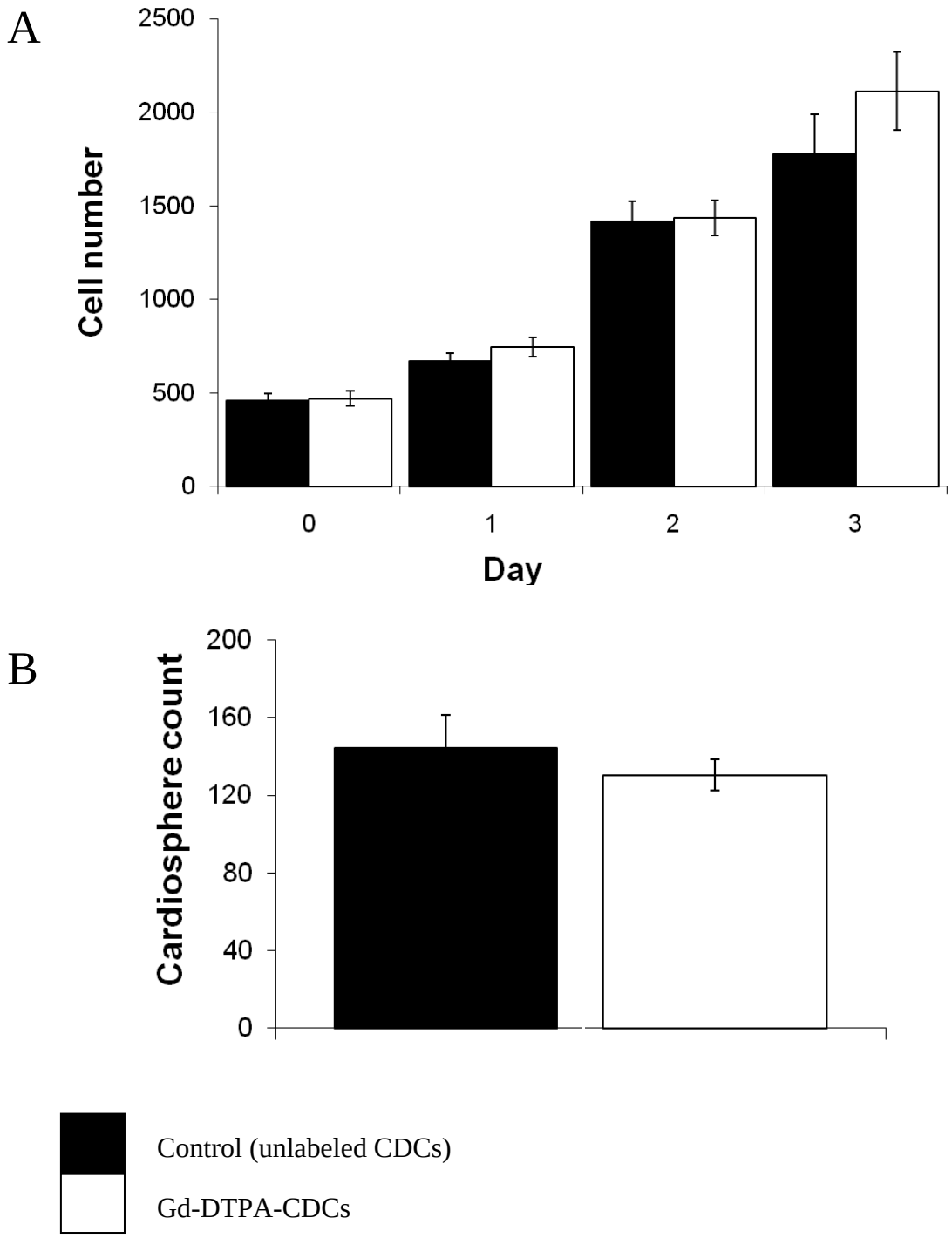

Figure 5.2: (A) Proliferation of Gd-DTPA-CDCs (n=3) and (B) cardiosphere number were the same as unlabelled CDCs (n=3). Data are presented as mean ± SD. Statistical analysis was performed using student t-test.

5.3.2.2 Ex vivo quantification of Gd-DTPA labelled CDCs by T1 mapping using a mixed inversion recovery spin echo (IR-SE) sequence

To test whether quantification of Gd-DTPA CDCs was possible, T1 maps of labelled-cells were measured using an IR-SE sequence. Gd-DTPA CDCs were serial diluted using unlabelled cells (Figure 5.3). Normalized signal intensities were plotted against multiple inversion times for different Gd-DTPA CDC densities (Figure 5.4), and T1 values were obtained by fitting Equation 1 (see *Section 5.3.1, page 104*). Relaxation rate (R1 = 1/T1) was found to correlate directly with Gd-DTPA cell number, indicating Gd-DTPA-labelled cell number can be estimated by mapping T1 (Figure 5.5).

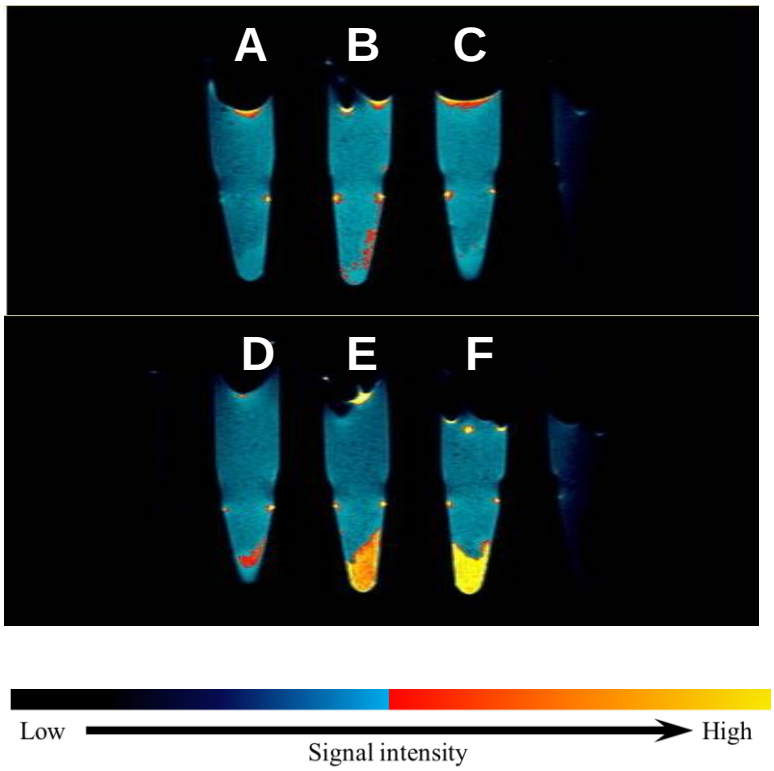

Figure 5.3: Representative T1-weighted MR images of Gd-DTPA-CDC pellets of different cell densities: (A) 0.01 x 10^6, (B)0.05 x 10^6, (C)0.125 x 10^6, (D) 0.25 x 10^6, (E)0.5 x 10^6 and (F) 1 x 10^6 cells (n=2).

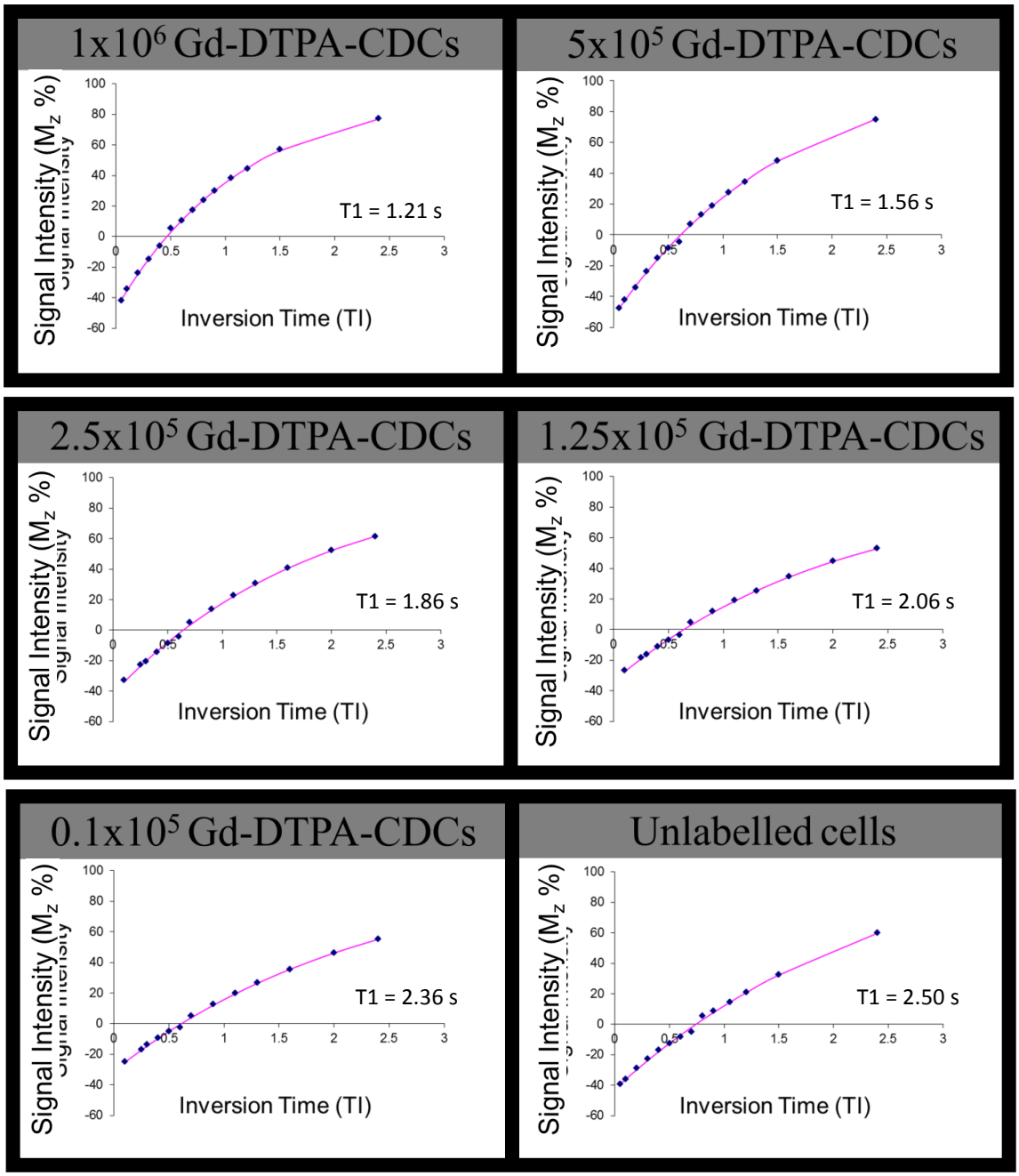

Figure 5.4: T1 relaxation time was calculated from signal intensities of different Gd-DTPA CDC densities plotted against multiple inversion times (TI) (n=1). Solid lines represent Equation 1, diamonds represent experimental data.

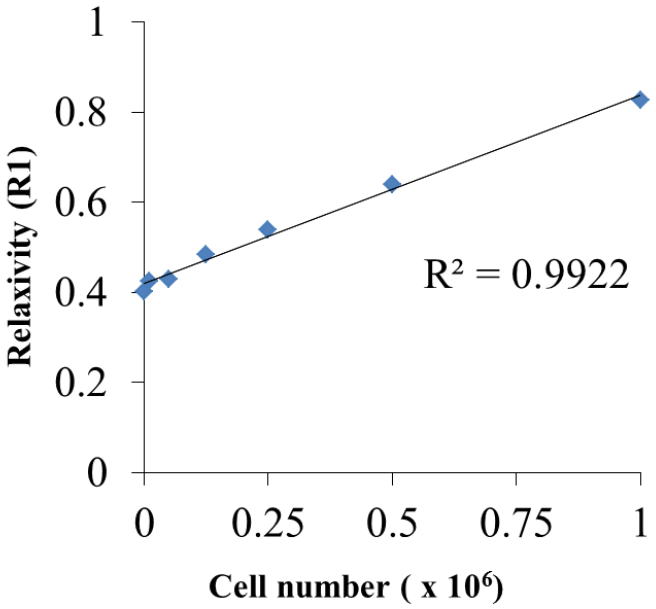

Figure 5.5: T1 relaxation rate (R1=1/T1) is linearly related to Gd-DTPA-CDC number (n=1).

5.3.2.3 Minimal cell detection sensitivity

To relate the *ex vivo* phantom study to *in vivo* detection, Gd-DTPA labelled cells were calculated as cells per mm^3 (Table 5.1) and plotted against normalized signal intensity (Figure 5.6). The minimal detectable cell number for analysis was 1.4 x 10^5 cells/mm^2. However, CDCs migrated across the infarct region, as showed by colocalization of the signal void from labelled iron particles (*Chapter 3*). Assuming one million CDCs were injected intramyocardially, and were distributed evenly throughout an infarct size of 10 mm^2 in a rat heart, it may be possible to detect 1 x 10^5 cells per mm^2, provided the cell administration resulted in full engraftment with no cell loss. However, immediate cell loss upon intramyocardial injection has been reported with ~10% cell retention after 24 hours (118). Therefore, the estimated cell density per mm^2 in the infarct region would more likely be much lower than 1 x 10^5 cells and thus, below the level of detection.

Table 5.1 Calculation to obtain cell number per mm^2

Cell number per 14 mm^3 pellet	Cell number per mm^3	Cell number within ROI*	Cell number per mm^2 image	Normalized Signal intensity
10000	714	1,429	2.9 x 10^3	1.25
125000	8929	17,857	3.5 x 10^4	1.16
250000	17857	35,714	7.1 x 10^4	1.27
500000	35714	71,429	1.4 x 10^5	2.26
1000000	71429	142,857	2.9 x 10^5	2.77

**ROI; region of interest = 4 mm^2 x 0.5 mm.*

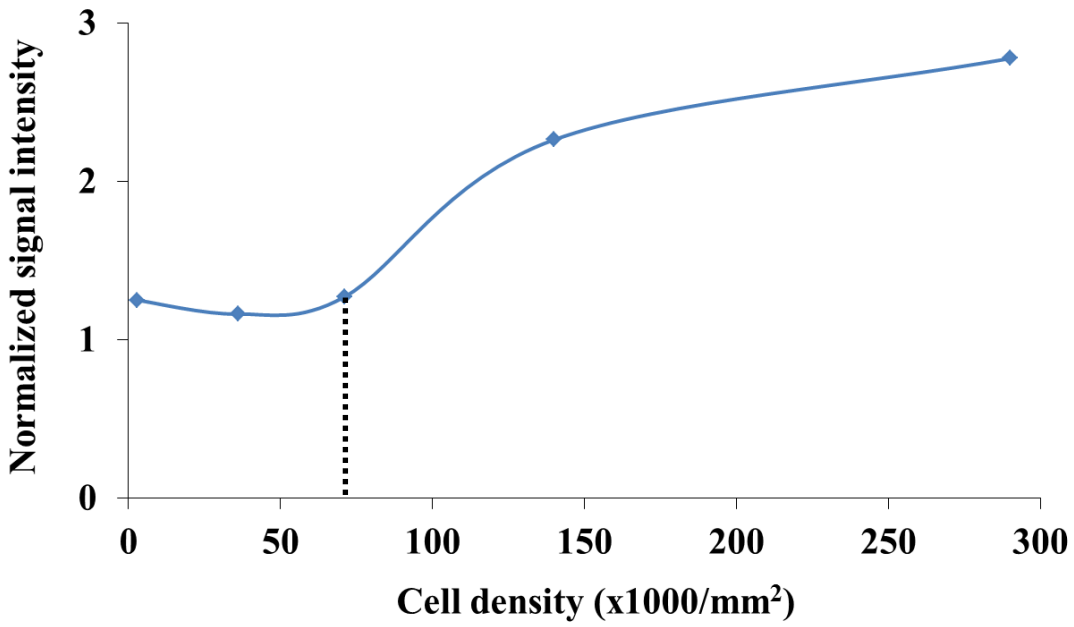

Figure 5.6: Contrast for labelled cells at less than 70 x 10^{3}cells/mm^2 could not be seen on T1-weighted images using the GRE sequence (n=1). Normalized signal for unlabeled cells = 1.

5.4 GADONANOTUBE (Gd^{3+}@US) AS A LABELLING AGENT FOR POSITIVE CONTRAST DETECTION AT 11.7 T

5.4.1 METHODS

Cell labelling and cytotoxicity assay

Gadonanotubes (Gd^{3+}@US) were a gift from Lon J Wilson's laboratory. Gadonanotube stock solution (76 µM) was prepared in 0.17% Pluronic F-108 solution. Passage 2 and 3 CDCs were labelled with gadonanotubes according to Tran's protocol (119) (see *Chapter Two*). CDCs were labelled at different gadonanotube concentrations (Table 5.2), and the gadonanotube toxicity was examined using AlamarBlue®. Briefly, about 5,000 CDCs were seeded into a 96 well plate and cultured under standard cell culture conditions overnight. The labelled cells were incubated with 10% AlamarBlue® in CEM for 4 hours, the plate was read on a fluorescent microplate reader and the relative fluorescence intensity was recorded from at least 5 samples.

Table 5.2 Summary of gadonanotube concentrations used in the cytotoxicity experiment.

Gadonanotube concentration %(v/v)	Gadonanotube concentration (µM)
5	3.8
10	7.6
15	11.4
20	15.2
25	19.0
30	22.8
35	26.6

Phantom study

The imaging parameters of the T1W-GRE were as follows: repetition time (TR), 4.5 ms; echo time (TE), 1.709 ms; flip angle, 10^{o}. The field-of-view (FOV) and matrix size were 25.6 x 60 mm and 256 x 256, respectively. A region-of-interest (ROI) of 4 mm^2 was used on each MR image to measure signal intensity.

5.4.2 RESULTS

5.4.2.1 Cytotoxicity of gadonanotubes

To determine the cytotoxicity of gadonanotubes, concentrations of 3.8 µM, 7.6 µM, 11.4 µM, 15.2 µM, 19.0 µM, 22.8 µM, and 26.6 µM were used to label CDCs, and cell viability was assessed using AlamarBlue®. A concentration of 26.6 µM had been recommended for labelling mesenchymal stem cells, as it gave the best signal intensity in MR images at 1.5T (119). However, cell viability was significantly lower than that of the unlabeled CDCs, when a labelling concentration of > 19 µM was used (Figure 5.7).

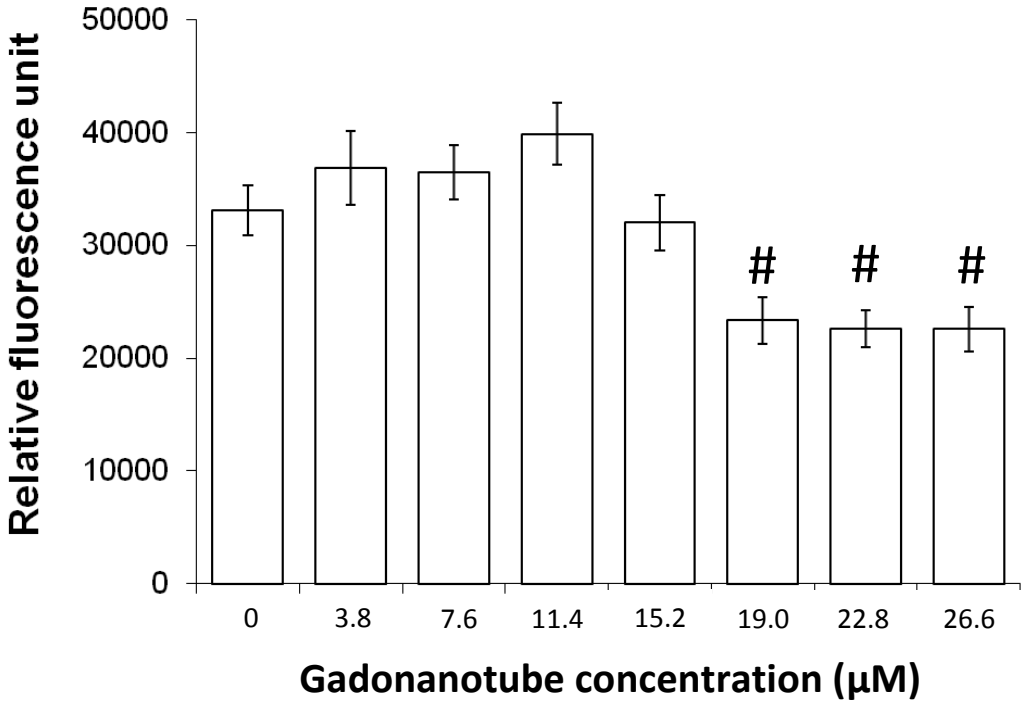

Figure 5.7: Passage 2 CDCs were plated on a 96 well plate and labelled with 3.8 µM, 7.6 µM, 11.4 µM, 15.2 µM, 19.0 µM, 22.8 µM, and 26.6 µM gadonanotubes. CDC viability decreased after labelling with 19.0 µM, 22.8 µM, and 26.6 µM of gadonanotubes (n=3). Data are presented as mean ± SD. # Statistical significance, determined using one-way ANOVA, was taken at $p < 0.05$, compared with unlabelled cells.

5.4.2.2 MR phantom study

CDCs were labelled with 7.6 µM and 15.2 µM gadonanotubes, the two optimal labelling concentrations determined in the cell cytotoxicity test. Phantoms of one million gadonanotube-labelled CDCs were studied. Surprisingly, gadonanotube-CDCs showed negative contrast in T1 weighted images, compared with the positive control Gd-DTPA-CDCs (Figure 5.8). As high gadolinium concentrations may also contribute to shortening of transverse proton relaxation time (T2), a series of phantoms were studied using lower gadonanotube concentrations. Signal intensities generated at labelling concentrations of 10 x 10^{-3} µM, 9 x 10^{-3} µM, 7 x 10^{-3} µM, and 5 x 10^{-3} µM were measured. The highest signal was obtained from cells with 9 x 10^{-3} µM gadonanotubes, but the intensity was weaker than CDCs labelled with 25 mM Gd-DTPA (Figure 5.9).

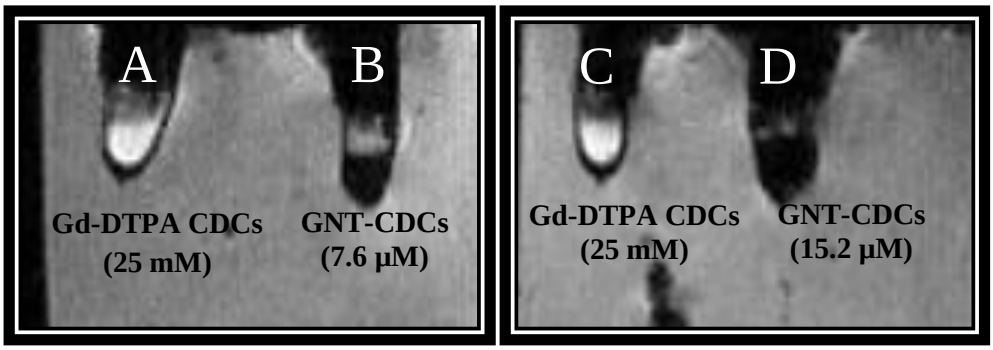

Figure 5.8: CDCs labelled with 7.6 µM and 15.2 µM gadonanotubes were pelleted at the bottom of 100 µl eppendorf tube and topped with 2% agarose in DMEM/F12 medium. However, CDCs labelled with gadonanotubes at both concentrations showed hypointense contrast on T1-weighted image.GNT;gadonanotubes (n=1).

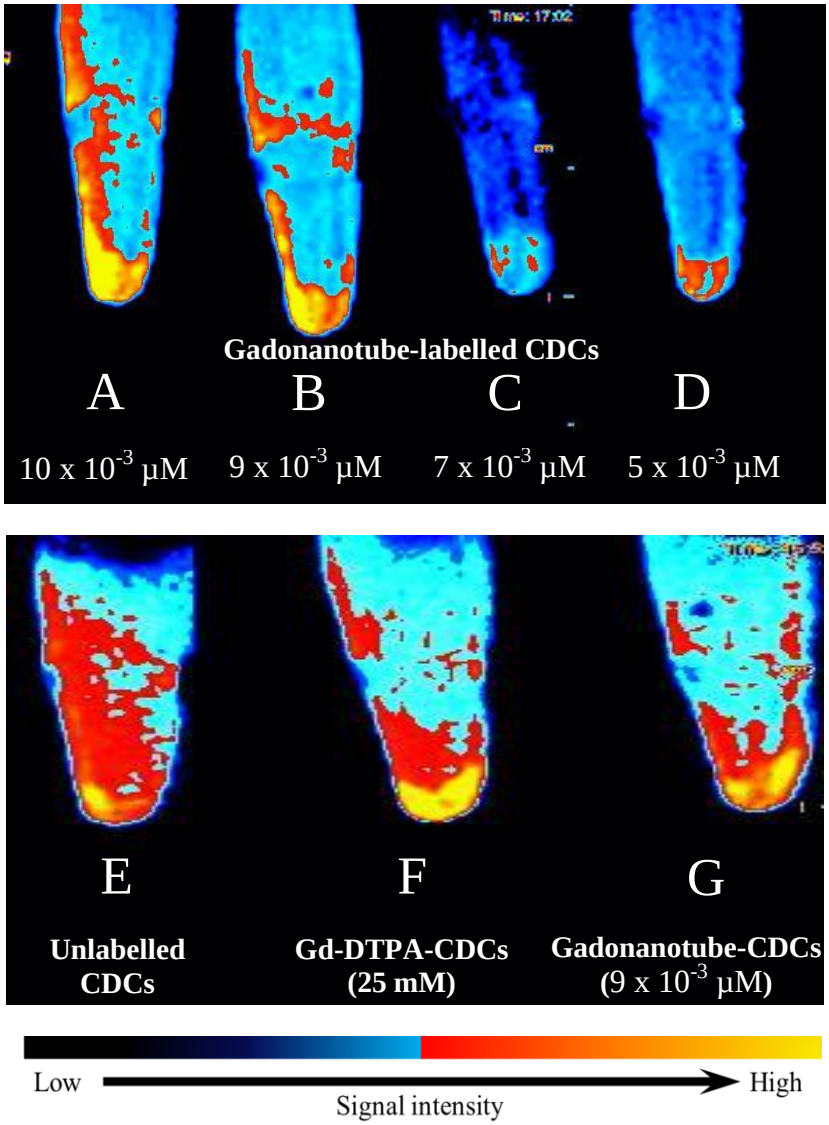

Figure 5.9: T1-weighted MRI of gadonanotube-labelled CDCs at 10 x 10^{-3} µM (A), 9 x 10^{-3} µM (B), 7 x 10^{-3} µM (C), 5 x 10^{-3} µM (D), and unlabelled control (E). Signal intensity from gadonanotube-labelled CDCs (9 x 10^{-3} µM, G) was lower than that of Gd-DTPA-CDCs (25 mM) (F). (n=1).

5.4.2.3 Re-evaluation of cytotoxicity and MR phantoms using freshly prepared gadonanotubes

The cytotoxic characteristic of gadonanotubes observed in *Section 5.4.2.1* may have been due to gadonanotube instability in solution after storage for a long period of time (Lesa Tran, personal communication). Therefore, CDC cytotoxicity was re-evaluated using a freshly prepared gadonanotube solution (prepared by Lesa Tran, Rice University, US). No sign of toxicity was observed in CDCs at a concentration of 26.6 µM (Figure 5.10), suggesting that the gadonanotubes used in the earlier studies may have deteriorated. CDCs were labelled

with fresh gadonanotubes at 26.6 µM, but again, the contrast generated from gadonanotube-labelled cells was lower than the unlabelled control (Figure 5.11).

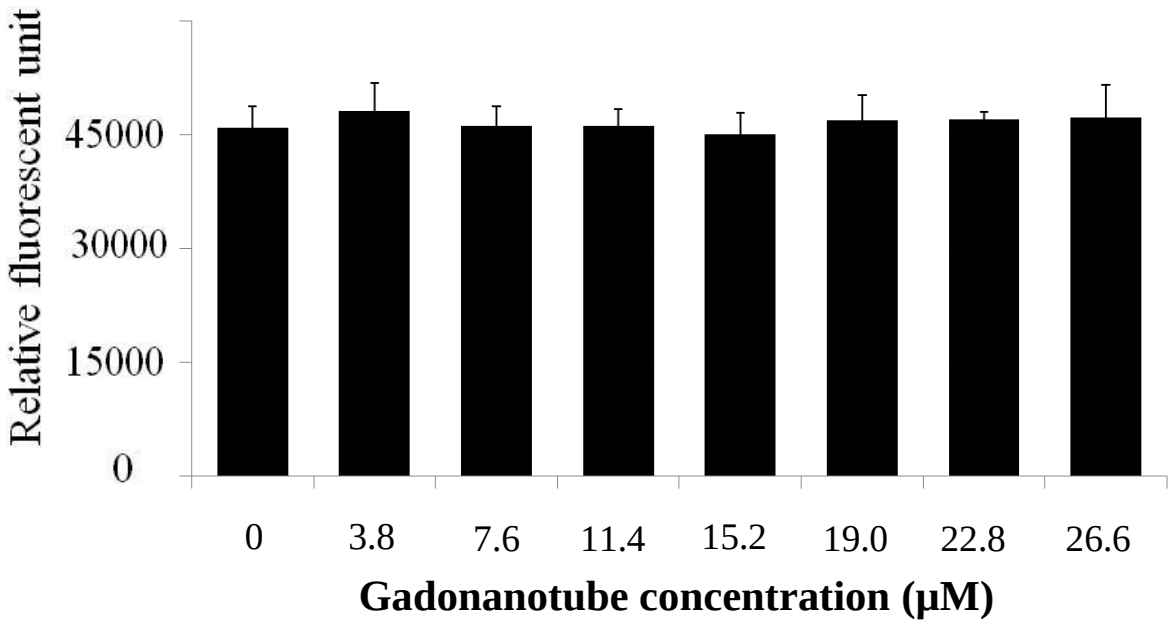

Figure 5.10: Passage 2 CDCs were plated on 96 well plate and the viability experiment repeated by labeling with 3.8 µM, 7.6 µM, 11.4 µM, 15.2 µM, 19.0 µM, 22.8 µM, and 26.6 µM gadonanotubes. No sign of toxicity was observed in CDCs after labelling with freshly-prepared gadonanotubes. Data are presented as mean ± SD (n=3).

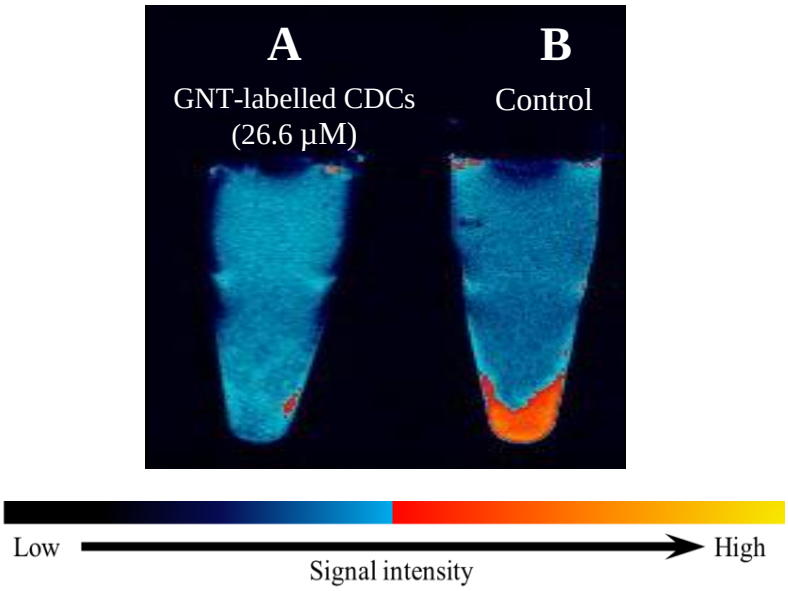

Figure 5.11: A T1 weighted image of CDCs labelled with 26.6 µM gadonanotubes (A) had a lower contrast than the unlabelled control (B) (n=1). GNT; gadonanotubes

5.5 DISCUSSION

Most pre-clinical studies of stem cell therapy are conducted using small animal models, which normally require high field MRI systems to produce high resolution images. Here, Gd-DTPA labelling was studied for cell tracking at 11.7 T, for a preclinical investigation of cell tracking in small animals using MRI. Calcium-phosphate precipitation was used to load Gd-DTPA into cells, a technique which had been used to label embryonic and neural stem cells, with high cell viability and labelling efficiency (209). Gd-DTPA did not compromise cell viability and function after labelling. In addition, the number of Gd-DTPA labelled CDCs could be estimated by mapping T1, thereby opening the possibility to track and quantify cell number *in vivo* using Gd-DTPA. High detection sensitivity is important, as low cell retention in cardiac cell therapy is common due to immediate cell loss after administration (211, 212). However, a high Gd-DTPA labelled CDC density of 1.4 $x10^5$ cells/mm^3 was required to produce positive contrast on MR imaging, despite the use of a highly T1-weighted gradient-recalled echo sequence. The low detection sensitivity would limit the use of Gd-DTPA for cell tracking *in vivo*.

Gadonanotubes exhibited greater T1-shortening than Gd-DTPA at 1.5 T (210). Thus, gadonanotubes were evaluated for improvement of sensitivity and detection threshold. Gadonanotubes were non-toxic to CDCs at 26.6 μM, but gadonanotube solutions were unstable, which caused cytotoxicity, due to leakage of cytotoxic free gadolinium ions (Gd^{3+}) from carbon nanotubes after more than a month at room temperature. In addition, gadonanotubes exhibited a dominant T2 effect at 11.7 T and caused hypointense contrast at high concentrations, in agreement with a recent report from Sitharaman, who showed that gadonanotube had a large T2 effect at 7 T (213). CDCs labelled with a much lower gadonanotube concentration (9×10^{-3} μM) had hyperintense contrast, but signal intensity was lower than that of Gd-DTPA labelled CDCs. Owing to the field dependent nature of T1, ultra

high field systems yield a significant slowing of T1 relaxation, such that the T2 shortening effect produced by Gd^{3+} becomes dominant, and results in loss of signal.

Others have reported superior signal enhancement in MCF-7 human breast cancer cells after labelling with gadonanotubes compared with Gd-DTPA at 9.4 T (214). However, this difference may be attributed to the Gd-DTPA labelling method employed as Gd-DTPA was solubilized in bovine serum albumin solution and incubated with cells overnight with no transfection agent. No internalization of Gd-DTPA into the cells was observed, as confirmed using inductively coupled plasma optical emission spectroscopy (ICP-OES) measurements. Here, calcium-phosphate was used to internalize Gd-DTPA into CDCs, which had a labelling efficiency of more than 80% in mouse embryonic stem cells (215). In addition, there was no hyperintense contrast in gadonanotube-labelled cells at 11.7 T, possibly due to a difference in cell type, labelling efficiency and the applied field strength in the experiment.

Nevertheless, there were limitations to this study. First, the cellular uptake of Gd-DTPA was not measured due to the limited equipment available. Hence, it could not be confirmed that the Gd-DTPA labelling concentration (25 mM) suggested by Rudelius was optimum for CDCs (215). In addition, CDCs contain cells of different sizes, and the amount of loaded Gd-DTPA or gadonanotube could vary from cell to cell. Thus, the signal intensity generated on the MR image may be dependent on the small:large cell ratio of the CDC population.

In conclusion, cell labelling using Gd-DTPA did not yield high detection sensitivity using MRI at 11.7 T. Gadonanotubes were tried to increase detection sensitivity, but resulted in loss of MR signal due to dominant T2 shortening when using high labelling concentrations at high field. A low gadonanotube labelling concentration (9×10^{-3} µM) showed hyperintense contrast, but the signal intensity was lower than labelling with Gd-DTPA. Hence, Gd-DTPA

and gadonanotubes are not ideal contrast agents for cell labelling and positive contrast detection at 11.7 T.

Chapter 6

General discussion

GENERAL DISCUSSION

Endogenous cardiac stem cells (CSCs) are a promising cell candidate for heart therapy. To advance the use of CSCs in the clinical setting and improve the therapeutic outcome, the method of isolation and culture must be optimized to provide sufficient CSCs in a reasonably short time period, whilst maintaining the stem cell phenotype. The main objective of the work described in this thesis was to isolate, characterize and optimize CSC culture conditions to allow rapid expansion, without compromising cell quality in terms of stemness and function, and to label cells with a positive contrast agent to allow imaging and tracking *in vivo* using MRI following cell administration.

Phenotypic characterization of cardiosphere-derived cells

In Chapter 3, the isolation and preliminary culture optimization of cardiosphere-derived cells (CDCs) were described, as were cell characterization and functional assessment *in vivo*. Culture conditions were optimized to reduce the time taken for cardiosphere formation to 4 days, which significantly shortened the time of expansion to 16 days and yielded 1.5 x 10^7 cells. CDCs expressed various stemness markers (c-kit, Oct3/4, SOX2, Klf4) and cardiomyocyte differentiation markers (Nkx2.5 and GATA4), confirming that CDCs were cardiac-derived stem cells. However, 71% of CDCs expressed CD90, indicating that most CDCs exhibited a mesenchymal phenotype, as has been shown in other studies (130). Some differentiated cells, including fibroblasts (expressing discoidin domain receptor-2), smooth muscle cells and, to a lesser extent, endothelial cells, were also detected in the CDC population. Nevertheless, 20% of CDCs were induced to differentiate into cardiomyocytes that expressed cardiac troponin I, despite there being only 3% c-kit positive cells present in CDCs. This suggested that some cardiomyocyte progenitors may arise from c-kit negative cells, for example the mesenchymal population (216), in CDCs. CDC cardiomyogenic

differentiation was also observed *in vivo* in the infarcted myocardium, confirming that CDCs are capable of cardiomyogenic differentiation, despite suggestions to the contrary (150).

Cardiosphere-derived cells ameliorated infarcted heart function

CDCs were labelled with micron-sized iron oxide particles (MPIOs), so that successful cell administration and retention in the infarcted rat heart could be confirmed using MRI. *In vitro* CDC proliferation and cardiosphere-forming capability were not affected by MPIO labelling, nor was the potential for *in vivo* myocyte differentiation, suggesting that MPIO-labelling is safe and has high biocompatibility. Serial measurements of hypointensities in MR images, which colocalized with MPIO-labelled CDCs, confirmed that CDCs engrafted in the myocardium for at least 16 weeks. A significant improvement in left ventricular ejection fraction (LVEF) was observed, with a better preserved peri-infarct wall thickness in the CDC treated hearts after 16 weeks, compared with that in untreated controls. Others have also found that CDC treatment improved heart function in mouse, rat and pig (99, 167, 168, 186, 217) (*Supplementary Table 2*). Furthermore, Chimenti and colleagues demonstrated that the regenerative mechanism of CDCs in the infarcted myocardium was both via indirect mechanisms, including secretion of paracrine factors that improved cardiomyocyte survival and activated endogenous cardiac stem cells and, via cardiomyocyte differentiation of administered CDCs, with differentiation accounting for 20-50% of the observed effects (167). Moreover, Smith *et al.* (2008) showed that a mixed population of CDCs (with ~20% c-kit$^+$ cells) possessed better regenerative potential *in vivo* than purified c-kit$^+$ or CD90$^+$ cells (102). Only a few reports failed to show the regenerative potential of CDCs, but these differences may be attributed to variations in the experimental design or the cell isolation and expansion methods employed in the studies (109, 150, 182).

Culture optimization and c-kit$^+$ cells in CDCs

The c-kit (CD117) receptor has a role in cell survival, proliferation and differentiation in hematopoietic stem cells by activating multiple biological signalling pathways (218). It is also expressed in many other cell types, such as mast cells (219), melanocytes (220), prostate stem cells (221), cancer stem cells (222), and the endogenous cardiac stem cells (28). To date, c-kit has been used simply as a marker to isolate, or indicate the presence of, cardiac stem cells.

It has been suggested that c-kit$^+$ CSCs and CDCs may share the same precursor (190), which could possibly be the epicardial-derived cells (EPDCs), which originate from an *in vivo* event called epithelial-mesenchymal transition (EMT) (223). EMT is a process of transformation of the epithelial cells, which normally residue near the basement membrane, to acquire a mesenchymal phenotype, with increased cell migratory and invasion capability, allowing the cells to migrate away from where they originated (224). In the developing heart, multipotent cells in the epicardium undergo EMT and give rise to EPDCs, which migrate into sub-epicardium and myocardium, and generate most heart components, including cardiomyocytes (225). In ischemic cardiomyopathy, c-kit$^+$ cells increase in the heart (78), and participate in myocardial regeneration (28). They are predominantly located in the subepicardium rather than the myocardium, where they are co-located with laminin (185).

A few recent studies have reported a reduction of c-kit expression, either in purified c-kit cells, or CDCs over time in culture, (182, 190, 216). Koninckx *et al.* (2010), demonstrated that clonogenic-derived c-kit$^+$ cells and CDCs lost c-kit expression after several passages in culture (190). This was explained by possible internalization of the c-kit receptor upon SCF activation (226), or by the destructive effect of trypsin on the antibody binding site of the c-kit receptor, thereby obscuring the c-kit receptor from detection. However, Gambini *et al.* (2010) showed that c-kit expression was significantly down-regulated at the RNA level after 4

passages, compared with freshly isolated c-kit$^+$ cells. This indicates that culture conditions may not be optimal for the growth of c-kit$^+$ cells.

Cardiosphere formation may increase the c-kit$^+$ population (99). However, here, CDCs had a comparable level of c-kit$^+$ cells (~3%) to those in explant-derived cells (EDCs). To increase the number of c-kit$^+$ cells, the optimal extracellular matrix (ECM) protein for CDC expansion was determined, by creating a niche-like environment to reduce spontaneous differentiation and preserve cell stemness. Hanging drop culture was the best method to induce cardiosphere formation, and CDCs cultured on collagen IV contained the highest c-kit$^+$ population. Although this combination increased passage two CDC c-kit$^+$ cells three-fold (to ~10%), a decline in c-kit level occurred when CDCs were kept longer in culture (data not shown).

Accumulating evidence suggests that cardiospheres possess better stem cell characteristics and potency than monolayer CDCs. Chimenti et al. (2010) compared cardiospheres, CDCs and normal human dermal fibroblasts for their secretion profile of growth factors (167), particularly looking at vascular endothelial growth factor (VEGF), hepatocyte growth factor (HGF) and insulin-like growth factor-1 (IGF-1), which possess a cardioprotective roles in myocardial infarction (227, 228). All three growth factors were secreted at a high level by cardiospheres, but the amount of secretion decreased in CDCs, with only VEGF released in a detectable amount (167). However, production of VEGF could be increased by reforming cardiospheres from CDCs (167), with the level of production dependent on sphere-size (191). This may be a result of the hypoxic environment created inside the three-dimensional sphere that up-regulates the hypoxia-inducible factor-1α (HIF-1α) and activates down-stream VEGF transcription (192). Many studies have shown that HIF-1α protein expression in human cancer cells is up-regulated by IGF-1 (229, 230), suggesting a synergistic relationship of the two signalling pathways in maintaining stem cell function (231, 232). Interestingly, a fall in

IGF-1 level (167) was found under the same conditions as down-regulation of c-kit expression in CDCs (233). Furthermore, IGF-1 up-regulates c-kit and induces cell cycling in neonatal myocytes (234). To date, no direct evidence shows that IGF-1 expression is related to c-kit expression in CDCs.

Cardiospheres exhibit strong expression of stemness genes, improved resistance to oxidative stress, and resembled a niche-like environment for c-kit^{+} cardiac stem cells (191, 233). The regenerative potency of cardiospheres in the infarcted myocardium results in superior therapeutic effects compared with CDCs, in attenuating progressive ventricular remodelling (235). However, cardiospheres need to be injected directly into the myocardium as they are too large for intracoronary delivery, which is more invasive and less accepted interventional procedure (168). Furthermore, the growth of cardiospheres was slower than that of CDCs, which may hamper generation of sufficient cells in short time. Therefore, in order to obtain relevant cell numbers within a reasonably short time, cell expansion in a monolayer was required.

Magnetic resonance (MR) positive contrast agent labelling

Superparamagnetic iron particles are the most widely used MR negative contrast agent for *in vivo* cell tracking. They are formulated to facilitate cell uptake and have been shown to be highly biocompatible. Iron particles offer high sensitivity for MR detection by generating hypointense signals in MR images. However, the magnetic field inhomogeneities can be confused by local sources of iron, such as blood clots (166). Furthermore, the hypointensities in MR images may not always represent the iron-loaded transplanted cells *in vivo*. When iron-labelled dead cells were administered, they were retained in the target tissue (236), or engulfed by macrophages (164). Thus, caution must be taken when measuring cell engraftment as signal void volume.

Positive contrast agents, such as gadolinium chelates, are less sensitive than iron particles, but are less likely be affected by artefacts. *Chapter 7* described an attempt to validate a MR positive contrast agent for *in vivo* stem cell tracking. This had been done using a clinical magnet (1.5 T), but rarely in high field MR systems (> 9 T) (*Supplementary Table 3*). Two MR agents, gadolinium-DTPA (Gd-DTPA) and gadonanotubes, were tested in the study. *In vitro* data showed that neither agent affected CDC viability. Gd-DTPA-labelled cells could be quantified by T1 mapping, but a high cell density was necessary for a detectable signal in the MR image. Gadonanotubes are a strong positive contrast agent at 1.5 T, but showed predominant T2 effects at 11.7 T, precluding their use for pre-clinical cell tracking experiments in small animals, where a high magnetic field strength is needed for MR resolution. An alternate positive contrast agent should be sought or developed to achieve this objective.

Study limitations

Although many studies have shown that cardiac-derived c-kit$^+$ stem cells are stem cells with multilineage differentiation potential (28), which contribute to heart regeneration following myocardial infarction (128), the role of c-kit$^+$ cells and their function in CDCs is unclear, and there is no direct evidence to date to show that the cardiomyocyte differentiating cells in CDCs arises mainly from the c-kit$^+$ population. Therefore, the use of c-kit as the only stem cell marker may lead to the effect of the changes to the culture protocol on other potential cardiac stem or progenitor cells that may be present in the population being overlooked.

Future directions

Many studies have shown CDCs improve cardiac function after myocardial infarction, which has led to a clinical trial (CArdiosphere-Derived aUtologous Stem CElls to Reverse ventricUlar dySfunction (CADUCEUS)). However, the protocol used here altered the original

characteristics and properties of cardiospheres after expansion into CDCs. Future research will focus on further optimization of CDC culture, with the ultimate aim of preserving most, if not all, the characteristics of cardiospheres in CDCs, in terms of paracrine secretion, differentiation and *in vivo* tissue regeneration. Culture conditions mimicking growth conditions in cardiospheres should be employed for CDC expansion, for example using collagen IV as the matrix for cell expansion, plus hypoxic preconditioning. The possible role of IGF-1 in preserving c-kit expressing cells in CDCs would also be investigated.

Recently, a new approach of imaging cells *in vivo* has used fluorine (^{19}F)-based particles (237). Unlike conventional paramagnetic contrast agents, such as gadolinium and iron particles, which rely on the alteration of ^{1}H spin of the water molecules in close proximity to the contrast agents, the ^{19}F nuclei can be imaged directly by the MR scanner. Due to negligible endogenous fluorine atoms in the body, ^{19}F MRI provides high specificity detection with a high signal to noise ratio, which permits more accurate localization and quantification of ^{19}F-labelled cells (238). Furthermore, tracking of fluorinated particle-labelled cells has been successful using clinical (1.5 T) and experimental (11.7 T) MR scanners (239). Therefore, future work would focus on the use of perfluorocarbon nanobeacons for CDC labelling.

In conclusion, cardiosphere-derived cells are a useful way to expand explant tissue, and possibly their resident cardiac stem cells, for uses to improve heart function after myocardial infarction. Hanging drop culture is the best method to generate cardiospheres and collagen IV is the best ECM for CDC expansion, although further optimization is needed to enhance the therapeutic effects of CDCs. Tracking of iron-labelled cells *in vivo* can be achieved using MRI. It would be preferable to use positive contrast in MR imaging to better visualize

injected cells without the confusion of endogenous signal voids, however, gadolinium-DTPA and gadonanotube are not ideal for cell tracking at high MR field strengths.

References:

1. http://www.who.int/mediacentre/factsheets/fs317/en/index.html
2. http://www.heartstats.org/datapage.asp?id=752
3. Hofstra, L., Liem, I. H., Dumont, E. A., Boersma, H. H., van Heerde, W. L., Doevendans, P. A., De Muinck, E., Wellens, H. J., Kemerink, G. J., Reutelingsperger, C. P., and Heidendal, G. A. (2000) Visualisation of cell death in vivo in patients with acute myocardial infarction. *Lancet* **356**, 209-212
4. Sutton, M. G., and Sharpe, N. (2000) Left ventricular remodeling after myocardial infarction: pathophysiology and therapy. *Circulation* **101**, 2981-2988
5. Keeley, E. C., and Hillis, L. D. (2007) Primary PCI for myocardial infarction with ST-segment elevation. *N Engl J Med* **356**, 47-54
6. Lange, R. A., and Hillis, L. D. (2002) Reperfusion therapy in acute myocardial infarction. *N Engl J Med* **346**, 954-955
7. King, S. B., 3rd, Marshall, J. J., and Tummala, P. E. (2010) Revascularization for coronary artery disease: stents versus bypass surgery. *Annu Rev Med* **61**, 199-213
8. Remme, W. J., Riegger, G., Hildebrandt, P., Komajda, M., Jaarsma, W., Bobbio, M., Soler-Soler, J., Scherhag, A., Lutiger, B., and Ryden, L. (2004) The benefits of early combination treatment of carvedilol and an ACE-inhibitor in mild heart failure and left ventricular systolic dysfunction. The carvedilol and ACE-inhibitor remodelling mild heart failure evaluation trial (CARMEN). *Cardiovasc Drugs Ther* **18**, 57-66
9. Huwer, H., Winning, J., Vollmar, B., Welter, C., Lohbach, C., Menger, M. D., and Schafers, H. J. (2003) Long-term cell survival and hemodynamic improvements after neonatal cardiomyocyte and satellite cell transplantation into healed myocardial cryoinfarcted lesions in rats. *Cell Transplant* **12**, 757-767
10. Odorico, J. S., Kaufman, D. S., and Thomson, J. A. (2001) Multilineage differentiation from human embryonic stem cell lines. *Stem Cells* **19**, 193-204
11. Nussbaum, J., Minami, E., Laflamme, M. A., Virag, J. A., Ware, C. B., Masino, A., Muskheli, V., Pabon, L., Reinecke, H., and Murry, C. E. (2007) Transplantation of undifferentiated murine embryonic stem cells in the heart: teratoma formation and immune response. *FASEB J* **21**, 1345-1357
12. Cao, F., Lin, S., Xie, X., Ray, P., Patel, M., Zhang, X., Drukker, M., Dylla, S. J., Connolly, A. J., Chen, X., Weissman, I. L., Gambhir, S. S., and Wu, J. C. (2006) In vivo visualization of embryonic stem cell survival, proliferation, and migration after cardiac delivery. *Circulation* **113**, 1005-1014
13. Draper, J. S., Pigott, C., Thomson, J. A., and Andrews, P. W. (2002) Surface antigens of human embryonic stem cells: changes upon differentiation in culture. *J Anat* **200**, 249-258
14. Takahashi, K., and Yamanaka, S. (2006) Induction of pluripotent stem cells from mouse embryonic and adult fibroblast cultures by defined factors. *Cell* **126**, 663-676
15. Zhang, J., Wilson, G. F., Soerens, A. G., Koonce, C. H., Yu, J., Palecek, S. P., Thomson, J. A., and Kamp, T. J. (2009) Functional cardiomyocytes derived from human induced pluripotent stem cells. *Circ Res* **104**, e30-41
16. Lister, R., Pelizzola, M., Kida, Y. S., Hawkins, R. D., Nery, J. R., Hon, G., Antosiewicz-Bourget, J., O'Malley, R., Castanon, R., Klugman, S., Downes, M., Yu, R., Stewart, R., Ren, B., Thomson, J. A., Evans, R. M., and Ecker, J. R. (2011) Hotspots of aberrant epigenomic reprogramming in human induced pluripotent stem cells. *Nature*
17. Wagers, A. J., and Weissman, I. L. (2004) Plasticity of adult stem cells. *Cell* **116**, 639-648
18. Kamihata, H., Matsubara, H., Nishiue, T., Fujiyama, S., Tsutsumi, Y., Ozono, R., Masaki, H., Mori, Y., Iba, O., Tateishi, E., Kosaki, A., Shintani, S., Murohara, T.,

Imaizumi, T., and Iwasaka, T. (2001) Implantation of Bone Marrow Mononuclear Cells Into Ischemic Myocardium Enhances Collateral Perfusion and Regional Function via Side Supply of Angioblasts, Angiogenic Ligands, and Cytokines. *Circulation* **104**, 1046-1052

19. Tse, H.-F., Kwong, Y.-L., Chan, J. K. F., Lo, G., Ho, C.-L., and Lau, C.-P. (2003) Angiogenesis in ischaemic myocardium by intramyocardial autologous bone marrow mononuclear cell implantation. *The Lancet* **361**, 47-49
20. Orlic, D., Kajstura, J., Chimenti, S., Jakoniuk, I., Anderson, S. M., Li, B., Pickel, J., McKay, R., Nadal-Ginard, B., Bodine, D. M., Leri, A., and Anversa, P. (2001) Bone marrow cells regenerate infarcted myocardium. *Nature* **410**, 701-705
21. Limbourg, F. P., Ringes-Lichtenberg, S., Schaefer, A., Jacoby, C., Mehraein, Y., Jager, M. D., Limbourg, A., Fuchs, M., Klein, G., Ballmaier, M., Schlitt, H. J., Schrader, J., Hilfiker-Kleiner, D., and Drexler, H. (2005) Haematopoietic stem cells improve cardiac function after infarction without permanent cardiac engraftment. *Eur J Heart Fail* **7**, 722-729
22. Numaguchi, Y., Sone, T., Okumura, K., Ishii, M., Morita, Y., Kubota, R., Yokouchi, K., Imai, H., Harada, M., Osanai, H., Kondo, T., and Murohara, T. (2006) The impact of the capability of circulating progenitor cell to differentiate on myocardial salvage in patients with primary acute myocardial infarction. *Circulation* **114**, I114-119
23. Shintani, S., Murohara, T., Ikeda, H., Ueno, T., Honma, T., Katoh, A., Sasaki, K., Shimada, T., Oike, Y., and Imaizumi, T. (2001) Mobilization of endothelial progenitor cells in patients with acute myocardial infarction. *Circulation* **103**, 2776-2779
24. Tang, J., Xie, Q., Pan, G., Wang, J., and Wang, M. (2006) Mesenchymal stem cells participate in angiogenesis and improve heart function in rat model of myocardial ischemia with reperfusion. *Eur J Cardiothorac Surg* **30**, 353-361
25. Silva, G. V., Litovsky, S., Assad, J. A. R., Sousa, A. L. S., Martin, B. J., Vela, D., Coulter, S. C., Lin, J., Ober, J., Vaughn, W. K., Branco, R. V. C., Oliveira, E. M., He, R., Geng, Y.-J., Willerson, J. T., and Perin, E. C. (2005) Mesenchymal Stem Cells Differentiate into an Endothelial Phenotype, Enhance Vascular Density, and Improve Heart Function in a Canine Chronic Ischemia Model. *Circulation* **111**, 150-156
26. Murry, C. E., Wiseman, R. W., Schwartz, S. M., and Hauschka, S. D. (1996) Skeletal myoblast transplantation for repair of myocardial necrosis. *J Clin Invest* **98**, 2512-2523
27. Taylor, D. A., Atkins, B. Z., Hungspreugs, P., Jones, T. R., Reedy, M. C., Hutcheson, K. A., Glower, D. D., and Kraus, W. E. (1998) Regenerating functional myocardium: improved performance after skeletal myoblast transplantation. *Nat Med* **4**, 929-933
28. Beltrami, A. P., Barlucchi, L., Torella, D., Baker, M., Limana, F., Chimenti, S., Kasahara, H., Rota, M., Musso, E., Urbanek, K., Leri, A., Kajstura, J., Nadal-Ginard, B., and Anversa, P. (2003) Adult cardiac stem cells are multipotent and support myocardial regeneration. *Cell* **114**, 763-776
29. Deb, A., Wang, S., Skelding, K. A., Miller, D., Simper, D., and Caplice, N. M. (2003) Bone marrow-derived cardiomyocytes are present in adult human heart: A study of gender-mismatched bone marrow transplantation patients. *Circulation* **107**, 1247-1249
30. Bayes-Genis, A., Salido, M., Sole Ristol, F., Puig, M., Brossa, V., Camprecios, M., Corominas, J. M., Marinoso, M. L., Baro, T., Vela, M. C., Serrano, S., Padro, J. M., Bayes de Luna, A., and Cinca, J. (2002) Host cell-derived cardiomyocytes in sex-mismatch cardiac allografts. *Cardiovasc Res* **56**, 404-410
31. Laflamme, M. A., Myerson, D., Saffitz, J. E., and Murry, C. E. (2002) Evidence for cardiomyocyte repopulation by extracardiac progenitors in transplanted human hearts. *Circ Res* **90**, 634-640

32. Martin-Rendon, E., Brunskill, S. J., Hyde, C. J., Stanworth, S. J., Mathur, A., and Watt, S. M. (2008) Autologous bone marrow stem cells to treat acute myocardial infarction: a systematic review. *Eur Heart J* **29**, 1807-1818
33. Terada, N., Hamazaki, T., Oka, M., Hoki, M., Mastalerz, D. M., Nakano, Y., Meyer, E. M., Morel, L., Petersen, B. E., and Scott, E. W. (2002) Bone marrow cells adopt the phenotype of other cells by spontaneous cell fusion. *Nature* **416**, 542-545
34. Fujii, H., Tomita, S., Nakatani, T., Fukuhara, S., Hanatani, A., Ohtsu, Y., Ishida, M., Yutani, C., Miyatake, K., and Kitamura, S. (2004) A novel application of myocardial contrast echocardiography to evaluate angiogenesis by autologous bone marrow cell transplantation in chronic ischemic pig model. *J Am Coll Cardiol* **43**, 1299-1305
35. Asahara, T., Masuda, H., Takahashi, T., Kalka, C., Pastore, C., Silver, M., Kearne, M., Magner, M., and Isner, J. M. (1999) Bone marrow origin of endothelial progenitor cells responsible for postnatal vasculogenesis in physiological and pathological neovascularization. *Circ Res* **85**, 221-228
36. Murry, C. E., Soonpaa, M. H., Reinecke, H., Nakajima, H., Nakajima, H. O., Rubart, M., Pasumarthi, K. B. S., Ismail Virag, J., Bartelmez, S. H., Poppa, V., Bradford, G., Dowell, J. D., Williams, D. A., and Field, L. J. (2004) Haematopoietic stem cells do not transdifferentiate into cardiac myocytes in myocardial infarcts. *Nature* **428**, 664-668
37. Nygren, J. M., Jovinge, S., Breitbach, M., Sawen, P., Roll, W., Hescheler, J., Taneera, J., Fleischmann, B. K., and Jacobsen, S. E. W. (2004) Bone marrow-derived hematopoietic cells generate cardiomyocytes at a low frequency through cell fusion, but not transdifferentiation. *Nat Med* **10**, 494-501
38. Li, T. S., Komota, T., Ohshima, M., Qin, S. L., Kubo, M., Ueda, K., and Hamano, K. (2008) TGF-beta induces the differentiation of bone marrow stem cells into immature cardiomyocytes. *Biochem Biophys Res Commun* **366**, 1074-1080
39. Xaymardan, M., Cimini, M., Fazel, S., Weisel, R. D., Lu, W.-Y., Martin, U., Harvey, R. P., and Li, R.-K. (2009) c-Kit Function Is Necessary for In Vitro Myogenic Differentiation of Bone Marrow Hematopoietic Cells. *STEM CELLS* **27**, 1911-1920
40. Peichev, M., Naiyer, A. J., Pereira, D., Zhu, Z., Lane, W. J., Williams, M., Oz, M. C., Hicklin, D. J., Witte, L., Moore, M. A. S., and Rafii, S. (2000) Expression of VEGFR-2 and AC133 by circulating human CD34+ cells identifies a population of functional endothelial precursors. *Blood* **95**, 952-958
41. Yoder, M. C., Mead, L. E., Prater, D., Krier, T. R., Mroueh, K. N., Li, F., Krasich, R., Temm, C. J., Prchal, J. T., and Ingram, D. A. (2007) Redefining endothelial progenitor cells via clonal analysis and hematopoietic stem/progenitor cell principals. *Blood* **109**, 1801-1809
42. Kocher, A. A., Schuster, M. D., Szabolcs, M. J., Takuma, S., Burkhoff, D., Wang, J., Homma, S., Edwards, N. M., and Itescu, S. (2001) Neovascularization of ischemic myocardium by human bone-marrow-derived angioblasts prevents cardiomyocyte apoptosis, reduces remodeling and improves cardiac function. *Nat Med* **7**, 430-436
43. Kawamoto, A., Gwon, H.-C., Iwaguro, H., Yamaguchi, J.-I., Uchida, S., Masuda, H., Silver, M., Ma, H., Kearney, M., Isner, J. M., and Asahara, T. (2001) Therapeutic Potential of Ex Vivo Expanded Endothelial Progenitor Cells for Myocardial Ischemia. *Circulation* **103**, 634-637
44. Wu, Y., Ip, J. E., Huang, J., Zhang, L., Matsushita, K., Liew, C.-C., Pratt, R. E., and Dzau, V. J. (2006) Essential Role of ICAM-1/CD18 in Mediating EPC Recruitment, Angiogenesis, and Repair to the Infarcted Myocardium. *Circ Res* **99**, 315-322
45. Badorff, C., Brandes, R. P., Popp, R., Rupp, S., Urbich, C., Aicher, A., Fleming, I., Busse, R., Zeiher, A. M., and Dimmeler, S. (2003) Transdifferentiation of blood-derived human adult endothelial progenitor cells into functionally active cardiomyocytes. *Circulation* **107**, 1024-1032

46. Yeh, E. T., Zhang, S., Wu, H. D., Korbling, M., Willerson, J. T., and Estrov, Z. (2003) Transdifferentiation of human peripheral blood CD34+-enriched cell population into cardiomyocytes, endothelial cells, and smooth muscle cells in vivo. *Circulation* **108**, 2070-2073
47. Murasawa, S., Kawamoto, A., Horii, M., Nakamori, S., and Asahara, T. (2005) Niche-dependent translineage commitment of endothelial progenitor cells, not cell fusion in general, into myocardial lineage cells. *Arterioscler Thromb Vasc Biol* **25**, 1388-1394
48. Wollert, K. C., and Drexler, H. (2005) Mesenchymal stem cells for myocardial infarction: promises and pitfalls. *Circulation* **112**, 151-153
49. Horwitz, E. M., Le Blanc, K., Dominici, M., Mueller, I., Slaper-Cortenbach, I., Marini, F. C., Deans, R. J., Krause, D. S., and Keating, A. (2005) Clarification of the nomenclature for MSC: The International Society for Cellular Therapy position statement. *Cytotherapy* **7**, 393-395
50. Shake, J. G., Gruber, P. J., Baumgartner, W. A., Senechal, G., Meyers, J., Redmond, J. M., Pittenger, M. F., and Martin, B. J. (2002) Mesenchymal stem cell implantation in a swine myocardial infarct model: engraftment and functional effects. *Ann Thorac Surg* **73**, 1919-1925; discussion 1926
51. Nagaya, N., Fujii, T., Iwase, T., Ohgushi, H., Itoh, T., Uematsu, M., Yamagishi, M., Mori, H., Kangawa, K., and Kitamura, S. (2004) Intravenous administration of mesenchymal stem cells improves cardiac function in rats with acute myocardial infarction through angiogenesis and myogenesis. *Am J Physiol Heart Circ Physiol* **287**, H2670-2676
52. Olivares, E. L., Costa-e-Sousa, R. H., Werneck-de-Castro, J. o. P. S., Pinho-Ribeiro, V., Silva, M. r. G., Ribeiro, K. C., Mattos, E. C., Goldenberg, R. C. S., de Carvalho, A. C. C., and Masuda, M. O. (2007) Cellular cardiomyoplasty in large myocardial infarction: Can the beneficial effect be enhanced by ACE-inhibitor therapy? *European Journal of Heart Failure* **9**, 558-567
53. Uemura, R., Xu, M., Ahmad, N., and Ashraf, M. (2006) Bone Marrow Stem Cells Prevent Left Ventricular Remodeling of Ischemic Heart Through Paracrine Signaling. *Circ Res* **98**, 1414-1421
54. Carr, C. A., Stuckey, D. J., Tatton, L., Tyler, D. J., Hale, S. J., Sweeney, D., Schneider, J. E., Martin-Rendon, E., Radda, G. K., Harding, S. E., Watt, S. M., and Clarke, K. (2008) Bone marrow-derived stromal cells home to and remain in the infarcted rat heart but fail to improve function: an in vivo cine-MRI study. *Am J Physiol Heart Circ Physiol* **295**, H533-542
55. Kuang, S., and Rudnicki, M. A. (2008) The emerging biology of satellite cells and their therapeutic potential. *Trends Mol Med* **14**, 82-91
56. Pagani, F. D., DerSimonian, H., Zawadzka, A., Wetzel, K., Edge, A. S., Jacoby, D. B., Dinsmore, J. H., Wright, S., Aretz, T. H., Eisen, H. J., and Aaronson, K. D. (2003) Autologous skeletal myoblasts transplanted to ischemia-damaged myocardium in humans. Histological analysis of cell survival and differentiation. *J Am Coll Cardiol* **41**, 879-888
57. Siminiak, T., Kalawski, R., Fiszer, D., Jerzykowska, O., Rzezniczak, J., Rozwadowska, N., and Kurpisz, M. (2004) Autologous skeletal myoblast transplantation for the treatment of postinfarction myocardial injury: phase I clinical study with 12 months of follow-up. *American heart journal* **148**, 531-537
58. Gavira, J. J., Herreros, J., Perez, A., Garcia-Velloso, M. J., Barba, J., Martin-Herrero, F., Cañizo, C., Martin-Arnau, A., Martí-Climent, J. M., Hernández, M., López-Holgado, N., González-Santos, J. M., Martín-Luengo, C., Alegria, E., and Prósper, F. (2006) Autologous skeletal myoblast transplantation in patients with nonacute myocardial infarction: 1-year follow-up. *The Journal of Thoracic and Cardiovascular Surgery* **131**, 799-804

59. Menasche, P., Hagege, A. A., Scorsin, M., Pouzet, B., Desnos, M., Duboc, D., Schwartz, K., Vilquin, J. T., and Marolleau, J. P. (2001) Myoblast transplantation for heart failure. *Lancet* **357**, 279-280
60. Menasche, P., Alfieri, O., Janssens, S., McKenna, W., Reichenspurner, H., Trinquart, L., Vilquin, J. T., Marolleau, J. P., Seymour, B., Larghero, J., Lake, S., Chatellier, G., Solomon, S., Desnos, M., and Hagege, A. A. (2008) The Myoblast Autologous Grafting in Ischemic Cardiomyopathy (MAGIC) trial: first randomized placebo-controlled study of myoblast transplantation. *Circulation* **117**, 1189-1200
61. Menasche, P. (2008) Skeletal myoblasts and cardiac repair. *Journal of molecular and cellular cardiology* **45**, 545-553
62. Rubart, M., Soonpaa, M. H., Nakajima, H., and Field, L. J. (2004) Spontaneous and evoked intracellular calcium transients in donor-derived myocytes following intracardiac myoblast transplantation. *The Journal of clinical investigation* **114**, 775-783
63. http://clinicaltrials.gov/ct2/show/NCT00908622?term=myoblast&rank=1
64. Kucia, M., Reca, R., Campbell, F. R., Zuba-Surma, E., Majka, M., Ratajczak, J., and Ratajczak, M. Z. (2006) A population of very small embryonic-like (VSEL) CXCR4(+)SSEA-1(+)Oct-4+ stem cells identified in adult bone marrow. *Leukemia* **20**, 857-869
65. Ratajczak, M. Z., Kucia, M., Ratajczak, J., and Zuba-Surma, E. K. (2009) A multi-instrumental approach to identify and purify very small embryonic like stem cells (VSELs) from adult tissues. *Micron* **40**, 386-393
66. Dawn, B., Tiwari, S., Kucia, M. J., Zuba-Surma, E. K., Guo, Y., Sanganalmath, S. K., Abdel-Latif, A., Hunt, G., Vincent, R. J., Taher, H., Reed, N. J., Ratajczak, M. Z., and Bolli, R. (2008) Transplantation of bone marrow-derived very small embryonic-like stem cells attenuates left ventricular dysfunction and remodeling after myocardial infarction. *Stem Cells* **26**, 1646-1655
67. Zuba-Surma, E. K., Guo, Y., Taher, H., Sanganalmath, S. K., Hunt, G., Vincent, R. J., Kucia, M., Abdel-Latif, A., Tang, X. L., Ratajczak, M. Z., Dawn, B., and Bolli, R. (2010) Transplantation of expanded bone marrow-derived very small embryonic-like stem cells (VSEL-SCs) improves left ventricular function and remodeling after myocardial infarction. *J Cell Mol Med*
68. Olivetti, G., Abbi, R., Quaini, F., Kajstura, J., Cheng, W., Nitahara, J. A., Quaini, E., Di Loreto, C., Beltrami, C. A., Krajewski, S., Reed, J. C., and Anversa, P. (1997) Apoptosis in the failing human heart. *N Engl J Med* **336**, 1131-1141
69. Kajstura, J., Hosoda, T., Bearzi, C., Rota, M., Maestroni, S., Urbanek, K., Leri, A., and Anversa, P. (2008) The human heart: a self-renewing organ. *Clin Transl Sci* **1**, 80-86
70. Hsieh, P. C., Segers, V. F., Davis, M. E., MacGillivray, C., Gannon, J., Molkentin, J. D., Robbins, J., and Lee, R. T. (2007) Evidence from a genetic fate-mapping study that stem cells refresh adult mammalian cardiomyocytes after injury. *Nat Med* **13**, 970-974
71. Kajstura, J., Urbanek, K., Rota, M., Bearzi, C., Hosoda, T., Bolli, R., Anversa, P., and Leri, A. (2008) Cardiac stem cells and myocardial disease. *J Mol Cell Cardiol* **45**, 505-513
72. Ellison, G. M., Torella, D., Karakikes, I., and Nadal-Ginard, B. (2007) Myocyte death and renewal: modern concepts of cardiac cellular homeostasis. *Nat Clin Pract Cardiovasc Med* **4 Suppl 1**, S52-59
73. Pfister, O., Oikonomopoulos, A., Sereti, K. I., Sohn, R. L., Cullen, D., Fine, G. C., Mouquet, F., Westerman, K., and Liao, R. (2008) Role of the ATP-binding cassette transporter Abcg2 in the phenotype and function of cardiac side population cells. *Circ Res* **103**, 825-835

74. Martin, C. M., Meeson, A. P., Robertson, S. M., Hawke, T. J., Richardson, J. A., Bates, S., Goetsch, S. C., Gallardo, T. D., and Garry, D. J. (2004) Persistent expression of the ATP-binding cassette transporter, Abcg2, identifies cardiac SP cells in the developing and adult heart. *Dev Biol* **265**, 262-275
75. Oyama, T., Nagai, T., Wada, H., Naito, A. T., Matsuura, K., Iwanaga, K., Takahashi, T., Goto, M., Mikami, Y., Yasuda, N., Akazawa, H., Uezumi, A., Takeda, S., and Komuro, I. (2007) Cardiac side population cells have a potential to migrate and differentiate into cardiomyocytes in vitro and in vivo. *J Cell Biol* **176**, 329-341
76. Higashikuni, Y., Sainz, J., Nakamura, K., Takaoka, M., Enomoto, S., Iwata, H., Sahara, M., Tanaka, K., Koibuchi, N., Ito, S., Kusuhara, H., Sugiyama, Y., Hirata, Y., Nagai, R., and Sata, M. (2010) The ATP-binding cassette transporter BCRP1/ABCG2 plays a pivotal role in cardiac repair after myocardial infarction via modulation of microvascular endothelial cell survival and function. *Arterioscler Thromb Vasc Biol* **30**, 2128-2135
77. Pfister, O., Mouquet, F., Jain, M., Summer, R., Helmes, M., Fine, A., Colucci, W. S., and Liao, R. (2005) CD31- but Not CD31+ cardiac side population cells exhibit functional cardiomyogenic differentiation. *Circ Res* **97**, 52-61
78. Fransioli, J., Bailey, B., Gude, N. A., Cottage, C. T., Muraski, J. A., Emmanuel, G., Wu, W., Alvarez, R., Rubio, M., Ottolenghi, S., Schaefer, E., and Sussman, M. A. (2008) Evolution of the c-kit-positive cell response to pathological challenge in the myocardium. *Stem Cells* **26**, 1315-1324
79. Urbanek, K., Torella, D., Sheikh, F., De Angelis, A., Nurzynska, D., Silvestri, F., Beltrami, C. A., Bussani, R., Beltrami, A. P., Quaini, F., Bolli, R., Leri, A., Kajstura, J., and Anversa, P. (2005) Myocardial regeneration by activation of multipotent cardiac stem cells in ischemic heart failure. *Proc Natl Acad Sci U S A* **102**, 8692-8697
80. Torella, D., Ellison, G. M., Karakikes, I., and Nadal-Ginard, B. (2007) Growth-factor-mediated cardiac stem cell activation in myocardial regeneration. *Nat Clin Pract Cardiovasc Med* **4 Suppl 1**, S46-51
81. Miyamoto, S., Kawaguchi, N., Ellison, G. M., Matsuoka, R., Shin'oka, T., and Kurosawa, H. (2010) Characterization of long-term cultured c-kit+ cardiac stem cells derived from adult rat hearts. *Stem Cells Dev* **19**, 105-116
82. Kawaguchi, N., Smith, A. J., Waring, C. D., Hasan, M. K., Miyamoto, S., Matsuoka, R., and Ellison, G. M. (2010) c-kitpos GATA-4 high rat cardiac stem cells foster adult cardiomyocyte survival through IGF-1 paracrine signalling. *PLoS One* **5**, e14297
83. Tang, X. L., Rokosh, G., Sanganalmath, S. K., Yuan, F., Sato, H., Mu, J., Dai, S., Li, C., Chen, N., Peng, Y., Dawn, B., Hunt, G., Leri, A., Kajstura, J., Tiwari, S., Shirk, G., Anversa, P., and Bolli, R. (2010) Intracoronary administration of cardiac progenitor cells alleviates left ventricular dysfunction in rats with a 30-day-old infarction. *Circulation* **121**, 293-305
84. Oh, H., Bradfute, S. B., Gallardo, T. D., Nakamura, T., Gaussin, V., Mishina, Y., Pocius, J., Michael, L. H., Behringer, R. R., Garry, D. J., Entman, M. L., and Schneider, M. D. (2003) Cardiac progenitor cells from adult myocardium: homing, differentiation, and fusion after infarction. *Proc Natl Acad Sci U S A* **100**, 12313-12318
85. Matsuura, K., Nagai, T., Nishigaki, N., Oyama, T., Nishi, J., Wada, H., Sano, M., Toko, H., Akazawa, H., Sato, T., Nakaya, H., Kasanuki, H., and Komuro, I. (2004) Adult cardiac Sca-1-positive cells differentiate into beating cardiomyocytes. *J Biol Chem* **279**, 11384-11391
86. Tang, Y. L., Shen, L., Qian, K., and Phillips, M. I. (2007) A novel two-step procedure to expand cardiac Sca-1+ cells clonally. *Biochem Biophys Res Commun* **359**, 877-883
87. Smits, A. M., van Vliet, P., Metz, C. H., Korfage, T., Sluijter, J. P., Doevendans, P. A., and Goumans, M. J. (2009) Human cardiomyocyte progenitor cells differentiate

into functional mature cardiomyocytes: an in vitro model for studying human cardiac physiology and pathophysiology. *Nat Protoc* **4**, 232-243

88. Schmidt, S., Vieweger, A., Obst, M., Mueller, S., Gross, V., Gutberlet, M., Steinbrink, J., Taubert, S., Misselwitz, B., Luedemann, L., and Spuler, S. (2009) Dysferlin-deficient muscular dystrophy: gadofluorine M suitability at MR imaging in a mouse model. *Radiology* **250**, 87-94
89. Wang, X., Hu, Q., Nakamura, Y., Lee, J., Zhang, G., From, A. H., and Zhang, J. (2006) The role of the sca-1+/CD31- cardiac progenitor cell population in postinfarction left ventricular remodeling. *Stem Cells* **24**, 1779-1788
90. Tateishi, K., Ashihara, E., Takehara, N., Nomura, T., Honsho, S., Nakagami, T., Morikawa, S., Takahashi, T., Ueyama, T., Matsubara, H., and Oh, H. (2007) Clonally amplified cardiac stem cells are regulated by Sca-1 signaling for efficient cardiovascular regeneration. *J Cell Sci* **120**, 1791-1800
91. Laugwitz, K. L., Moretti, A., Lam, J., Gruber, P., Chen, Y., Woodard, S., Lin, L. Z., Cai, C. L., Lu, M. M., Reth, M., Platoshyn, O., Yuan, J. X., Evans, S., and Chien, K. R. (2005) Postnatal isl1+ cardioblasts enter fully differentiated cardiomyocyte lineages. *Nature* **433**, 647-653
92. Laugwitz, K. L., Moretti, A., Caron, L., Nakano, A., and Chien, K. R. (2008) Islet1 cardiovascular progenitors: a single source for heart lineages? *Development* **135**, 193-205
93. Bollini, S., Smart, N., and Riley, P. R. (2010) Resident cardiac progenitor cells: At the heart of regeneration. *J Mol Cell Cardiol*
94. Vieira, J. M., and Riley, P. R. (2011) Epicardium-derived cells: a new source of regenerative capacity. *Heart* **97**, 15-19
95. Wessels, A., and Perez-Pomares, J. M. (2004) The epicardium and epicardially derived cells (EPDCs) as cardiac stem cells. *Anat Rec A Discov Mol Cell Evol Biol* **276**, 43-57
96. Riley, P. R., and Smart, N. (2009) Thymosin beta4 induces epicardium-derived neovascularization in the adult heart. *Biochem Soc Trans* **37**, 1218-1220
97. Cai, C. L., Martin, J. C., Sun, Y., Cui, L., Wang, L., Ouyang, K., Yang, L., Bu, L., Liang, X., Zhang, X., Stallcup, W. B., Denton, C. P., McCulloch, A., Chen, J., and Evans, S. M. (2008) A myocardial lineage derives from Tbx18 epicardial cells. *Nature* **454**, 104-108
98. Winter, E. M., Grauss, R. W., Hogers, B., van Tuyn, J., van der Geest, R., Lie-Venema, H., Steijn, R. V., Maas, S., DeRuiter, M. C., deVries, A. A., Steendijk, P., Doevendans, P. A., van der Laarse, A., Poelmann, R. E., Schalij, M. J., Atsma, D. E., and Gittenberger-de Groot, A. C. (2007) Preservation of left ventricular function and attenuation of remodeling after transplantation of human epicardium-derived cells into the infarcted mouse heart. *Circulation* **116**, 917-927
99. Messina, E., De Angelis, L., Frati, G., Morrone, S., Chimenti, S., Fiordaliso, F., Salio, M., Battaglia, M., Latronico, M. V., Coletta, M., Vivarelli, E., Frati, L., Cossu, G., and Giacomello, A. (2004) Isolation and expansion of adult cardiac stem cells from human and murine heart. *Circ Res* **95**, 911-921
100. Smith, R. R., Barile, L., Cho, H. C., Leppo, M. K., Hare, J. M., Messina, E., Giacomello, A., Abraham, M. R., and Marban, E. (2007) Regenerative potential of cardiosphere-derived cells expanded from percutaneous endomyocardial biopsy specimens. *Circulation* **115**, 896-908
101. Messina, E., De Angelis, L., Frati, G., Morrone, S., Chimenti, S., Fiordaliso, F., Salio, M., Battaglia, M., Latronico, M. V. G., Coletta, M., Vivarelli, E., Frati, L., Cossu, G., and Giacomello, A. (2004) Isolation and Expansion of Adult Cardiac Stem Cells From Human and Murine Heart. *Circ Res* **95**, 911-921

102. Smith, R. R., Chimenti, I., and Marban, E. (2008) Abstract 3417: Unselected Human Cardiosphere-derived Cells are Functionally Superior to c-Kit- or CD90-Purified Cardiosphere-derived Cells. *Circulation* **118**, S_420-a-
103. Linke, A., Müller, P., Nurzynska, D., Casarsa, C., Torella, D., Nascimbene, A., Castaldo, C., Cascapera, S., Böhm, M., Quaini, F., Urbanek, K., Leri, A., Hintze, T. H., Kajstura, J., and Anversa, P. (2005) Stem cells in the dog heart are self-renewing, clonogenic, and multipotent and regenerate infarcted myocardium, improving cardiac function. *Proceedings of the National Academy of Sciences of the United States of America* **102**, 8966-8971
104. Oh, H., Bradfute, S. B., Gallardo, T. D., Nakamura, T., Gaussin, V., Mishina, Y., Pocius, J., Michael, L. H., Behringer, R. R., Garry, D. J., Entman, M. L., and Schneider, M. D. (2003) Cardiac progenitor cells from adult myocardium: Homing, differentiation, and fusion after infarction. *Proceedings of the National Academy of Sciences of the United States of America* **100**, 12313-12318
105. Matsuura, K., Nagai, T., Nishigaki, N., Oyama, T., Nishi, J., Wada, H., Sano, M., Toko, H., Akazawa, H., Sato, T., Nakaya, H., Kasanuki, H., and Komuro, I. (2004) Adult Cardiac Sca-1-positive Cells Differentiate into Beating Cardiomyocytes. *Journal of Biological Chemistry* **279**, 11384-11391
106. Oyama, T., Nagai, T., Wada, H., Naito, A. T., Matsuura, K., Iwanaga, K., Takahashi, T., Goto, M., Mikami, Y., Yasuda, N., Akazawa, H., Uezumi, A., Takeda, S. i., and Komuro, I. (2007) Cardiac side population cells have a potential to migrate and differentiate into cardiomyocytes in vitro and in vivo. *The Journal of Cell Biology* **176**, 329-341
107. Liang, S. X., Tan, T. Y. L., Gaudry, L., and Chong, B. (2010) Differentiation and migration of Sca1+/CD31- cardiac side population cells in a murine myocardial ischemic model. *International Journal of Cardiology* **138**, 40-49
108. Laugwitz, K.-L., Moretti, A., Lam, J., Gruber, P., Chen, Y., Woodard, S., Lin, L.-Z., Cai, C.-L., Lu, M. M., Reth, M., Platoshyn, O., Yuan, J. X. J., Evans, S., and Chien, K. R. (2005) Postnatal isl1+ cardioblasts enter fully differentiated cardiomyocyte lineages. *Nature* **433**, 647-653
109. Davis, D. R., Zhang, Y., Smith, R. R., Cheng, K., Terrovitis, J., Malliaras, K., Li, T. S., White, A., Makkar, R., and Marban, E. (2009) Validation of the cardiosphere method to culture cardiac progenitor cells from myocardial tissue. *PLoS One* **4**, e7195
110. Tallini, Y. N., Greene, K. S., Craven, M., Spealman, A., Breitbach, M., Smith, J., Fisher, P. J., Steffey, M., Hesse, M., Doran, R. M., Woods, A., Singh, B., Yen, A., Fleischmann, B. K., and Kotlikoff, M. I. (2009) c-kit expression identifies cardiovascular precursors in the neonatal heart. *Proc Natl Acad Sci U S A* **106**, 1808-1813
111. Brenner, W., Aicher, A., Eckey, T., Massoudi, S., Zuhayra, M., Koehl, U., Heeschen, C., Kampen, W. U., Zeiher, A. M., Dimmeler, S., and Henze, E. (2004) 111In-labeled CD34+ hematopoietic progenitor cells in a rat myocardial infarction model. *J Nucl Med* **45**, 512-518
112. Westbrook, C., Roth, C. K., and Talbot, J. M. (2005) *MRI in practice*, Blackwell Publishing, Oxford
113. Ly, H. Q., Frangioni, J. V., and Hajjar, R. J. (2008) Imaging in cardiac cell-based therapy: in vivo tracking of the biological fate of therapeutic cells. *Nat Clin Pract Cardiovasc Med* **5 Suppl 2**, S96-102
114. Stuckey, D. J., Carr, C. A., Martin-Rendon, E., Tyler, D. J., Willmott, C., Cassidy, P. J., Hale, S. J., Schneider, J. E., Tatton, L., Harding, S. E., Radda, G. K., Watt, S., and Clarke, K. (2006) Iron particles for noninvasive monitoring of bone marrow stromal cell engraftment into, and isolation of viable engrafted donor cells from, the heart. *Stem Cells* **24**, 1968-1975

115. Amado, L. C., Saliaris, A. P., Schuleri, K. H., St John, M., Xie, J. S., Cattaneo, S., Durand, D. J., Fitton, T., Kuang, J. Q., Stewart, G., Lehrke, S., Baumgartner, W. W., Martin, B. J., Heldman, A. W., and Hare, J. M. (2005) Cardiac repair with intramyocardial injection of allogeneic mesenchymal stem cells after myocardial infarction. *Proc Natl Acad Sci U S A* **102**, 11474-11479
116. Kraitchman, D. L., Heldman, A. W., Atalar, E., Amado, L. C., Martin, B. J., Pittenger, M. F., Hare, J. M., and Bulte, J. W. (2003) In vivo magnetic resonance imaging of mesenchymal stem cells in myocardial infarction. *Circulation* **107**, 2290-2293
117. Himes, N., Min, J. Y., Lee, R., Brown, C., Shea, J., Huang, X., Xiao, Y. F., Morgan, J. P., Burstein, D., and Oettgen, P. (2004) In vivo MRI of embryonic stem cells in a mouse model of myocardial infarction. *Magn Reson Med* **52**, 1214-1219
118. Cheng, K., Li, T. S., Malliaras, K., Davis, D. R., Zhang, Y., and Marban, E. (2010) Magnetic targeting enhances engraftment and functional benefit of iron-labeled cardiosphere-derived cells in myocardial infarction. *Circ Res* **106**, 1570-1581
119. Tran, L. A., Krishnamurthy, R., Muthupillai, R., Cabreira-Hansen Mda, G., Willerson, J. T., Perin, E. C., and Wilson, L. J. (2010) Gadonanotubes as magnetic nanolabels for stem cell detection. *Biomaterials* **31**, 9482-9491
120. Shen, J., Cheng, L. N., Zhong, X. M., Duan, X. H., Guo, R. M., and Hong, G. B. (2010) Efficient in vitro labeling rabbit neural stem cell with paramagnetic Gd-DTPA and fluorescent substance. *Eur J Radiol* **75**, 397-405
121. Tseng, C. L., Shih, I. L., Stobinski, L., and Lin, F. H. (2010) Gadolinium hexanedione nanoparticles for stem cell labeling and tracking via magnetic resonance imaging. *Biomaterials* **31**, 5427-5435
122. Adler, E. D., Bystrup, A., Briley-Saebo, K. C., Mani, V., Young, W., Giovanonne, S., Altman, P., Kattman, S. J., Frank, J. A., Weinmann, H. J., Keller, G. M., and Fayad, Z. A. (2009) In vivo detection of embryonic stem cell-derived cardiovascular progenitor cells using Cy3-labeled Gadofluorine M in murine myocardium. *JACC Cardiovasc Imaging* **2**, 1114-1122
123. Mosmann, T. (1983) Rapid colorimetric assay for cellular growth and survival: application to proliferation and cytotoxicity assays. *J Immunol Methods* **65**, 55-63
124. Michael, L. H., Entman, M. L., Hartley, C. J., Youker, K. A., Zhu, J., Hall, S. R., Hawkins, H. K., Berens, K., and Ballantyne, C. M. (1995) Myocardial ischemia and reperfusion: a murine model. *Am J Physiol* **269**, H2147-2154
125. Tyler, D. J., Lygate, C. A., Schneider, J. E., Cassidy, P. J., Neubauer, S., and Clarke, K. (2006) CINE-MR imaging of the normal and infarcted rat heart using an 11.7 T vertical bore MR system. *J Cardiovasc Magn Reson* **8**, 327-333
126. Rasband, W. S. (1997-2009) ImageJ, U. S. National Institutes of Health, Bethesda, Maryland, USA,. http://rsb.info.nih.gov/ij/
127. Nahrendorf, M., Wiesmann, F., Hiller, K. H., Hu, K., Waller, C., Ruff, J., Lanz, T. E., Neubauer, S., Haase, A., Ertl, G., and Bauer, W. R. (2001) Serial cine-magnetic resonance imaging of left ventricular remodeling after myocardial infarction in rats. *J Magn Reson Imaging* **14**, 547-555
128. Tang, Y. L., Zhu, W., Cheng, M., Chen, L., Zhang, J., Sun, T., Kishore, R., Phillips, M. I., Losordo, D. W., and Qin, G. (2009) Hypoxic preconditioning enhances the benefit of cardiac progenitor cell therapy for treatment of myocardial infarction by inducing CXCR4 expression. *Circ Res* **104**, 1209-1216
129. Itzhaki-Alfia, A., Leor, J., Raanani, E., Sternik, L., Spiegelstein, D., Netser, S., Holbova, R., Pevsner-Fischer, M., Lavee, J., and Barbash, I. M. (2009) Patient characteristics and cell source determine the number of isolated human cardiac progenitor cells. *Circulation* **120**, 2559-2566
130. Tateishi, K., Ashihara, E., Honsho, S., Takehara, N., Nomura, T., Takahashi, T., Ueyama, T., Yamagishi, M., Yaku, H., Matsubara, H., and Oh, H. (2007) Human

cardiac stem cells exhibit mesenchymal features and are maintained through Akt/GSK-3beta signaling. *Biochem Biophys Res Commun* **352**, 635-641

131. Lipinski, M. J., Biondi-Zoccai, G. G., Abbate, A., Khianey, R., Sheiban, I., Bartunek, J., Vanderheyden, M., Kim, H. S., Kang, H. J., Strauer, B. E., and Vetrovec, G. W. (2007) Impact of intracoronary cell therapy on left ventricular function in the setting of acute myocardial infarction: a collaborative systematic review and meta-analysis of controlled clinical trials. *Journal of the American College of Cardiology* **50**, 1761-1767
132. Schachinger, V., Erbs, S., Elsasser, A., Haberbosch, W., Hambrecht, R., Holschermann, H., Yu, J., Corti, R., Mathey, D. G., Hamm, C. W., Suselbeck, T., Assmus, B., Tonn, T., Dimmeler, S., and Zeiher, A. M. (2006) Intracoronary bone marrow-derived progenitor cells in acute myocardial infarction. *N Engl J Med* **355**, 1210-1221
133. Li, Y. M., Schilling, T., Benisch, P., Zeck, S., Meissner-Weigl, J., Schneider, D., Limbert, C., Seufert, J., Kassem, M., Schutze, N., Jakob, F., and Ebert, R. (2007) Effects of high glucose on mesenchymal stem cell proliferation and differentiation. *Biochem Biophys Res Commun* **363**, 209-215
134. Kim, Y. H., Heo, J. S., and Han, H. J. (2006) High glucose increase cell cycle regulatory proteins level of mouse embryonic stem cells via PI3-K/Akt and MAPKs signal pathways. *J Cell Physiol* **209**, 94-102
135. Kim, M. H., Kim, M. O., Kim, Y. H., Kim, J. S., and Han, H. J. (2009) Linoleic acid induces mouse embryonic stem cell proliferation via Ca2+/PKC, PI3K/Akt, and MAPKs. *Cell Physiol Biochem* **23**, 53-64
136. Aguiari, P., Leo, S., Zavan, B., Vindigni, V., Rimessi, A., Bianchi, K., Franzin, C., Cortivo, R., Rossato, M., Vettor, R., Abatangelo, G., Pozzan, T., Pinton, P., and Rizzuto, R. (2008) High glucose induces adipogenic differentiation of muscle-derived stem cells. *Proc Natl Acad Sci U S A* **105**, 1226-1231
137. Urbich, C., Dernbach, E., Rossig, L., Zeiher, A. M., and Dimmeler, S. (2008) High glucose reduces cathepsin L activity and impairs invasion of circulating progenitor cells. *J Mol Cell Cardiol* **45**, 429-436
138. Parker, G. C., Acsadi, G., and Brenner, C. A. (2009) Mitochondria: determinants of stem cell fate? *Stem Cells Dev* **18**, 803-806
139. St John, J. C., Amaral, A., Bowles, E., Oliveira, J. F., Lloyd, R., Freitas, M., Gray, H. L., Navara, C. S., Oliveira, G., Schatten, G. P., Spikings, E., and Ramalho-Santos, J. (2006) The analysis of mitochondria and mitochondrial DNA in human embryonic stem cells. *Methods Mol Biol* **331**, 347-374
140. Armstrong, L., Tilgner, K., Saretzki, G., Atkinson, S. P., Stojkovic, M., Moreno, R., Przyborski, S., and Lako, M. (2010) Human induced pluripotent stem cell lines show stress defense mechanisms and mitochondrial regulation similar to those of human embryonic stem cells. *Stem Cells* **28**, 661-673
141. Neubauer, S. (2007) The failing heart--an engine out of fuel. *N Engl J Med* **356**, 1140-1151
142. Winter, E. M., Hogers, B., van der Graaf, L. M., Gittenberger-de Groot, A. C., Poelmann, R. E., and van der Weerd, L. (2010) Cell tracking using iron oxide fails to distinguish dead from living transplanted cells in the infarcted heart. *Magnetic Resonance in Medicine* **63**, 817-821
143. Terrovitis, J., Stuber, M., Youssef, A., Preece, S., Leppo, M., Kizana, E., Schar, M., Gerstenblith, G., Weiss, R. G., Marban, E., and Abraham, M. R. (2008) Magnetic Resonance Imaging Overestimates Ferumoxide-Labeled Stem Cell Survival After Transplantation in the Heart. *Circulation* **117**, 1555-1562

144. Izadpanah, R., Kaushal, D., Kriedt, C., Tsien, F., Patel, B., Dufour, J., and Bunnell, B. A. (2008) Long-term in vitro expansion alters the biology of adult mesenchymal stem cells. *Cancer Res* **68**, 4229-4238
145. Riekstina, U., Muceniece, R., Cakstina, I., Muiznieks, I., and Ancans, J. (2008) Characterization of human skin-derived mesenchymal stem cell proliferation rate in different growth conditions. *Cytotechnology* **58**, 153-162
146. Mannello, F., and Tonti, G. A. (2007) Concise review: no breakthroughs for human mesenchymal and embryonic stem cell culture: conditioned medium, feeder layer, or feeder-free; medium with fetal calf serum, human serum, or enriched plasma; serum-free, serum replacement nonconditioned medium, or ad hoc formula? All that glitters is not gold! *Stem Cells* **25**, 1603-1609
147. D'Amour, K. A., Agulnick, A. D., Eliazer, S., Kelly, O. G., Kroon, E., and Baetge, E. E. (2005) Efficient differentiation of human embryonic stem cells to definitive endoderm. *Nat Biotechnol* **23**, 1534-1541
148. Tomita, Y., Matsumura, K., Wakamatsu, Y., Matsuzaki, Y., Shibuya, I., Kawaguchi, H., Ieda, M., Kanakubo, S., Shimazaki, T., Ogawa, S., Osumi, N., Okano, H., and Fukuda, K. (2005) Cardiac neural crest cells contribute to the dormant multipotent stem cell in the mammalian heart. *J Cell Biol* **170**, 1135-1146
149. Zakharova, L., Mastroeni, D., Mutlu, N., Molina, M., Goldman, S., Diethrich, E., and Gaballa, M. A. (2010) Transplantation of cardiac progenitor cell sheet onto infarcted heart promotes cardiogenesis and improves function. *Cardiovasc Res* **87**, 40-49
150. Andersen, D. C., Andersen, P., Schneider, M., Jensen, H. B., and Sheikh, S. P. (2009) Murine "cardiospheres" are not a source of stem cells with cardiomyogenic potential. *Stem Cells* **27**, 1571-1581
151. Seeger, F. H., Tonn, T., Krzossok, N., Zeiher, A. M., and Dimmeler, S. (2007) Cell isolation procedures matter: a comparison of different isolation protocols of bone marrow mononuclear cells used for cell therapy in patients with acute myocardial infarction. *Eur Heart J* **28**, 766-772
152. Orlic, D., Fischer, R., Nishikawa, S., Nienhuis, A. W., and Bodine, D. M. (1993) Purification and characterization of heterogeneous pluripotent hematopoietic stem cell populations expressing high levels of c-kit receptor. *Blood* **82**, 762-770
153. Li, T. S., Cheng, K., Lee, S. T., Matsushita, S., Davis, D., Malliaras, K., Zhang, Y., Matsushita, N., Smith, R. R., and Marban, E. (2010) Cardiospheres recapitulate a niche-like microenvironment rich in stemness and cell-matrix interactions, rationalizing their enhanced functional potency for myocardial repair. *Stem Cells* **28**, 2088-2098
154. Cheng, K., Li, T.-S., Malliaras, K., Sun, B., Matsushita, N., Marban, L., Smith, R., Blusztajn, A., Terrovitis, J., and Marban, E. (2010) Abstract 20957: Paracrine and Functional Superiority of Human Cardiosphere-Derived Cells as Compared to Mesenchymal Stem Cells, Adipose-Derived Stem Cells or Bone Marrow Mononuclear Cells. *Circulation* **122**, A20957-
155. Finck, B. N., and Kelly, D. P. (2007) Peroxisome proliferator-activated receptor gamma coactivator-1 (PGC-1) regulatory cascade in cardiac physiology and disease. *Circulation* **115**, 2540-2548
156. Zhu, L., Sun, G., Zhang, H., Zhang, Y., Chen, X., Jiang, X., Krauss, S., Zhang, J., Xiang, Y., and Zhang, C. Y. (2009) PGC-1alpha is a key regulator of glucose-induced proliferation and migration in vascular smooth muscle cells. *PLoS One* **4**, e4182
157. Vander Heiden, M. G., Cantley, L. C., and Thompson, C. B. (2009) Understanding the Warburg effect: the metabolic requirements of cell proliferation. *Science* **324**, 1029-1033
158. Garber, K. (2004) Energy boost: the Warburg effect returns in a new theory of cancer. *J Natl Cancer Inst* **96**, 1805-1806

159. Warburg, O. (1956) On the origin of cancer cells. *Science* **123**, 309-314
160. Brand, K. A., and Hermfisse, U. (1997) Aerobic glycolysis by proliferating cells: a protective strategy against reactive oxygen species. *FASEB J* **11**, 388-395
161. Kondoh, H., Lleonart, M. E., Nakashima, Y., Yokode, M., Tanaka, M., Bernard, D., Gil, J., and Beach, D. (2007) A high glycolytic flux supports the proliferative potential of murine embryonic stem cells. *Antioxid Redox Signal* **9**, 293-299
162. DeBerardinis, R. J., Lum, J. J., Hatzivassiliou, G., and Thompson, C. B. (2008) The biology of cancer: metabolic reprogramming fuels cell growth and proliferation. *Cell Metab* **7**, 11-20
163. Ferreira, L. M. (2010) Cancer metabolism: the Warburg effect today. *Exp Mol Pathol* **89**, 372-380
164. Terrovitis, J., Stuber, M., Youssef, A., Preece, S., Leppo, M., Kizana, E., Schar, M., Gerstenblith, G., Weiss, R. G., Marban, E., and Abraham, M. R. (2008) Magnetic resonance imaging overestimates ferumoxide-labeled stem cell survival after transplantation in the heart. *Circulation* **117**, 1555-1562
165. Amsalem, Y., Mardor, Y., Feinberg, M. S., Landa, N., Miller, L., Daniels, D., Ocherashvilli, A., Holbova, R., Yosef, O., Barbash, I. M., and Leor, J. (2007) Iron-oxide labeling and outcome of transplanted mesenchymal stem cells in the infarcted myocardium. *Circulation* **116**, I38-45
166. Rigol, M., Solanes, N., Roque, M., Farre, J., Batlle, M., Roura, S., Bellera, N., Prat-Vidal, C., Sionis, A., Ramirez, J., Sitges, M., Sanz, G., Bayes-Genis, A., and Heras, M. (2008) Hemosiderin deposits confounds tracking of iron-oxide-labeled stem cells: an experimental study. *Transplant Proc* **40**, 3619-3622
167. Chimenti, I., Smith, R. R., Li, T. S., Gerstenblith, G., Messina, E., Giacomello, A., and Marban, E. (2010) Relative roles of direct regeneration versus paracrine effects of human cardiosphere-derived cells transplanted into infarcted mice. *Circ Res* **106**, 971-980
168. Johnston, P. V., Sasano, T., Mills, K., Evers, R., Lee, S. T., Smith, R. R., Lardo, A. C., Lai, S., Steenbergen, C., Gerstenblith, G., Lange, R., and Marban, E. (2009) Engraftment, differentiation, and functional benefits of autologous cardiosphere-derived cells in porcine ischemic cardiomyopathy. *Circulation* **120**, 1075-1083, 1077 p following 1083
169. Chimenti, I., Smith, R. R., Li, T. S., Gerstenblith, G., Messina, E., Giacomello, A., and Marban, E. Relative roles of direct regeneration versus paracrine effects of human cardiosphere-derived cells transplanted into infarcted mice. *Circ Res* **106**, 971-980
170. Mouquet, F., Pfister, O., Jain, M., Oikonomopoulos, A., Ngoy, S., Summer, R., Fine, A., and Liao, R. (2005) Restoration of cardiac progenitor cells after myocardial infarction by self-proliferation and selective homing of bone marrow-derived stem cells. *Circ Res* **97**, 1090-1092
171. Taylor, D. A., and Zenovich, A. G. (2008) Cardiovascular cell therapy and endogenous repair. *Diabetes Obes Metab* **10 Suppl 4**, 5-15
172. Andersen, D. C., Andersen, P., Schneider, M., Jensen, H. B., and Sheikh, S. P. (2009) Murine "Cardiospheres" Are Not a Source of Stem Cells with Cardiomyogenic Potential. *Stem Cells* **27**, 1571-1581
173. Vidarsson, H., Hyllner, J., and Sartipy, P. (2010) Differentiation of human embryonic stem cells to cardiomyocytes for in vitro and in vivo applications. *Stem Cell Rev* **6**, 108-120
174. Hofmeister, C. C., Zhang, J., Knight, K. L., Le, P., and Stiff, P. J. (2007) Ex vivo expansion of umbilical cord blood stem cells for transplantation: growing knowledge from the hematopoietic niche. *Bone Marrow Transplant* **39**, 11-23
175. Scadden, D. T. (2006) The stem-cell niche as an entity of action. *Nature* **441**, 1075-1079

176. Fuchs, E., Tumbar, T., and Guasch, G. (2004) Socializing with the neighbors: stem cells and their niche. *Cell* **116**, 769-778
177. Watt, F. M., and Hogan, B. L. (2000) Out of Eden: stem cells and their niches. *Science* **287**, 1427-1430
178. Chen, S. S., Fitzgerald, W., Zimmerberg, J., Kleinman, H. K., and Margolis, L. (2007) Cell-cell and cell-extracellular matrix interactions regulate embryonic stem cell differentiation. *Stem Cells* **25**, 553-561
179. Tate, M. C., Shear, D. A., Hoffman, S. W., Stein, D. G., Archer, D. R., and LaPlaca, M. C. (2002) Fibronectin promotes survival and migration of primary neural stem cells transplanted into the traumatically injured mouse brain. *Cell Transplant* **11**, 283-295
180. Stern, M. M., Myers, R. L., Hammam, N., Stern, K. A., Eberli, D., Kritchevsky, S. B., Soker, S., and Van Dyke, M. (2009) The influence of extracellular matrix derived from skeletal muscle tissue on the proliferation and differentiation of myogenic progenitor cells ex vivo. *Biomaterials* **30**, 2393-2399
181. Mauney, J. R., Volloch, V., and Kaplan, D. L. (2005) Matrix-mediated retention of adipogenic differentiation potential by human adult bone marrow-derived mesenchymal stem cells during ex vivo expansion. *Biomaterials* **26**, 6167-6175
182. Li, Z., Lee, A., Huang, M., Chun, H., Chung, J., Chu, P., Hoyt, G., Yang, P., Rosenberg, J., Robbins, R. C., and Wu, J. C. (2009) Imaging survival and function of transplanted cardiac resident stem cells. *J Am Coll Cardiol* **53**, 1229-1240
183. Bowers, S. L. K., Banerjee, I., and Baudino, T. A. (2010) The extracellular matrix: At the center of it all. *Journal of Molecular and Cellular Cardiology* **48**, 474-482
184. Urbanek, K., Cesselli, D., Rota, M., Nascimbene, A., De Angelis, A., Hosoda, T., Bearzi, C., Boni, A., Bolli, R., Kajstura, J., Anversa, P., and Leri, A. (2006) Stem cell niches in the adult mouse heart. *Proc Natl Acad Sci U S A* **103**, 9226-9231
185. Castaldo, C., Di Meglio, F., Nurzynska, D., Romano, G., Maiello, C., Bancone, C., Muller, P., Bohm, M., Cotrufo, M., and Montagnani, S. (2008) CD117-positive cells in adult human heart are localized in the subepicardium, and their activation is associated with laminin-1 and alpha6 integrin expression. *STEM CELLS* **26**, 1723-1731
186. Davis, D. R., Kizana, E., Terrovitis, J., Barth, A. S., Zhang, Y., Smith, R. R., Miake, J., and Marban, E. (2010) Isolation and expansion of functionally-competent cardiac progenitor cells directly from heart biopsies. *J Mol Cell Cardiol* **49**, 312-321
187. Davis, D. R., Ruckdeschel Smith, R., and Marban, E. (2010) Human cardiospheres are a source of stem cells with cardiomyogenic potential. *Stem Cells* **28**, 903-904
188. Nakanishi, C., Yamagishi, M., Yamahara, K., Hagino, I., Mori, H., Sawa, Y., Yagihara, T., Kitamura, S., and Nagaya, N. (2008) Activation of cardiac progenitor cells through paracrine effects of mesenchymal stem cells. *Biochem Biophys Res Commun* **374**, 11-16
189. Shenje, L. T., Field, L. J., Pritchard, C. A., Guerin, C. J., Rubart, M., Soonpaa, M. H., Ang, K. L., and Galinanes, M. (2008) Lineage tracing of cardiac explant derived cells. *PLoS One* **3**, e1929
190. Koninckx, R., Daniels, A., Windmolders, S., Carlotti, F., Mees, U., Steels, P., Rummens, J. L., Hendrikx, M., and Hensen, K. (2010) Mesenchymal stem cells or cardiac progenitors for cardiac repair? A comparative study. *Cell Mol Life Sci*
191. Bartosh, T. J., Wang, Z., Rosales, A. A., Dimitrijevich, S. D., and Roque, R. S. (2008) 3D-model of adult cardiac stem cells promotes cardiac differentiation and resistance to oxidative stress. *J Cell Biochem* **105**, 612-623
192. Pugh, C. W., and Ratcliffe, P. J. (2003) Regulation of angiogenesis by hypoxia: role of the HIF system. *Nat Med* **9**, 677-684

193. Forsythe, J. A., Jiang, B. H., Iyer, N. V., Agani, F., Leung, S. W., Koos, R. D., and Semenza, G. L. (1996) Activation of vascular endothelial growth factor gene transcription by hypoxia-inducible factor 1. *Mol Cell Biol* **16**, 4604-4613
194. Daley, W. P., Peters, S. B., and Larsen, M. (2008) Extracellular matrix dynamics in development and regenerative medicine. *J Cell Sci* **121**, 255-264
195. Hakuno, D., Takahashi, T., Lammerding, J., and Lee, R. T. (2005) Focal adhesion kinase signaling regulates cardiogenesis of embryonic stem cells. *J Biol Chem* **280**, 39534-39544
196. Xiao, Q., Zeng, L., Zhang, Z., Hu, Y., and Xu, Q. (2007) Stem cell-derived Sca-1+ progenitors differentiate into smooth muscle cells, which is mediated by collagen IV-integrin Î±1/Î²1/Î±v and PDGF receptor pathways. *American Journal of Physiology - Cell Physiology* **292**, C342-C352
197. Wollert, K. C., Meyer, G. P., Lotz, J., Ringes-Lichtenberg, S., Lippolt, P., Breidenbach, C., Fichtner, S., Korte, T., Hornig, B., Messinger, D., Arseniev, L., Hertenstein, B., Ganser, A., and Drexler, H. (2004) Intracoronary autologous bone-marrow cell transfer after myocardial infarction: the BOOST randomised controlled clinical trial. *Lancet* **364**, 141-148
198. Strauer, B. E., Yousef, M., and Schannwell, C. M. The acute and long-term effects of intracoronary Stem cell Transplantation in 191 patients with chronic heARt failure: the STAR-heart study. *Eur J Heart Fail* **12**, 721-729
199. Erbs, S., Linke, A., Schachinger, V., Assmus, B., Thiele, H., Diederich, K. W., Hoffmann, C., Dimmeler, S., Tonn, T., Hambrecht, R., Zeiher, A. M., and Schuler, G. (2007) Restoration of microvascular function in the infarct-related artery by intracoronary transplantation of bone marrow progenitor cells in patients with acute myocardial infarction: the Doppler Substudy of the Reinfusion of Enriched Progenitor Cells and Infarct Remodeling in Acute Myocardial Infarction (REPAIR-AMI) trial. *Circulation* **116**, 366-374
200. Meyer, G. P., Wollert, K. C., Lotz, J., Pirr, J., Rager, U., Lippolt, P., Hahn, A., Fichtner, S., Schaefer, A., Arseniev, L., Ganser, A., and Drexler, H. (2009) Intracoronary bone marrow cell transfer after myocardial infarction: 5-year follow-up from the randomized-controlled BOOST trial. *Eur Heart J* **30**, 2978-2984
201. Graham, J. J., Foltz, W. D., Vaags, A. K., Ward, M. R., Yang, Y., Connelly, K. A., Vijayaraghavan, R., Detsky, J. S., Hough, M. R., Stewart, D. J., Wright, G. A., and Dick, A. J. (2010) Long-term tracking of bone marrow progenitor cells following intracoronary injection post-myocardial infarction in swine using MRI. *Am J Physiol Heart Circ Physiol* **299**, H125-133
202. Frangioni, J. V., and Hajjar, R. J. (2004) In vivo tracking of stem cells for clinical trials in cardiovascular disease. *Circulation* **110**, 3378-3383
203. Shapiro, E. M., Sharer, K., Skrtic, S., and Koretsky, A. P. (2006) In vivo detection of single cells by MRI. *Magn Reson Med* **55**, 242-249
204. Zhang, Z., van den Bos, E. J., Wielopolski, P. A., de Jong-Popijus, M., Bernsen, M. R., Duncker, D. J., and Krestin, G. P. (2005) In vitro imaging of single living human umbilical vein endothelial cells with a clinical 3.0-T MRI scanner. *MAGMA* **18**, 175-185
205. Lau, J. F., Anderson, S. A., Adler, E., and Frank, J. A. (2010) Imaging approaches for the study of cell-based cardiac therapies. *Nat Rev Cardiol* **7**, 97-105
206. Goyen, M., and Debatin, J. F. (2004) Gadopentetate dimeglumine-enhanced three-dimensional MR-angiography: dosing, safety, and efficacy. *J Magn Reson Imaging* **19**, 261-273
207. Oshinski, J. N., Yang, Z., Jones, J. R., Mata, J. F., and French, B. A. (2001) Imaging time after Gd-DTPA injection is critical in using delayed enhancement to determine infarct size accurately with magnetic resonance imaging. *Circulation* **104**, 2838-2842

208. Shen, J., Cheng, L. N., Zhong, X. M., Duan, X. H., Guo, R. M., and Hong, G. B. (2009) Efficient in vitro labeling rabbit neural stem cell with paramagnetic Gd-DTPA and fluorescent substance. *Eur J Radiol* **75**, 397-405
209. Rudelius, M., Daldrup-Link, H. E., Heinzmann, U., Piontek, G., Settles, M., Link, T. M., and Schlegel, J. (2003) Highly efficient paramagnetic labelling of embryonic and neuronal stem cells. *Eur J Nucl Med Mol Imaging* **30**, 1038-1044
210. Sitharaman, B., Kissell, K. R., Hartman, K. B., Tran, L. A., Baikalov, A., Rusakova, I., Sun, Y., Khant, H. A., Ludtke, S. J., Chiu, W., Laus, S., Toth, E., Helm, L., Merbach, A. E., and Wilson, L. J. (2005) Superparamagnetic gadonanotubes are high-performance MRI contrast agents. *Chem Commun (Camb)*, 3915-3917
211. Yau, T. M., Kim, C., Ng, D., Li, G., Zhang, Y., Weisel, R. D., and Li, R. K. (2005) Increasing transplanted cell survival with cell-based angiogenic gene therapy. *Ann Thorac Surg* **80**, 1779-1786
212. Teng, C. J., Luo, J., Chiu, R. C., and Shum-Tim, D. (2006) Massive mechanical loss of microspheres with direct intramyocardial injection in the beating heart: implications for cellular cardiomyoplasty. *J Thorac Cardiovasc Surg* **132**, 628-632
213. Sitharaman, B., Van Der Zande, M., Ananta, J. S., Shi, X., Veltien, A., Walboomers, X. F., Wilson, L. J., Mikos, A. G., Heerschap, A., and Jansen, J. A. (2010) Magnetic resonance imaging studies on gadonanotube-reinforced biodegradable polymer nanocomposites. *J Biomed Mater Res A* **93**, 1454-1462
214. Hassan, A. A., Chan, B. T., Tran, L. A., Hartman, K. B., Ananta, J. S., Mackeyev, Y., Hu, L., Pautler, R. G., Wilson, L. J., and Lee, A. V. (2010) Serine-derivatized gadonanotubes as magnetic nanoprobes for intracellular labeling. *Contrast Media Mol Imaging* **5**, 34-38
215. Rudelius, M., Daldrup-Link, H. E., Heinzmann, U., Piontek, G., Settles, M., Link, T. M., and Schlegel, J. (2003) Highly efficient paramagnetic labelling of embryonic and neuronal stem cells. *European Journal of Nuclear Medicine and Molecular Imaging* **30**, 1038-1044
216. Gambini, E., Pompilio, G., Biondi, A., Alamanni, F., Capogrossi, M. C., Agrifoglio, M., and Pesce, M. (2011) C-kit+ cardiac progenitors exhibit mesenchymal markers and preferential cardiovascular commitment. *Cardiovasc Res* **89**, 362-373
217. Mishra, R., Vijayan, K., Colletti, E. J., Harrington, D. A., Matthiesen, T. S., Simpson, D., Goh, S. K., Walker, B. L., Almeida-Porada, G., Wang, D., Backer, C. L., Dudley, S. C., Jr., Wold, L. E., and Kaushal, S. (2011) Characterization and Functionality of Cardiac Progenitor Cells in Congenital Heart Patients. *Circulation*
218. Linnekin, D. (1999) Early signaling pathways activated by c-Kit in hematopoietic cells. *Int J Biochem Cell Biol* **31**, 1053-1074
219. Meininger, C., Yano, H., Rottapel, R., Bernstein, A., Zsebo, K., and Zetter, B. (1992) The c-kit receptor ligand functions as a mast cell chemoattractant. *Blood* **79**, 958-963
220. Yoshida, H., Kunisada, T., Grimm, T., Nishimura, E. K., Nishioka, E., and Nishikawa, S. I. (2001) Review: melanocyte migration and survival controlled by SCF/c-kit expression. *J Investig Dermatol Symp Proc* **6**, 1-5
221. Leong, K. G., Wang, B. E., Johnson, L., and Gao, W. Q. (2008) Generation of a prostate from a single adult stem cell. *Nature* **456**, 804-808
222. Adhikari, A. S., Agarwal, N., Wood, B. M., Porretta, C., Ruiz, B., Pochampally, R. R., and Iwakuma, T. (2010) CD117 and Stro-1 identify osteosarcoma tumor-initiating cells associated with metastasis and drug resistance. *Cancer Res* **70**, 4602-4612
223. Di Meglio, F., Castaldo, C., Nurzynska, D., Romano, V., Miraglia, R., Bancone, C., Langella, G., Vosa, C., and Montagnani, S. (2010) Epithelial-mesenchymal transition of epicardial mesothelium is a source of cardiac CD117-positive stem cells in adult human heart. *J Mol Cell Cardiol* **49**, 719-727

224. Kalluri, R., and Weinberg, R. A. (2009) The basics of epithelial-mesenchymal transition. *J Clin Invest* **119**, 1420-1428
225. Zhou, B., Ma, Q., Rajagopal, S., Wu, S. M., Domian, I., Rivera-Feliciano, J., Jiang, D., von Gise, A., Ikeda, S., Chien, K. R., and Pu, W. T. (2008) Epicardial progenitors contribute to the cardiomyocyte lineage in the developing heart. *Nature* **454**, 109-113
226. Jahn, T., Seipel, P., Coutinho, S., Urschel, S., Schwarz, K., Miething, C., Serve, H., Peschel, C., and Duyster, J. (2002) Analysing c-kit internalization using a functional c-kit-EGFP chimera containing the fluorochrome within the extracellular domain. *Oncogene* **21**, 4508-4520
227. Hausenloy, D. J., and Yellon, D. M. (2009) Cardioprotective growth factors. *Cardiovasc Res* **83**, 179-194
228. Jin, H., Wyss, J. M., Yang, R., and Schwall, R. (2004) The therapeutic potential of hepatocyte growth factor for myocardial infarction and heart failure. *Curr Pharm Des* **10**, 2525-2533
229. Feldser, D., Agani, F., Iyer, N. V., Pak, B., Ferreira, G., and Semenza, G. L. (1999) Reciprocal positive regulation of hypoxia-inducible factor 1alpha and insulin-like growth factor 2. *Cancer Res* **59**, 3915-3918
230. Fukuda, R., Hirota, K., Fan, F., Jung, Y. D., Ellis, L. M., and Semenza, G. L. (2002) Insulin-like growth factor 1 induces hypoxia-inducible factor 1-mediated vascular endothelial growth factor expression, which is dependent on MAP kinase and phosphatidylinositol 3-kinase signaling in colon cancer cells. *J Biol Chem* **277**, 38205-38211
231. Ivanovic, Z. (2009) Hypoxia or in situ normoxia: The stem cell paradigm. *J Cell Physiol* **219**, 271-275
232. Torella, D., Rota, M., Nurzynska, D., Musso, E., Monsen, A., Shiraishi, I., Zias, E., Walsh, K., Rosenzweig, A., Sussman, M. A., Urbanek, K., Nadal-Ginard, B., Kajstura, J., Anversa, P., and Leri, A. (2004) Cardiac stem cell and myocyte aging, heart failure, and insulin-like growth factor-1 overexpression. *Circ Res* **94**, 514-524
233. Li, T.-S., Cheng, K., Lee, S.-T., Matsushita, S., Davis, D., Malliaras, K., Zhang, Y., Matsushita, N., Smith, R. R., and Marbán, E. (2010) Cardiospheres Recapitulate a Niche-Like Microenvironment Rich in Stemness and Cell-Matrix Interactions, Rationalizing Their Enhanced Functional Potency for Myocardial Repair. *Stem Cells* **28**, 2088-2098
234. Yu, X. Y., Geng, Y. J., Li, X. H., Lin, Q. X., Shan, Z. X., Lin, S. G., Song, Y. H., and Li, Y. (2009) The effects of mesenchymal stem cells on c-kit up-regulation and cell-cycle re-entry of neonatal cardiomyocytes are mediated by activation of insulin-like growth factor 1 receptor. *Mol Cell Biochem* **332**, 25-32
235. Lee, S. T., White, A. J., Matsushita, S., Malliaras, K., Steenbergen, C., Zhang, Y., Li, T. S., Terrovitis, J., Yee, K., Simsir, S., Makkar, R., and Marban, E. (2011) Intramyocardial injection of autologous cardiospheres or cardiosphere-derived cells preserves function and minimizes adverse ventricular remodeling in pigs with heart failure post-myocardial infarction. *J Am Coll Cardiol* **57**, 455-465
236. Winter, E. M., Hogers, B., van der Graaf, L. M., Gittenberger-de Groot, A. C., Poelmann, R. E., and van der Weerd, L. (2010) Cell tracking using iron oxide fails to distinguish dead from living transplanted cells in the infarcted heart. *Magn Reson Med* **63**, 817-821
237. Janjic, J. M., and Ahrens, E. T. (2009) Fluorine-containing nanoemulsions for MRI cell tracking. *Wiley Interdiscip Rev Nanomed Nanobiotechnol* **1**, 492-501
238. Chen, J., Lanza, G. M., and Wickline, S. A. (2010) Quantitative magnetic resonance fluorine imaging: today and tomorrow. *Wiley Interdiscip Rev Nanomed Nanobiotechnol* **2**, 431-440

239. Partlow, K. C., Chen, J., Brant, J. A., Neubauer, A. M., Meyerrose, T. E., Creer, M. H., Nolta, J. A., Caruthers, S. D., Lanza, G. M., and Wickline, S. A. (2007) 19F magnetic resonance imaging for stem/progenitor cell tracking with multiple unique perfluorocarbon nanobeacons. *FASEB J* **21**, 1647-1654
240. Meyer, G. P., Wollert, K. C., Lotz, J., Steffens, J., Lippolt, P., Fichtner, S., Hecker, H., Schaefer, A., Arseniev, L., Hertenstein, B., Ganser, A., and Drexler, H. (2006) Intracoronary bone marrow cell transfer after myocardial infarction: eighteen months' follow-up data from the randomized, controlled BOOST (BOne marrOw transfer to enhance ST-elevation infarct regeneration) trial. *Circulation* **113**, 1287-1294
241. Lunde, K., Solheim, S., Aakhus, S., Arnesen, H., Abdelnoor, M., Egeland, T., Endresen, K., Ilebekk, A., Mangschau, A., Fjeld, J. G., Smith, H. J., Taraldsrud, E., Grogaard, H. K., Bjornerheim, R., Brekke, M., Muller, C., Hopp, E., Ragnarsson, A., Brinchmann, J. E., and Forfang, K. (2006) Intracoronary injection of mononuclear bone marrow cells in acute myocardial infarction. *N Engl J Med* **355**, 1199-1209
242. Janssens, S., Dubois, C., Bogaert, J., Theunissen, K., Deroose, C., Desmet, W., Kalantzi, M., Herbots, L., Sinnaeve, P., Dens, J., Maertens, J., Rademakers, F., Dymarkowski, S., Gheysens, O., Van Cleemput, J., Bormans, G., Nuyts, J., Belmans, A., Mortelmans, L., Boogaerts, M., and Van de Werf, F. (2006) Autologous bone marrow-derived stem-cell transfer in patients with ST-segment elevation myocardial infarction: double-blind, randomised controlled trial. *Lancet* **367**, 113-121
243. Ge, J., Li, Y., Qian, J., Shi, J., Wang, Q., Niu, Y., Fan, B., Liu, X., Zhang, S., Sun, A., and Zou, Y. (2006) Efficacy of emergent transcatheter transplantation of stem cells for treatment of acute myocardial infarction (TCT-STAMI). *Heart* **92**, 1764-1767
244. Hirsch, A., Nijveldt, R., van der Vleuten, P. A., Tio, R. A., van der Giessen, W. J., Marques, K. M., Doevendans, P. A., Waltenberger, J., Ten Berg, J. M., Aengevaeren, W. R., Biemond, B. J., Tijssen, J. G., van Rossum, A. C., Piek, J. J., and Zijlstra, F. (2008) Intracoronary infusion of autologous mononuclear bone marrow cells in patients with acute myocardial infarction treated with primary PCI: Pilot study of the multicenter HEBE trial. *Catheter Cardiovasc Interv* **71**, 273-281
245. Huikuri, H. V., Kervinen, K., Niemela, M., Ylitalo, K., Saily, M., Koistinen, P., Savolainen, E. R., Ukkonen, H., Pietila, M., Airaksinen, J. K., Knuuti, J., and Makikallio, T. H. (2008) Effects of intracoronary injection of mononuclear bone marrow cells on left ventricular function, arrhythmia risk profile, and restenosis after thrombolytic therapy of acute myocardial infarction. *Eur Heart J* **29**, 2723-2732
246. Beitnes, J. O., Hopp, E., Lunde, K., Solheim, S., Arnesen, H., Brinchmann, J. E., Forfang, K., and Aakhus, S. (2009) Long-term results after intracoronary injection of autologous mononuclear bone marrow cells in acute myocardial infarction: the ASTAMI randomised, controlled study. *Heart* **95**, 1983-1989
247. Tendera, M., Wojakowski, W., Ruzyllo, W., Chojnowska, L., Kepka, C., Tracz, W., Musialek, P., Piwowarska, W., Nessler, J., Buszman, P., Grajek, S., Breborowicz, P., Majka, M., and Ratajczak, M. Z. (2009) Intracoronary infusion of bone marrow-derived selected CD34+CXCR4+ cells and non-selected mononuclear cells in patients with acute STEMI and reduced left ventricular ejection fraction: results of randomized, multicentre Myocardial Regeneration by Intracoronary Infusion of Selected Population of Stem Cells in Acute Myocardial Infarction (REGENT) Trial. *Eur Heart J* **30**, 1313-1321
248. Hirsch, A., Nijveldt, R., van der Vleuten, P. A., Tijssen, J. G., van der Giessen, W. J., Tio, R. A., Waltenberger, J., Ten Berg, J. M., Doevendans, P. A., Aengevaeren, W. R., Zwaginga, J. J., Biemond, B. J., van Rossum, A. C., Piek, J. J., and Zijlstra, F. (2010) Intracoronary infusion of mononuclear cells from bone marrow or peripheral blood compared with standard therapy in patients after acute myocardial infarction treated by

primary percutaneous coronary intervention: results of the randomized controlled HEBE trial. *Eur Heart J*

249. Roncalli, J., Mouquet, F., Piot, C., Trochu, J. N., Le Corvoisier, P., Neuder, Y., Le Tourneau, T., Agostini, D., Gaxotte, V., Sportouch, C., Galinier, M., Crochet, D., Teiger, E., Richard, M. J., Polge, A. S., Beregi, J. P., Manrique, A., Carrie, D., Susen, S., Klein, B., Parini, A., Lamirault, G., Croisille, P., Rouard, H., Bourin, P., Nguyen, J. M., Delasalle, B., Vanzetto, G., Van Belle, E., and Lemarchand, P. (2010) Intracoronary autologous mononucleated bone marrow cell infusion for acute myocardial infarction: results of the randomized multicenter BONAMI trial. *Eur Heart J*
250. Takehara, N., Tsutsumi, Y., Tateishi, K., Ogata, T., Tanaka, H., Ueyama, T., Takahashi, T., Takamatsu, T., Fukushima, M., Komeda, M., Yamagishi, M., Yaku, H., Tabata, Y., Matsubara, H., and Oh, H. (2008) Controlled delivery of basic fibroblast growth factor promotes human cardiosphere-derived cell engraftment to enhance cardiac repair for chronic myocardial infarction. *J Am Coll Cardiol* **52**, 1858-1865
251. Terrovitis, J., Lautamaki, R., Bonios, M., Fox, J., Engles, J. M., Yu, J., Leppo, M. K., Pomper, M. G., Wahl, R. L., Seidel, J., Tsui, B. M., Bengel, F. M., Abraham, M. R., and Marban, E. (2009) Noninvasive quantification and optimization of acute cell retention by in vivo positron emission tomography after intramyocardial cardiac-derived stem cell delivery. *J Am Coll Cardiol* **54**, 1619-1626
252. Daldrup-Link, H. E., Rudelius, M., Oostendorp, R. A., Settles, M., Piontek, G., Metz, S., Rosenbrock, H., Keller, U., Heinzmann, U., Rummeny, E. J., Schlegel, J., and Link, T. M. (2003) Targeting of hematopoietic progenitor cells with MR contrast agents. *Radiology* **228**, 760-767
253. Daldrup-Link, H. E., Rudelius, M., Metz, S., Piontek, G., Pichler, B., Settles, M., Heinzmann, U., Schlegel, J., Oostendorp, R. A., and Rummeny, E. J. (2004) Cell tracking with gadophrin-2: a bifunctional contrast agent for MR imaging, optical imaging, and fluorescence microscopy. *Eur J Nucl Med Mol Imaging* **31**, 1312-1321
254. Vuu, K., Xie, J., McDonald, M. A., Bernardo, M., Hunter, F., Zhang, Y., Li, K., Bednarski, M., and Guccione, S. (2005) Gadolinium-rhodamine nanoparticles for cell labeling and tracking via magnetic resonance and optical imaging. *Bioconjug Chem* **16**, 995-999
255. Sitharaman, B., Tran, L. A., Pham, Q. P., Bolskar, R. D., Muthupillai, R., Flamm, S. D., Mikos, A. G., and Wilson, L. J. (2007) Gadofullerenes as nanoscale magnetic labels for cellular MRI. *Contrast Media Mol Imaging* **2**, 139-146
256. Shyu, W. C., Chen, C. P., Lin, S. Z., Lee, Y. J., and Li, H. (2007) Efficient tracking of non-iron-labeled mesenchymal stem cells with serial MRI in chronic stroke rats. *Stroke* **38**, 367-374
257. Klasson, A., Ahren, M., Hellqvist, E., Soderlind, F., Rosen, A., Kall, P. O., Uvdal, K., and Engstrom, M. (2008) Positive MRI contrast enhancement in THP-1 cells with Gd2O3 nanoparticles. *Contrast Media Mol Imaging* **3**, 106-111

APPENDIX 1 – CELL CULTURE MEDIUM

Cardiac explant medium (CEM)

Iscove's modified Dulbecco's medium (IMDM) was supplemented with 20% (v/v) fetal bovine serum (FBS; Biosera), 1× penicillin-streptomycin-glutamine (added from 100× solution which contained 10,000 U/ml penicillin, 10,000 μg/ml streptomycin, and 29.2 mg/ml L-glutamine/ml in 0.85% saline; Invitrogen) and 0.1 mM 2-mercaptoethanol (Sigma).

Cardiosphere-growth medium (CGM)

Cardiosphere-growth medium was made of 65% (v/v) Dulbecco's modified Eagle's medium (DMEM)/F12 (Invitrogen) and 35% (v/v) Iscove's modified Dulbecco's medium (IMDM; Invitrogen), supplemented with: 7% (v/v) fetal bovine serum (Biosera), 1× penicillin-streptomycin-glutamine (added from 100× solution, which contains 10,000 U/ml penicillin, 10,000 μg/ml streptomycin, and 29.2 mg/ml L-glutamine/ml in 0.85% saline; Invitrogen), 0.1 mM 2-mercaptoethanol (Sigma), 2% (v/v) B27 supplement (Invitrogen), 25 ng/ml cardiotrophin (Peprotech), 20 ng/ml bFGF (Promega), 10 ng/ml EGF (Peprotech), 5 U thrombin (Sigma).

Cardiomyocyte differentiation medium

Cardiomyocyte differentiation medium was made of 50% (v/v) Dulbecco's modified Eagle's medium (DMEM)/F12 (Invitrogen) and 50% (v/v) Iscove's modified Dulbecco's medium (IMDM; Invitrogen), supplemented with 10% fetal bovine serum (embryonic cell-qualified, Invitrogen), 1 μM dimethyl sulfoxide (DMSO) (Sigma), 300 μM ascorbic acid (Sigma), and 1 x insulin-selenium-transferrin solution (added from 100 x solution, which contained 67 ng/ml sodium selenite, 1 mg/ml insulin and 0.55 mg/ml transferrin).

APPENDIX 2 – IMMUNOBLOTTING REAGENTS

Lysis buffer

Lysis buffer was made of 75 mM Tris HCl (pH6.8), 4 M urea, 1% triton (v/v), 3.8% sodium dodecyl sulfate (SDS) and 20% glycerol in distilled water. The lysis buffer (10ml) was supplemented with one tablet of protease inhibitor cocktails (Roche) for preparing cell lysate.

Laemmli loading buffer (pH 6.8)

Laemmli loading buffer was made of 187.5 mM tris-HCl, 0.003% Bromophenol Blue, 6% SDS (w/v) and 30% glycerol (v/v) in distilled water.

Tris-buffered saline (TBS)-Tween (pH 7.4)

TBS-Tween solution was made of 10 mM tris-base, 0.05% Tween (v/v), and 0.9% sodium chloride (w/v) in distilled water.

SDS transfer buffer

SDS transfer buffer was made of 39 mM glycine, 48 mM Tris, 0.0375% SDS (w/v) and 20% methanol in distilled water.

Supplementary Table 1:
List of clinical trials involving cell therapy using bone marrow mononuclear cells for acute myocardial infarction

Reference	Trial	Year	Duration	Number of patients	Route of cell delivery	LVEF
(197)	BOOST	2004	6 months	60	Intracoronary	+7%
(240)	BOOST#	2006	18 months	60	Intracoronary	N.D.
(241)	ASTAMI	2006	6 months	100	Intracoronary	N.D.
(132)	REPAIR	2006	4 months	204	Intracoronary	+6%
(242)	Jassen	2006	4 months	67	Intracoronary	N.D.
(243)	TCT-STAMI	2006	6 months	20	Intracoronary	+10%
(244)	HEBE (pilot study)	2008	4 months	200	Intracoronary	+2%
(245)	FINCELL	2008	6 months	80	Intracoronary	+7%
(200)	BOOST#	2009	5 years	56	Intracoronary	N.D.
(246)	ASTAMI#	2009	3 years	97	Intracoronary	N.D.
(247)	REGENT	2009	6 months	200	Intracoronary	+3%
(248)	HEBE	2010	4 months	200	Intracoronary	+4%
(249)	BONAMI	2010	3 months	101	Intracoronary	N.D.

 # Follow-up study, N.D; no significant difference compared with untreated patients

Supplementary Table 2:
In vivo animal studies using explant-derived cells, cardiospheres or cardiosphere-derived cells

Reference	Model	Cell delivery method	Cell type	Cell number	Imaging method	Time after transplant	Results
(99)	AMI SCID-beige mice	IM	Mouse cardiospheres	60 spheres	Echocardiography	18 days	Better preservation of infarcted anterior wall thickness and fractional shortening.
(100)	AMI adult male SCID-beige mice	IM	Human CDCs	1×10^5	Echocardiography	20 days	Improved LVEF and cardiomyocytes survival in the infarct
(250)	CMI Pigs	IM	Human CDCs	2.0×10^7	MRI (1.5T)	4 weeks	LVEF, + 8.3%, RWM, +12.3%, reduced infract size, improved cell engraftment*.
(251)	AMI female Wistar-Kyoto rats	IM	Rat CDCs	2×10^6	Echocardiography	21 days	Improved fractional area change.
(182)	AMI FVB mice	IM	L2G85 transgenic mice CDCs	5×10^5	Echocardiography	56 days	No improvement.
(168)	AMI pigs	IC	Porcine CDCs	2.5×10^7	MRI (3T)	8 weeks	Preserved LVEF, reduced infarct size, improved hemodynamic function.
(233)	AMI adult male SCID-beige mice	IM	Human CDCs and cardiospheres	1×10^5	Echocardiography	3 weeks	CDCs preserved LVEF, CSp improved LVEF and cell engraftment .
(186)	AMI Wistar-Kyoto rats	IM	Rat EDCs and CDCs	1×10^6	MRI (9.4T)	6 weeks	Improved LVEF and cardiomyocytes survival in the infarct .
(118)	AMI Wistar-Kyoto rats	IM	Rat CDCs	1×10^6	Echocardiography	3 weeks	Improved LVEF, reduced infract size, improved cell engraftment§.
(167)	AMI SCID-beige mice	IM	Human CDCs	1×10^5	Echocardiography	3 weeks	Improved LVEF and cardiomyocytes survival in the infarct .
(217)	AMI immunodeficient male nude rats	IM	Human CDCs	1×10^6	Echocardiography	28 days	Improved LVEF and fractional shortening.
(235)	AMI pigs	IM	Cardiosphere or CDCs	1×10^7	Echocardiography	8 weeks	CDCs and cardiospheres improved LVEF, cardiospheres exerted superior improvement in hempdynamics and regional function.

AMI; acute myocardial infarction, CMI; chronic myocardial infarction, SCID;severe combined immunodeficiency, IM; intramyocardial injection, IC; intracoronary injection, LVEF; left ventricle ejection fraction, bFGF; basic fibroblast growth factor, RWM; regional wall motion, T; tesla, CDCs; cardiosphere-derived cells, EDCs; explant-derived cells

*Injection involved combinations o hCDCs and bFGF-containing hydrogel.

§cell engraftment was enhanced by magnetic targeting

Supplementary Table 3:
Previous studies of gadolinium based MR contrast agent

Reference	Contrast agent	Cell type	Labeling method	MR field strength
(209)	Gd-DTPA	Mouse ESCs and NSCs	Calcium-phosphate precipitation	1.5 T
(252)	Gd-DTPA	HPCs	Transfection with Lipofectin	1.5 T
(253)	Gadophrin-2	Human peripheral blood cells	Transfection with Lipofectin	1.5 T
(254)	Gadolinium Rhodamine nanoparticles	Human T47D breast cancer cells	Endocytosis	7 T
(255)	Gadofullerenes	NIH 3T3 mouse fibroblast cells	Endocytosis	1.5 T
(256)	Gd-DTPA	Human MSCs	Transfection with Effectene	3 T
(257)	Gadolinium oxide nanoparticles	THP-1 monocytic cell line,	Endocytosis	1.5 T
(122)	Gadofluorine M	Murine ES cells	Endocytosis	9.4 T
(120)	Gd-DTPA	Rabbit NSCs	Transfection with Effectene	1.5 T
(121)	Gadolinium hexanedione nanoparticles	Human MSCs	Endocytosis	3 T
(119)	Gadonanotubes	Pig MSCs	Endocytosis	1.5 T

Gd-DTPA; gadolinium diethylenetriamine penta-acetic acid, HPCs; hematopoietic progenitor cells, ESC; embryonic stem cells, NSC; neural stem cells, MSC; bone marrow mesenchymal stem cells, T; Tesla, NI; not indicated